AD_____

Award Number: W81XWH-05-1-0055

TITLE: Dendritic Cell-Based Genetic Immunotherapy for Ovarian Cancer

PRINCIPAL INVESTIGATOR: James M. Mathis, Ph.D.

CONTRACTING ORGANIZATION: Louisiana State University
Shreveport, LA 71130-3932

REPORT DATE: December 2008

TYPE OF REPORT: Final Report

PREPARED FOR: U.S. Army Medical Research and Materiel Command
Fort Detrick, Maryland 21702-5012

DISTRIBUTION STATEMENT:

☒ Approved for public release; distribution unlimited

The views, opinions and/or findings contained in this report are those of the author(s) and should not be construed as an official Department of the Army position, policy or decision unless so designated by other documentation.

REPORT DOCUMENTATION PAGE

Form Approved
OMB No. 0704-0188

1. REPORT DATE *(DD-MM-YYYY)*	2. REPORT TYPE	3. DATES COVERED *(From - To)*
01-12-2008	Final	12/01/2004 – 11/30/2008

4. TITLE AND SUBTITLE
Dendritic Cell-Based Genetic Immunotherapy for Ovarian Cancer

5a. CONTRACT NUMBER

5b. GRANT NUMBER
W81XWH-05-1-0055

5c. PROGRAM ELEMENT NUMBER

6. AUTHOR(S)
James Michael Mathis, Ph.D.

5d. PROJECT NUMBER

5e. TASK NUMBER

5f. WORK UNIT NUMBER

7. PERFORMING ORGANIZATION NAME(S) AND ADDRESS(ES)
Louisiana State University

Shreveport, LA 71130-3932

8. PERFORMING ORGANIZATION REPORT NUMBER

9. SPONSORING / MONITORING AGENCY NAME(S) AND ADDRESS(ES)
U.S. Army Medical Research and Materiel Command

Fort Detrick, MD 21702-5012

10. SPONSOR/MONITOR'S ACRONYM(S)

11. SPONSOR/MONITOR'S REPORT NUMBER(S)

12. DISTRIBUTION / AVAILABILITY STATEMENT
Approved for public release; distribution unlimited

13. SUPPLEMENTARY NOTES

14. ABSTRACT
Adenovirus (Ad)-mediated transduction of dendritic cells (DCs) is inefficient because of the lack of the primary Ad receptor, CAR. CD40 is a surface marker expressed by DCs that plays a crucial role in their maturation and subsequent stimulation of T cells. DC infection with Ad targeted to the CD40 results in increased gene transfer. Cells transduced with CD40-targeted Ad5-SV40-TAg vector showed increased expression of transgene and expression of co-stimulatory molecules at 48 hours post-infection compared to cells transduced with untargeted Ad5-SV40-TAg vector. We demonstrated that CD40-targeted gene transfer promotes DC maturation with induction of a complex signaling cascade accompanied by characteristic changes in cytokine production. These results demonstrate that DCs can be successfully transduced using a CD40 targeted adenoviral vector and that transduced DCs show activation.

15. SUBJECT TERMS
ovarian cancer; gene therapy; dendritic cells; adenovirus; cd40; tumor antigen; vaccination; targeting; ctl response; antigen presenting cell; syngeneic tumor model; immunization; preclinical

16. SECURITY CLASSIFICATION OF:			17. LIMITATION OF ABSTRACT	18. NUMBER OF PAGES	19a. NAME OF RESPONSIBLE PERSON
					USAMRMC
a. REPORT	b. ABSTRACT	c. THIS PAGE	UU	91	19b. TELEPHONE NUMBER *(include area code)*
U	U	U			

TABLE OF CONTENTS

INTRODUCTION:

1. General Introduction

1.1. Strategies of immune evasion adopted by tumor cells.

The combined effort of many researchers during the last thirty years has provided significant progress understanding the immunological features of cancer cells. Most cancers possess tumor-specific antigens, or over-express antigens present in normal tissues, that can serve as targets for the immune system [14]. The reasons for the failure of the immune system to prevent cancer have just begun to be elucidated. Immunological ignorance of tumor antigens is due to an imbalance in the combination of signals between cancer cells and T-cells, necessary to initiate an immune response [15] . The interaction between MHC class I molecules on the tumor cells and the T-cell receptor (signal 1) on T-lymphocytes and between adhesion/costimulatory molecules (signal 2) are both necessary for cytotoxic T-lymphocyte (CTL) activation. In accordance with this model, tumor cells that down regulate MHC class I molecule expression (signal 1), and lack co-stimulatory molecules (signal 2), fail to activate T-cells because of errors at one or both signals [16-20]. Some tumor cells have defects in the antigen-processing and presentation pathway such that they do not present tumor antigens on their cell surface along with MHC, for example, mutation or down-regulation of TAP-1/2 or LMP-2/7 proteins [21-23]. There can even be physical exclusion of immune cells from the tumor due to the presence of the tumor in immune-privileged sites like the nervous system, or due to the lack/repression of expression of various Cellular Adhesion Molecules (CAMs) on the blood vessels in the tumor which prevent the transmigration and thus homing of the lymphocytes from the blood vessels into the tumor tissue [24]. Other mechanisms adopted by tumor cells to evade the immune system is shedding of tumor antigens into the serum and lymph such as to induce tolerance against them or antigenic modulation by tumor cells, such as down-modulation of antigen expression on their cell-surface when the immune cells are present in their vicinity [25-27]. Some tumor cells also secrete immunosuppressive cytokines such as Transforming Growth Factor-β (TGF-β), Interleukin-10 (IL-10) and Vascular Endothelial Growth Factor (VEGF) which act to inhibit the induced immune response [28, 29]. Other immune evasion mechanisms adopted by the tumor cells include mechanisms of escape from immune cell-mediated apoptosis such as modulation of expression of FAS ligand and FAS on cell surface, loss of receptors that can lead to induction of apoptosis or over-expression of proteins that can inhibit apoptosis [30-32]. Some tumor cells are also known to induce tolerance by activating regulatory T-cells (T_{regs}) [33, 34]. These T_{regs} cells suppress the function, proliferation and cytokine secretion by CD4 positive, CD25 negative and CD8 positive T-cells [32]. The aim of cancer immunotherapy is to augment the efficiency of the existing immune system to detect and kill cancer cells and to make the tumor cells more vulnerable to killing by the immune cells.

1.2. Immunotherapy strategies for cancer treatment.

The immunotherapies used to treat cancer can be classified into three types [6]:

1) Active specific immunotherapies that stimulates the body's own immune system to fight the tumor, *e.g.,* cancer vaccines.
2) Passive specific immunotherapies that do not stimulate the body's own immune system to induce an anti-tumor response, but use components of the immune system such as tumor-specific antibodies or T-cells that are generated *in vitro*, to detect and kill cancer cells in the body upon infusion, *e.g.,* monoclonal antibody therapy and adoptive T-cell therapy.
3) Non-specific immunotherapies and adjuvants that stimulate the immune system in a general way, *e.g.,* Cytokines, BCG, Incomplete Freund's Adjuvant (IFA).

Components of the immune system that are used in passive and nonspecific immunotherapies though effective, have their own half-life and the success of these therapies depends on the survival and stability of the T-cells, antibodies and cytokines in the body. In addition, once these agents are cleared from the body, there is no protection against future relapses of the cancer. Active specific immunotherapies stimulate the body's own immune system against the tumor, which produces effector tumor-specific T and B cells and inflammatory cytokines until the antigenic stimulus, *i.e.,* the tumor, is present in the body. This ensures that the induced immune response will remain active until the tumor is cleared. In addition, the memory generated by the induced anti-tumor immune response will protect against future relapses of the same tumor.

To induce an anti-tumor immune response, the immune cells must be stimulated against antigens that are specifically expressed or over-expressed in tumor cells. The identification of tumor associated-antigens (TAA) recognized by T-cells has opened new directions for immunogene therapy. The different cancer vaccines currently being developed to induce a specific anti-tumor immune response can be classified as follows [35]:

1) Tumor cell vaccines
2) Antigen vaccines
3) Anti-idiotype vaccines
4) DNA vaccines

5) Dendritic cell (DC)-based vaccines

Tumor cell vaccines use the tumor cells or cell lines obtained from surgery as vaccine to stimulate the immune system [35]. The tumor cells are killed, usually by radiation, before they are injected back into the patient. The advantages of using tumor cell as vaccine is that immunity is raised against all the antigens that are presented by the tumor cell. The disadvantages of the tumor cell vaccines are that sometimes autoimmune response can be induced, some tumor cells do not induce an effective immune response because of poor presentation of the tumor antigens or lack of co-stimulatory molecules on their cell surface. In such cases the tumor cells can even be genetically modified *in vitro* to enhance their antigen processing and presentation capacity and to express co-stimulatory molecules on their cell-surface to activate the immune cells.

Antigen vaccines stimulate the immune system by using the individual TAAs or tumor specific antigens (TSAs) [35]. The identification of various TAAs and TSAs has revolutionized the field of cancer vaccination. The advantage of using antigen vaccines is that the immune response is stimulated against the antigens that are more specifically expressed by tumor cells and thus minimizing the possibility of an autoimmune response. The antigen vaccine is usually a peptide that corresponds to the immunogenic epitope of the tumor antigen given by itself or along with an adjuvant. The major obstacle with the use of antigen vaccines is its inherent lack of immunogenicity and biodegradability. The peptide can be modified to increase its immunogenic potential such as substitution of amino acid to increase its binding potential to MHC or TCR and fusion to immunostimulatory molecules like cytokines to produce recombinant peptide vaccine. Even then the success of this vaccine depends on the uptake of the peptide antigen by cells that can efficiently present them to lymphocytes and induce a strong immune response . For example, the NY-ESO-1 is an antigen vaccine. The NY-ESO-1 is a cancer-testis antigen [36]. Cancer-testis antigens are a category of tumor antigens that are normally expressed by male germ calls in the testis, but not by adult somatic tissues. The regulation of this gene is however disrupted in malignancy , and the gene is over-expressed in several tumor types, including 40% of epithelial ovarian cancers and it has been selected as a prototypic human cancer antigen for vaccine development.

Anti-idiotype vaccines use the immunogenicity of the anti-TAA antibodies (Ab1) to raise antibodies (Ab2) against the idiotypic component of the anti-TAA antibodies. Some of these anti-idiotype antibodies (Ab2i) represent the internal image of the antigenic epitope of the TAA against which the anti-TAA antibodies (Ab1) were raised and thus can be used as surrogate antigens for immunization [35]. In 1982, Levy and colleagues used anti-idiotypic monoclonal antibodies to induce remission in patients with B-cell lymphoma. The advantage of this vaccine is that again there is reduced possibility of induction of autoimmune response. The anti-idiotype vaccines are antibodies and thus the success of this vaccine depends on the stability of these antibodies in the body. In addition, this type of vaccine will mainly induce a humoral response, which may not be sufficient to induce killing of all tumor cells.

DNA vaccines use the DNA encoding tumor antigens to immunize the patients [35]. The cells that take up the DNA molecule will express the tumor antigen and present it on its cell surface to the lymphocytes resulting in induction of an anti-tumor immune response. The advantage of using the genetic material instead of the antigen protein itself is the prolonged expression and presentation of the tumor antigens to the immune system. Naked DNA vaccination approaches, in which a plasmid encoding a tumor antigen is administered subcutaneously or intradermally have proven useful in eliciting antibody and cellular anti-tumor responses. Recombinant virus-mediated delivery of tumor antigens into the skin or muscle has also proven to elicit anti-tumor responses. Recombinant vaccinia, adenovirus and fowlpox vaccines expressing carcinoembryonic antigens, human papillomavirus E6/E7 and NY-ESO-1 have shown immune responses in humans. Like antigen vaccines, the drawbacks of the DNA vaccines lie in its intrinsic lack of immunogenicity and biodegradability. The antigen recombinant viral vectors can also lead to liver toxicity. In addition, the effectiveness of the DNA vaccine is dependent on its uptake, expression and presentation of the expressed tumor antigen by an appropriate cell type to induce a strong immune response.

Dendritic cell vaccines use dendritic cells (DCs), which are the professional antigen presenting cells of the immune system, to process and present the tumor antigens and provide co-stimulatory signals to the antigen-specific lymphocytes to induce a robust anti-tumor immune response [35]. The DCs also secrete inflammatory cytokines and chemokines that further augment the induced immune response. The DCs can be cultured *in vitro* by isolating monocytes from the blood of the tumor bearing patients, and culturing them *in vitro* in the presence of cytokines to induce their differentiation into DCs. The tumor antigens can be loaded onto or expressed in the DCs using tumor cell lysates, peptides corresponding to the antigenic epitopes of the tumor antigen, plasmid or viral vectors carrying the DNA that encodes for tumor antigens. The pulsed or transfected DCs are then injected back into the patient as autologous DC vaccine. The loading or infection of the DCs can be carried out *ex vivo* or by targeting the DCs *in vivo*. Targeting DCs *in vivo* using different targeting recombinant vectors or molecules would alleviate the need for culturing the DCs *in vitro*. The advantage of using dendritic cell vaccines is that DCs are the most potent antigen presenting cells. The presentation of tumor antigens released upon tumor cell death and captured by APC (a phenomenon called “cross-presentation’) has been

proposed as a more potent strategy than direct presentation of tumor antigens by the tumor cells themselves. Thus, antigens that may not have been immunogenic when presented by the tumor cells may induce a strong immune response when presented by the DCs. The DCs are also more stable than peptides or DNA molecules and thus a longer period of stimulation of the immune response is ensured. DCs are not toxic by themselves and thus do not pose that risk. The DCs, dependent on the nature and source of the antigen, can elicit both cellular as well as humoral immune response.

1.3. Dendritic cells as candidate effector cell for presentation of tumor antigens.

Dendritic cells (DCs) are the most potent APCs so far identified and as such, they are also the most potent initiators of immunity [37, 38] They can capture, process and present antigens in combination with MHC class I and class II molecules to naive CD8+ (cytotoxic) and CD4+ (helper) T lymphocytes, respectively. Through this process, specific cytotoxic T lymphocytes for that antigen are activated that can recognize a target cell and kill it. DCs possess particular characteristics that make them suitable for antigen presentation. They are found in different maturation cell states that confer them distinct abilities. In their immature state, DCs are predominantly antigen-capturing cells, through phagocytosis, macropinocytosis and receptor-mediated endocytosis. Upon capturing, antigens enter the endocytic pathway where they are processed and loaded in MHC class II molecules for presentation to CD4-expressing T lymphocytes. Antigens that have access to the cytosol, like viral proteins synthesized inside the DC upon infection, can associate with MHC class I proteins and be presented to CD8+ T-cells.

The exogenous pathway, in which antigens not synthesized inside the DC can also be presented in association with MHC class I, is a mechanism recently identified and is responsible for cross-presentation. In this regard, it has recently been shown that DCs can acquire antigens from apoptotic cells through a receptor-mediated mechanism that can generate class I-restricted responses [39]. This would explain how DCs can process and present, in an MHC class I-restricted manner, antigens from tumor cells that otherwise would not be cytosol-accessible. Immature DCs are found at many tissues, in particular at the port of entry of infectious agents such as skin (the Langerhans cells). Although immature cells are specialized in capturing and processing, their T-cell activation ability is limited. DC maturation can be driven by antigens themselves, by cytokines, and by interaction with T-cells. In the mature state, DCs up regulate their expression of MHC, and co-stimulatory proteins necessary for T-cell activation. They also acquire their distinctive stellate shape and increase their motility allowing them to migrate to lymphoid centers where antigen presentation takes place. Specific naive cytotoxic and helper T-cells are thus activated and the immune response initiated. It is upon the interaction with T-cells that DCs acquire their final maturation phenotype; characterized by loss of phagocytic capacity, further expression of costimulatory molecules, and synthesis of cytokines such as IL-12. This final maturation step is not insignificant. It has recently been described that interaction of DCs through CD40 with T helper cells expressing CD40 ligand (CD40L) can bring the DC to a state that triggers cytotoxic T-cell responses [40-42]. Therefore, this final maturation based upon CD40-CD40L interactions allows DC to present antigens and activate CD8+ T-cells. Shortly after complete maturation, DCs undergo activation-induced apoptosis and die.

1.4. The use of dendritic cells in tumor vaccination approaches.

The use of DCs as adjuvants for cancer therapy was boosted by the development of techniques to generate and culture sufficient amounts of DCs *ex vivo*. DCs originate from a hematopoietic precursor and they represent a low percentage in the circulation. Investigators have been able to derive DCs from different sources such as peripheral blood monocytes or bone marrow CD34+ cells, using the appropriate combination of cytokines. It is now feasible to obtain enough number of DCs and stimulate them *ex vivo* to present tumor-specific antigens. Subsequently, autologous DCs can be reinfused into the patient by intravenous or intradermal administration, and cells travel to the lymph node where presentation and activation of T-cells take place. A number of reports have shown preclinical data on the potency of DC-based vaccination [43-63] , and phase I and II clinical trials targeting different types of tumors have been initiated [64-66] .

The choice of current immunogen and vaccination protocols is broad: the immunogens typically used in DC-based vaccination fall into two major categories: single tumor antigens and multiple antigen mixtures. The rationale of using single defined tumor antigens is that some tumor antigens and even peptide fragments interacting with different MHC class I alleles have been identified and isolated. From a pharmacological standpoint, this approach provides a cleaner immunization system. However, one drawback is that negative selection of antigen-deficient cells may also occur. Immunization with mixtures containing multiple tumor antigens represents an alternative approach. In this case, unfractionated tumor material is generally used and therefore may contain proteins common in normal tissues. Although this approach may increase the chances of presentation of weak or undefined tumor antigens, it may also give rise to autoimmune responses. The most widespread approaches in vaccination protocols have been to load (pulse) dendritic cells with synthetic peptides that correspond to TAAs recognized by CD8+ T-cells in combination with a defined MHC allele.

Using this protocol, cells are co-cultured with the peptide, which in turn, associates with class II and also binds to

class I molecules. This method has been shown to promote protective anti-tumor immunity and regression of pre-established tumors [45, 48, 51, 60, 67, 68] . The main disadvantage of this approach is that not all tumor antigens are known for many tumors and not all MHC class I-restricted peptides are known for a given tumor-specific antigen. For this reason, DCs have been pulsed with peptides eluted from MHC-antigen complexes present in tumor cells [44] . This approach has shown therapeutic effects in weakly immunogenic tumors in experimental models. In the same regard, DCs have been pulsed with total soluble antigens from tumor extracts and shown to elicit tumor-specific immunity [56, 69, 70]. Although both eluted tumor peptides and tumor lysates do represent individualized approaches for each patient's tumor, the fact that they rely on the availability of tumor material restricts their use.

Different approaches based on genetic transduction, whereby a coding sequence for a tumor antigen is introduced and expressed in DCs, have also been attempted. In this case, most of the endogenously synthesized antigen is channeled mainly into class I molecules and CD8+ responses are elicited. By providing the complete DNA sequence for a tumor antigen, presentation is not limited to a single epitope for a given MHC allele. Furthermore, the delivery of genetic material allows for prolonged expression and therefore presentation of antigens. Both nonviral [49, 54, 71, 72] and viral [53, 61-63, 73-78] methods have been described for introduction of DNA sequences, which have shown to promote specific CTL responses and protective and therapeutic anti-tumor immunity of tumors expressing the antigen sequence delivered. However, because the endogenously expressed antigens may have only limited access to the class II presentation pathway, it is possible that there will be a deficiency in generating CD4+ T helper cells, required for an effective and durable CTL response. An approach different from *ex vivo* DC pulsing and genetic transduction is the use of cell fusion between tumor cells and DCs [58, 79, 80]. This approach combines the presence of tumor antigens in tumor cells with the presentation capability of DCs. While the advantage of this approach may be the presentation of undefined tumor antigens both to CD4+ and CD8+ T lymphocytes, there is still some concern regarding the generation of autoimmune responses. In addition, the requirement of viable autologous tumor cells is a disadvantage for clinical implementation.

The promise of DC-based vaccination strategies is reflected in the fact that more than 50 DC-related clinical trial protocols have been published (results reviewed in [81]). However, there are critical issues in the DC-based vaccination approaches that may limit their employment in the clinic. With the advent of DC culturing techniques *ex vivo*, researchers have sought DC-specific markers. Although a panel of characteristic markers has been defined (*e.g.,* CD1a+, CD40+, CD80+, CD86+, MHC class I and class II, ICAM-l, LFA-3), it is now obvious that the collective name of DC, groups a heterogeneous population of cells, derived from different lineages, in different maturation states, and probably showing distinct functional features [82]. Thus, differentiation of DCs *ex vivo* may be subjected to different environmental modifications resulting in cells that do not totally represent their counterparts *in vivo*. This may translate into reduced potency to elicit effective anti-tumor responses. In addition, the *ex vivo* culture and manipulation of DCs is time-consuming, laborious and expensive. Therefore, the development of an *in vivo* approach based on DC vaccination without involving isolation and culturing of DCs *ex vivo* would be clinically significant.

1.5. Strategies for targeting Dendritic cells *in vivo*.

Many strategies currently used to target *in vivo* DCs utilize ligands or antibodies that can bind to the cell surface markers expressed by DCs. The tumor antigen or peptides are linked to the ligands/antibodies by either chemical coupling or genetic recombination. The cell surface receptors along with the bound chimeric antibody-peptide complex will be internalized by the DCs by receptor-mediated endocytosis, directing the antigens to different antigen processing and presentation pathways and the peptides will be presented along with the appropriate MHC molecules on the DC cell surface.

Other strategies that have been used to target DCs *in vivo* without specifically targeting any known cell surface receptor are targeting antigens to DCs *in vivo* using apoptosis, nanoparticles and lentiviral vectors [83-85]. Apoptosis was used to target DCs *in vivo* by using apoptotic antigen-bearing cells. The apoptotic antigen-bearing cells were engineered by co-expressing the immunogen and FAS in the same cell. The apoptotic death of the antigen-bearing cells *in vivo* led to increased acquisition of antigen by antigen presenting cells including DCs [83]. Poly(propylene sulfide) nanoparticles have been shown to be internalized by 40-50% of the lymph node DCs and APCs without the use of a targeting ligand , thus showing potential for immunotherapeutic applications [84]. Recently, lentivirus vectors have been successfully used to induce a robust and sustained antigen-specific CTL responses [85]. The absence of pre-existing immunity in humans makes lentiviral-based vaccines an attractive candidate for tumor immunotherapy. However, lentiviruses belong to the retovirus family and thus pose the risk of insertional mutagenesis and oncogenesis.

The various cell-surface markers that have been exploited for targeting DCs have been DEC-205, CD91, DC-SIGN and Dectin-1 [86-89]. Monoclonal antibody against DEC-205 chemically coupled with the target antigen was used to target DCs *in vivo*. It was observed that targeting steady-state DCs via DEC-205 lead to tolerance against the target antigen instead of immunity [86]. Whereas, simultaneous delivery of a DC-

maturation stimulus via CD40 along with the anti-DEC-205-antigen complex led to the induction of a strong immune response. Thus, binding of the antigen to the DC -surface followed by its uptake was not sufficient to generate an immune response, in fact, it could induce tolerance instead of immunity. The maturation status of the infected DCs is the determining factor of whether immunity or tolerance is induced, and thus the delivery of a maturation stimulus along with the antigen increases the possibility of induction of a robust immune response. Another example of induction of immunity via simultaneous delivery of antigen and maturation stimulus to the DCs is the liposome mediated delivery of encapsulated antigens and immunomodulatory agents such as lipopolysaccharide (LPS) or interferon-gamma (IFN-γ) to dendritic cells [90]. In this study, liposomes were targeted to the dendritic cells by using single chain antibody fragments specific for DC markers such as CD11c or DEC-205 that were attached to the vesicle surface by metal chelation for successful induction of antigen-specific immune response.

The above studies suggest that induction of an effective immune response by *in vivo* infection of DCs requires efficient targeting of the DCs and induction of maturation in the infected DCs without perturbation of DC function. CD40 is a transmembrane receptor expressed on DC cell surface that plays a crucial role in their maturation and subsequent stimulation of T-cells. Thus, targeting DCs via CD40 would not only mediate delivery of antigen to DCs, but also induce their maturation. Several studies have shown that targeting DCs using antigens linked to monoclonal antibodies specific for CD40 leads to DC maturation and induction of immunity against the antigen [91-93]. Delivery of genetic material encoding the tumor antigen instead of the antigen itself would sustain the presentation of the antigens by DCs for longer period of time. Several studies by Curiel *et al*., have used an adenoviral vector to deliver genes encoding target antigens to the DCs [78, 92-99].

Adenoviruses were initially vectored as vehicles for gene therapy. But, the attempts to replace faulty or missing genes by adenoviral gene transfer vehicles were mostly unsucessful in both, animals as well as humans, due to the innate and adaptive immune responses induced by adenoviral antigens. While this reduced their appeal as gene transfer vehicles, it potentiated their use as vaccine carriers. Adenovirus have been used as a recombinant viral carrier for vaccination against several infectious diseases because of several reasons [100-102]. Its genome is well characterized and can be easily manipulated. Its stability and type I immune adjuvant property make adenovirus very attractive as vaccine carriers. They can also be obtained in high titers (> 10^9 plaque forming untis per ml) by propagation on 293 or PER.C6 cells and can be easily purified. Most adenoviruses cause mild diseases in immunocompetent human adults such as cold and gastroenteritis, and by deletion of crucial regions of the viral genome can be rendered replication incompetent, which reduces their chance of causing disease. Adenoviruses have a broad tropism, infecting both dividing as well as non-dividing cells. The adenoviral genome has been shown to persist episomally in the target cell , rather than integrating into the host DNA. This reduces the risk of insertional mutagenesis. They can be administered by several routes such as intranasal, oral, intratracheal, intraperitoneal, intravenous, intramuscular and subcutaneous. As a result, Ad-based vaccines can induce not only a systemic immune response, but also a strong mucosal immune response, upon application to respiratory or intestinal tract. Mucosal immunity is particularly important to prevent infections caused by agents that infect the host via mucosal membranes such as Human Immunodeficiency Virus (HIV), Herpes Simplex Virus (HSV), *Mycobacterium tuberculosis*, rabies virus, SARS-coronavirus, Ebola virus, etc. Thus, currently three adenovirus-based vaccines are already in phase I and II clinical trials for HIV infection. A replication deficient adenoviral vaccine that expresses an immunodominant *Mycobacterium tuberculosis* antigen Ag85A (AdAg85A) has been shown to be a potent mucosally administrable vaccine in animal model [101]. An adenoviral vaccine expressing the HSV glycoprotein B (AdgB) has been shown to be effective in mouse models of HSV infection [101]. The adenoviral vector expressing the rabies virus glycoprotein was shown to induce protective antigen-specific neutralizing antibody titers very rapidly after a single application in animal models [100]. Adenoviral vectors expressing the spike protein, the membrane protein and the nucleoprotein of SARS virus were shown to induce virus-neutralizing antibodies and T cell responses in non-human primates.[100] Adenoviral vectors expressing the Ebola virus glycoprotein has been shown to induce a protective immune response in nonhuman primates against the Ebola virus, which causes hemorrhagic fever in humans [100]. Thus, adenoviral vaccine carriers, due to their genetic flexibility and ease of manipulation, the speed with which they induce a protective immune response, and potential for immunization via varied routes, have extremely bright potential for being developed as vaccine against several infectious diseases as well as cancer.

Adenoviruses cannot efficiently infect DCs because of deficiency of the native receptor of adenovirus, *i.e.,* Coxsackie and Adenovirus Receptor (CAR) on the DC cell surface. Thus, to target adenovirus to DCs , Curiel *et al* used bi-specific monoclonal antibodies specific for the fiber knob domain of adenovirus and CD40 receptor linked to each other by chemical coupling or genetic recombination. They successfully demonstrated enhanced infection of DCs by using CD40-targeted adenovirus compared with untargeted adenovirus. The infected DCs also showed increased expression of maturation markers and inflammatory cytokines such as IL-12 and enhanced allostimulatory capacity in a

mixed lymphocyte reaction (MLR). In one study, they have shown that adenoviral vectors targeted to CD40 enhance the efficacy of DC-based vaccination against human papillomavirus 16-induced tumors in a murine model [78]. The human papillomavirus virus (HPV) E7 antigen was the chosen target antigen in the study. The results showed that relative to DCs infected with untargeted Ad-E7, DCs infected with Ad-E7 targeted to the receptor CD40 enhanced protection against HPV-16 induced tumor cells in a murine model. The Curiel group also generated a single-component CD40-targeted adenoviral vector, where adenovirus is targeted to CD40 by genetic incorporation of the CD40 ligand in the capsid of the adenovirus. This single component CD40-targeted adenovirus achieved efficient infection and maturation of DCs *in vitro* as well as in a human skin substrate system [92]. Thus, there is enough evidence to support the use of CD40-targetd adenoviral vectors as a new vaccine modality for immunotherapy strategies. Our collaborators at the University of Alabama at Birmingham (UAB), generated Ad vector systems that specifically target mouse DCs via the CD40 receptor using bi-specific adapter molecule, CFm40L [103]. The bi-specific adapter molecule, CFm40L, consists of the ectodomain of CAR fused to mouse CD40 ligand via a trimerization motif. Their studies showed that CD40-targeted adenovirus could dramatically enhance gene transfer to DCs compared with untargeted adenovirus, induce phenotypic maturation and up-regulate expression of IL-12. Their studies also demonstrated that CD40-targeted adenovirus elicited specific immune response against a model antigen, β-gal, *in vivo*. The next step was to test the potential of this CD40-targeted adenoviral vector to infect DCs *in vivo* and generate an effective anti-tumor immune response in a murine model of cancer.

1.6. Hypothesis and Specific Aims

Our goal was to study the efficacy of this CD40-targeted adenoviral vector expressing the tumor antigen, SV40 T-Ag, to generate anti-tumor immunity in a mouse model of ovarian cancer. Untargeted adenovirus cannot efficiently infect DCs due to deficiency of expression of the native receptor of adenovirus, *i.e.,* CAR on DC cell surface. CD40 is a co-stimulatory protein expressed by antigen presenting cells of the immune system including DCs. Our hypothesis was that the CD40-targeted adenoviral vector will infect *in vivo* APCs including DCs more efficiently and will induce a greater cytotoxic immune response against the target SV40 T-Ag, than the untargeted adenovirus. Our second hypothesis was that CD40-targeted adenoviral vectors will induce lower liver toxicity, as by targeting the adenovirus to CD40 , the native tropism of the adenovirus for the liver would be altered. The main limitation in the use of adenoviral vector as treatment modality, is the liver toxicity that is induced by the virus because the native tropism of the adenovirus is for the liver.

Our hypothesis was that CD40-targeted adenovirus will infect DCs more efficiently than untargeted adenovirus and will also induce maturation of the DCs, thus increasing the activation potential of the infected DCs. Our Specific Aim I was to test the potential of the CD40-targeted adenovirus to infect dendritic cells *in vitro*, to characterize the changes in the activation potential of the infected DCs and to study the changes in cell signaling that occur in the DCs upon infection with CD40-targeted adenovirus. The expression of the target antigen in infected DCs will be determined by flow cytometric as well as Western blot analysis. The activation potential of the infected DCs was analyzed by measuring phenotypic expression of maturation markers on DC cell surface by flow cytometry and secretion of inflammatory cytokines and chemokines by the DCs using Bio-Plex cytokine analysis. The changes in cell signaling that occur in response to infection by CD40-targeted adenovirus will be studied by Western blot analysis of the cell signaling proteins.

According to our hypothesis, CD40-targeted adenovirus carrying the transgene that encodes the target tumor antigen, can infect DCs *in vivo* more efficiently than the untargeted adenovirus. The DCs infected by CD40-targeted adenovirus, will then express, process and present the tumor antigen on its cell surface to the lymphocytes, and induce a greater specific cytotoxic immune response against the target antigen than the DCs infected by untargeted adenovirus. Our Specific Aim II was to measure the cytotoxic T lymphocyte response against the target SV40 T-Ag, induced by CD40-targeted adenovirus and untargeted adenovirus carrying the gene that encodes the antigen, using the *in vitro* chromium release assay and *in vivo* CFSE-based CTL assay. According to our second hypothesis, the CD40-targeted adenovirus will induce lower liver toxicity than the untargeted adenovirus as we expect that the native tropism of the adenovirus, which is for the liver, will be altered by targeting the adenovirus to CD40.Our Specific Aim III was to analyze and compare the liver toxicities induced by CD40-targeted adenovirus and untargeted adenovirus. The liver toxicity was analyzed by histological studies of the liver sections, measuring *in vivo* infection of the liver by adenovirus using real-time PCR and PET and analyzing the serum for liver toxicity enzymes and inflammatory cytokines and chemokines. Our Specific Aim IV was to test and compare the potential of CD40-targeted adenovirus with that of untargeted adenovirus, both carrying the gene that encodes the target SV40 T-Ag, to elicit a prophylactic immune response in a murine model of ovarian cancer which expresses SV40 T-Ag. The tumor growth and progression in the immunized mice upon challenge with the tumor cells expressing SV40 T-Ag, was followed by measuring changes in weight of the animals and following their survival.

BODY:

2. In vitro infection and characterization of dendritic cells

2.1. Introduction

Dendritic cells are the professional antigen presenting cells of the immune system. They are the most potent activators of naïve T-cells. They sample the antigenic environment in the periphery, capture and phagocytose any foreign pathogen or particle that may be present. The DCs then travel to the local lymph nodes or the secondary lymphoid organs and present the foreign antigens to the lymphocytes. They activate the antigen-specific lymphocytes in the lymphoid organs. The activated antigen-specific lymphocytes then travel out of the lymphoid organs into the periphery, to the site of infection or inflammation and mount an immune esponse against the foreign pathogen.

The dendritic cells exist in two different states [104]. In the periphery, they exist in the immature state, where they are phagocytic and their main function is to capture all antigens that may be present in the peripheral organs. Maturation is induced by components of the pathogen or by host molecules associated with inflammation or tissue injury. The mature dendritic cells are specialized for T-cell activation. Mature dendritic cells are characterized by reduced phagocytic uptake, the development of cytoplasmic extensions, migration to lymphoid tissues and enhanced T-cell activation potential. Thus, the immature dendritic cells capture all particulate matter in the periphery, undergo maturation and then travel to the lymphoid organs. In the lymphoid organs, the mature DCs present the foreign antigens to the lymphocytes and activate them. The activated antigen-specific lymphocytes travel to the site of infection or tissue injury and mount an immune response against the foreign pathogen or injured self-tissue.

Observing defects in DC function and maturation in cancer patients as well as tumor-bearing animals lead to the hypothesis that dendritic cells could be used to induce an anti-tumor immune response, *i.e.,* DCs could be used as an anti-tumor vaccine. The ex-vivo generation of anti-tumor DC vaccine involves isolation of monocytes from the peripheral blood of cancer patients [105]. The monocytes are cultured *in vitro* in the presence of cytokines such as GM-CSF and IL-4. In the presence of these cytokines, monocytes differentiate into immature DCs. The immature DCs are then matured in the presence of maturation agents such as CD40L, LPS, and TNF-α, *etc*. The mature DCs are then pulsed with either tumor lysate, peptides which correspond to the antigenic epitopes of tumor antigens or infected by viral vectors which encode for tumor antigens. The result is mature DCs which express the tumor antigens on their cell surface along with MHC molecules. These autologous DCs are then injected back into the patients as anti-tumor vaccine. The DCs will present these tumor antigens and activate the antigen-specific lymphocytes. The activated antigen-specific lymphocytes will then mount an anti-tumor immune response in the patients and kill the tumor cells.

The entire process of *ex vivo* generation of DC-based anti-tumor vaccine is expensive, time-consuming and cumbersome. It would also require a laboratory to be attached to the hospital for the culture and processing of dendritic cells. An alternative would be to target DCs *in vivo* with a vector which encodes for the tumor antigen. The advantages of targeting DCs *in vivo* are that it would be less labor-intensive and expensive than the *ex vivo* approach. It would be an attractive off-the-shelf reagent. It would also be possible to exploit the physiological properties of DCs for efficient immunization. Among all the vectors available for infection, genetically modified adenoviral vectors are widely used because they can elicit both humoral and cellular immune responses, they do not perturb the DC function upon infection and do not cause cytopathic effects in DCs, except at a high multiplicity of infection (m.o.i.) [106]. One of the major limitations in the use of adenovirus is that wild-type Ad5 cannot efficiently infect DCs because of deficiency of the Ad5 receptor, CAR, on dendritic cells [71] .

Our collaborators at UAB have generated a DC-targeted Ad5 vector by using a bispecific adapter molecule, called CFm40L. The adapter protein consists of the extracellular portion of the native Ad receptor, CAR, fused to a trimerization motif of a 71 amino acid domain from the bacteriophage T4 fibritin protein, linked to the extracellular domain of the mouse CD40 ligand. CD40 ligand binds to the CD40 receptor, which is a cell-surface receptor expressed by dendritic cells. Thus, when the CFm40L adapter molecule and Ad5 viral particles are mixed, the adapter molecule binds to the fiber-knob domain of the adenovirus by the extracellular portion of the native Ad receptor, CAR. The adenovirus particle, coated by the adapter molecule, can bind to and infect any cell expressing CD40 receptor on its cell-surface by the CD40 ligand domain of the adapter molecule [103].

We tested the infection potential of the CD40-targeted Ad5 vector on DCs cultured *in vitro*. We also determined the maturation status of the infected DCs by measuring the expression of maturation markers such as CD80, CD86 and CD40 on the cell-surface of DCs after infection. We also determined the inflammatory

cytokines that were secreted by the DCs on infection. We also looked into the changes in the cell signaling pathways that occur in the DCs on infection, which lead to the increased expression of cell-surface maturation markers and secretion of inflammatory cytokines.

2.2. Materials and Methods

2.2.1. Adenoviruses. The replication-defective human adenovirus (serotype 5-derived) vectors were produced in 293 cells by homologous recombination between two transfected plasmids containing adenovirus DNA fragments overlapped at the E1a flanking region. High titer adenovirus stocks were purified by cesium chloride gradient centrifugation. Banded virus was removed, desalted by dialysis, and stored in small aliquots at -80ºC. Viral stocks and infected cells were handled only in a Class II laminar flow hood and maintained in a CO_2 incubator designated for that purpose. The concentration of total viral particles (v.p.) was determined by measuring absorption at 260 nm. The concentrations of infectious v.p. were defined as infection forming units (ifu) determined in 293 cells using an Adeno-X Rapid Titer Kit (Clontech). The Ad5-CMV-SV40 T-Ag vector was a gift of H-G Zhang [107].

2.2.2. CFm40L targeting ligand. This bispecific adapter protein consists of the extracellular portion of the native Ad receptor, CAR, fused to a trimerization motif of a 71 amino acid domain from the bacteriophage T4 fibritin protein, linked to the extracellular domain of the mouse CD40 ligand (CFm40L). The cDNA coding for the recombinant fusion protein was assembled in an expression plasmid and its integrity confirmed by DNA sequencing. Linearized plasmid DNA was then used to establish stable 293 cell lines producing CFm40L as a secreted CFm40L protein. Supernatants from the clones were tested for the presence of CFm40L by a dot-blot assay with anti-CAR antibodies (data not shown). A positive clone, constitutively secreting the product was expanded and the fusion protein was purified by metal affinity chromatography from the culture medium.

2.2.3. Isolation and culture of mouse Bone Marrow Derived Dendritic Cells (BMDCs). Bone marrow cells were isolated from the fibulas and femurs of 6-8 week old B6C3F1 mice. The cells were then cultured in complete media (RPMI-1640 containing 10% fetal bovine serum, 2 mM L-glutamine, 1% non-essential amino acids, 100 U/ml penicillin, 100 µg/ml streptomycin, 10 ng/ml GM-CSF and 10 ng/ml IL-4 for 5 days. On day 5, the BMDCs were harvested using versene and used for further experiments [103].

2.2.4. Gene transfer assay. The BMDCs were plated in 6-well dishes, with 1×10^6 cells per well. The cells were incubated in a humidified incubator at 37^0C for 48 h. After 48 h, the cells were infected with the untargeted adenovirus encoding Green Fluorescent Protein (Ad5-CMV-GFP) and Ad5-CMV-GFP complexed with increasing amounts of CFm40L (3, 30, 90, 120, 300, 600 ng). The multiplicity of infection used for the experiment was 100:1 (ifu:cell). The cells were incubated in a humidified incubator at 37^0C for 48 h. After 48 h, the cells were harvested using Versene (Invitrogen) and expression of GFP in the infected cells was measured using flow cytometry.

2.2.5. Infection of BMDCs. The cells were plated in 6-well dishes, with 1×10^6 cells plated per well. The cells were incubated in a humidified incubator at 37^0C, 5% CO_2 for 0, 6, 12, 24 and 48 h after infection. At each time point, BMDCs were infected with Ad5-CMV-SV40 T-Ag and Ad5-CMV-SV40 T-Ag complexed with CFm40L. The multiplicity of infection that was used for the experiments was 100:1 (ifu:cell). The concentration of the ligand used was 120 ng per 10^8 viral particles.

2.2.6. Western blot Analysis. For this analysis, the cells were infected as described above. The cells were harvested at given time-points and lysates were prepared. Protein concentrations of each sample were determined using the Bradford method, and all lysates were normalized to the lowest concentration of protein. Samples were loaded onto 10% SDS-polyacrylamide gels, separated by electrophoresis, and transferred to nitrocellulose membranes (15 V for 15 min). Membranes were blocked for 1 h with 5% bovine serum albumin in Tris-Cl buffered saline (TBS), followed by two 5 min washes with 1% Tween-20 in TBS (TTBS). The membranes were incubated for 1 h in TTBS containing a primary mouse anti-mouse SV40 T-Ag antibody (BD Pharmingen, clone PAb101), and washed three times for 30 min each with TTBS. Afterwards, the membranes were incubated for 1 h in TTBS containing a horseradish peroxidase-labeled goat anti-mouse IgG antibody (SantaCruz), and washed three times for 30 min each with TTBS. Finally the membranes were developed using the ECL substrate (Amersham), and exposed to x-ray film.

2.2.7. Flow cytometric analysis of Antigen Presenting Cells. The cells were infected as described above. As negative control, the cells were left untreated. After 48 h of incubation, the cells were harvested and stained, and 5×10^5 cells were stained per well for activation markers CD40 (BD Biosciences, clone HM40-3), CD80 (eBioscience, clone 16-10A1) and CD86 (eBioscience, clone GL1). The antibodies were used at 1 µg/ml. Labeled antibody were added to the cells of interest and incubated in the dark for 20 min at 4^0C. Isotype control antibodies were also used to set up compensation. The cells were fixed in 1%

paraformaldehyde for 5 min in the dark, washed twice and resuspended in 200 µl of FACS buffer. The cells were analyzed using a FACScan flow cytometer (Becton Dickinson).

2.2.8. Bio-Plex cytokine assay. The cells were plated and infected as described above. The supernatants were harvested at 24, 48 and 72 h post-infection. The concentrations of IL-1A, IL-1B, IL-2, IL-3, IL-4, IL-6, IL-12 (p40), IL-12 (p70), IL-13, IL-17, TNF-α, KC and MCP-1 were analyzed by the Bio-Plex multiplex mouse cytokine assay kit (Bio-Rad laboratories, Hercules, CA) and the cytokine reagent kit (Bio-Rad) according to the manufacturer's protocol. Briefly, 50 µl of diluted standards or culture supernatant were added to a 96-well plate coated with beads that have antibodies specific for cytokines conjugated to them. Thus, the cytokines present in the supernatant will bind to the antibodies that are coupled to the beads. The reaction was incubated at RT by vortexing at 300 rpm for 30 min. The plate was then washed thrice to remove any unbound protein. A mixture of biotinylated antibodies specific for a different epitope on the cytokines wa then added to the beads. The reaction was incubated again at RT by vortexing at 300 rpm for 30 min After three washes, Streptavidin-phycoerythrin (streptavidin-PE) was added to the reaction containing biotinylated antibodies bound to the cytokines in a sandwich. The reaction was incubated at RT by vortexing at 300 rpm for 10 min After three washes, the data from the reaction was collected and analyzed using the Bio-Plex suspension array system (Bio-Rad, Hercules, CA).

2.3. Results

2.3.1. Generation and primary characterization of CFm40L. Previous studies in the laboratory of our collaborator (A. Pereboev, M.D., Ph.D., University of Alabama at Birmingham) demonstrated that targeting to mouse CD40 enhanced Ad-mediated gene transfer, was accompanied by phenotypic changes characteristic for DCs maturation. This targeting was achieved by utilization of bi-specific chemically conjugated antibodies. The aim of the following experiments was to utilize recombinant adapter protein capable of achieving the same effects. The adapter protein consists of the extracellular portion of the native Ad receptor, CAR, fused to a trimerization motif of a 71 amino acid domain from the bacteriophage T4 fibritin protein, linked to the extracellular domain of the mouse CD40 ligand (CFm40L). The cDNA coding for the recombinant fusion protein was assembled in an expression plasmid and its integrity confirmed by DNA sequencing. Linearized plasmid DNA was then used to establish stable 293 cell lines producing CFm40L as a secreted CFm40L protein. Supernatants from the clones were tested for the presence of CFm40L by a dot-blot assay with anti-CAR antibodies (data not shown). A positive clone, constitutively secreting the product was expanded and the fusion protein was purified by metal affinity chromatography from the culture medium.

2.3.2. Flow cytometric analysis of expression of GFP transgene expression in DCs infected with CD40-targeted Ad5-CMV-GFP. The first aim of this project was to test the infection potential of a CD40-targeted adenoviral vector. In the experiment shown in Fig. 2.1, we determined if the CD40-targeted adenoviral vector could efficiently infect DCs. To do this, we performed a titration experiment in which DCs were infected *in vitro* at a multiplicity of infection (m.o.i.) of 100 infectious units (ifu)/cell using an adenoviral vector (Ad5-CMV-GFP) expressing green fluorescent protein (GFP) complexed with increasing concentrations of the targeting ligand, CFm40L. At 48 h post-infection, the cells were harvested and GFP expression was measured by flow cytometry. Without the CFm40L targeting ligand, a low infectivity representing approximately 7% of the DCs that were GFP-positive when treated with untargeted Ad5-CMV-GFP. When Ad-CMV-GFP was complexed at a ratio of 3 ng CFm40L/1 $\times$ 10^8 ifu virus no increase in infectivity was observed. However, the population DCs infected with Ad5-CMV-GFP increased from 7% to 32%, when Ad-CMV-GFP was complexed with 30 ng CFm40L/1 $\times$ 10^8 ifu virus. This increase was maximal, as a further increase in the ratio up to 600 ng CFm40L/1 $\times$ 10^8 ifu did not result in a further significant increase in the infectivity of DCs. Thus, the optimal CFm40L concentration (lowest amount of CFm40L achieving maximal DC infection) in this experiment was determined to be 30 ng CFm40L/1 $\times$ 10^8 ifu virus at an m.o.i. 100 infectious units (ifu)/cell. These results indicate that Ad vectors complexed with the CFm40L adapter protein become more efficient at infecting mouse DCs. However, there appears to be a population of DCs that remain refractory to Ad infection, despite adding CFm40L adapter protein.

2.3.3. Flow cytometric analysis of expression of GFP transgene in RAW 264.7 cells infected with CD40-targeted Ad5-CMV-GFP. RAW 264.7 is a murine macrophage cell line initially derived from BALB/c mice infected with Abelson leukemia virus, and is extremely sensitive to lipopolysaccharides, (LPS) which are potent inducers of DC maturation. Interestingly, this cell line can be induced to differentiate into DC-like cells by treatment LPS as demonstrated by the expression of surface phenotypic markers associated with dendritic cells. Thus we used RAW 264.7 as another model to test whether CFm40L could augment adenovirus infectivity. As shown in Fig. 2.2, the RAW 264.7 cells showed a low infectivity, representing approximately 4% of cells infected with untargeted Ad5-CMV-GFP at a m.o.i. of 100 ifu/cell. When Ad5-CMV-GFP was complexed at a ratio of 3 ng CFm40L/1 $\times$ 10^8 ifu virus no increase in infectivity was observed. However, the population of RAW 264.7 cells that were GFP-positive, increased from 4% to about 27 % when Ad5-CMV-GFP was complexed with 30 ng of CFm40L/1 $\times$ 10^8 ifu virus. This increase was maximal, as a further increase in the ratio up to 600 ng CFm40L/1 $\times$ 10^8 ifu did not result in a further significant increase in the

infectivity of RAW 264.7. Thus, the optimal CFm40L concentration (lowest amount of CFm40L achieving maximal RAW 264.7 infection) in this experiment was determined to be 30 ng CFm40L/1 $\times$ 10^8 ifu virus at an m.o.i. 100 ifu/cell. These results confirm the finding in RAW 264.7 that vectors complexed with the CFm40L adapter protein become more efficient at infecting cells through the CD40 receptor.

2.3.4. Western blot analysis of SV40 T-Ag transgene expression in DCs infected with CD40-targeted Ad5-CMV-SV40 T-Ag. To further characterize ability of CFm40L to enhance Ad vectors to cells expressing CD40, Western blot analysis was performed. In this experiment, DCs were infected *in vitro* with CD40-targeted and untargeted adenoviral vector expressing the SV40 large T antigen (Ad5-CMV-SV40 T-Ag) at m.o.i. of 100 ifu/cell. The SV40 T-Ag was chosen as the model tumor antigen since it is highly immunogenic, inducing both antibody and cytotoxic T lymphocyte (CTL) responses. In this experiment, DCs were infected with untargeted Ad5-CMV-SV40 T-Ag and Ad5-CMV-SV40 T-Ag complexed with 150 ng CFm40L/1 $\times$ 10^8 ifu virus. Uninfected DCs were used as a negative control. At 48 h after infection the cells were harvested and expression of SV40 T-Ag was measured. As shown in Fig. 2.3 A, DCs infected with untargeted Ad5-CMV-SV40 T-Ag (lane 2) demonstrated a weak signal at 53 kDa, indicative of low infection efficiency. However, DCs infected with CD40-targeted Ad5-CMV-SV40 T-Ag (lane 3) showed greater expression of SV40 T-Ag compared with DCs infected with untargeted Ad5-CMV-SV40 T-Ag. These results confirm that Ad vectors complexed with the CFm40L adapter protein were more efficient at infecting mouse DC than untargeted Ad vectors.

A second experiment was also performed to analyze the time-course of transgene expression in DCs infected with a CD40-targeted adenoviral vector. As shown in Fig. 2.3. B, DCs were infected *in vitro* with Ad5-CMV-SV40 T-Ag complexed with 150 ng CFm40L/1 $\times$ 10^8 ifu virus at an m.o.i. of 100 ifu/cell. Infected cells were harvested at 0, 6, 12, 24 and 48 h post-infection and expression of SV40 T-Ag was measured by Western blot analysis. In this experiment, the expression of SV40 T-Ag was first detected at 24 h post-infection but was maximal at 48 h post-infection. This observation is consistent with the time course of transgene expression in Ad infected cells previously characterized in our lab.

2.3.5. Western blot analysis of SV40 T-Ag transgene expression in RAW 264.7 cells infected with CD40-targeted Ad5-CMV-SV40 T-Ag. As a second model to analyze adenovirus infection, RAW 264.7 cells were also tested for the expression of the SV40 T-Ag transgene by Western blot analysis, after infection with CD40-targeted vector. RAW 264.7 cells were infected *in vitro* with CD40-targeted and untargeted Ad5-CMV-SV40 T-Ag, at an m.o.i. of 100 ifu/cell. Uninfected RAW 264.7 cells were used as a negative control. At 48 h after infection the cells were harvested and expression of SV40 T-Ag was measured. As shown in Fig. 2.4 A, RAW 264.7 cells infected with untargeted Ad5-CMV-SV40 T-Ag (lane 2) demonstrated a weak signal at 53 kDa, indicative of low infection efficiency. However, RAW 264.7 cells infected with CD40-targeted Ad5-CMV-SV40 T-Ag (lane 3) showed greater expression of SV40 T-Ag compared with RAW 264.7 cells infected with untargeted Ad5-CMV-SV40 T-Ag. These results confirm that Ad vectors complexed with the CFm40L adapter protein were more efficient at infecting RAW 264.7 cells than untargeted Ad vectors.

A second experiment was also performed to analyze the time-course of transgene expression in RAW 264.7 infected with a CD40-targeted adenoviral vector. As shown in Fig. 2.4. B, RAW 264.7 were infected *in vitro* with Ad5-CMV-SV40 T-Ag complexed with 150 ng CFm40L/1 $\times$ 10^8 ifu virus at an m.o.i. of 100 ifu/cell. Infected cells were harvested at 0, 6, 12, 24 and 48 h post-infection and expression of SV40 T-Ag was measured by Western blot analysis. In this experiment, the expression of SV40 T-Ag was first detected at 24 h post-infection but was maximal at 48 h post-infection. This observation is consistent with the time course of transgene expression in Ad infected DC cells shown above.

2.3.6. Flow cytometric analysis of maturation markers in DCs infected with CD40-targeted Ad5-CMV-SV40 T-Ag. The phenotypic maturation of human and murine DCs has previously been described as an effect of Ad infection targeted to CD40. To evaluate DC activation upon CD40-targeted Ad infection using the CFm40L adapter molecule, we infected DCs *in vitro* with untargeted as well as CD40-targeted Ad and then subjected them to phenotype analysis by flow cytometry. The maturation status of the DCs was determined by measuring the expression of the cell surface markers CD40, CD80 and CD86. In this experiment, DCs were infected *in vitro* with Ad5-CMV-SV40 T-Ag complexed with 120 ng CFm40L/1 $\times$ 10^8 ifu virus at an m.o.i. of 100 ifu/cell. Likewise, DCs were infected with untargeted Ad5-CMV-SV40 T-Ag at an m.o.i. of 100 ifu/cell. Uninfected DCs were used as controls. After 48 h post-infection, the cells were harvested and the cell surface expression of CD40, CD80 and CD86 was measured. As shown in Fig. 2.5, DCs infected with CD40-targeted Ad5-CMV-SV40 T-Ag showed an increased expression of maturation markers compared with DCs infected with untargeted Ad5-CMV-SV40 T-Ag or to uninfected DCs. Approximately 66% of the uninfected DCs were CD40-positive. The expression of CD40 increased to 71% in DCs infected with untargeted Ad5-CMV-SV40 T-Ag and to 79% in DCs infected with CD40-targeted Ad5-CMV-SV40 T-Ag. Only 13% of the uninfected DCs were CD80-positive. The expression of CD80 remained at 15% in DCs infected with untargeted Ad5-CMV-SV40 T-Ag and 13% in the DCs infected with CD40-targeted Ad5-CMV-SV40 T-Ag. Finally, 8% of uninfected DCs were

CD86-positive. The level of CD86-positive cells in DCs infected with untargeted Ad5-CMV-SV40 T-Ag was similar at 9%. The expression of CD86, however, increased to 13% in DCs infected with the CD40-targeted Ad5-CMV-SV40 T-Ag. Thus, compared to the uninfected cells, DCs infected with CD40-targeted Ad5-CMV-SV40 T-Ag exhibited signs of maturation, as demonstrated by elevated levels of the CD40 and CD86 maturation markers.

2.3.7. Flow cytometric analysis of maturation markers in RAW 264.7 cells infected with CD40-targeted Ad5-CMV-SV40 T-Ag. As a second model to analyze phenotypic maturation, RAW 264.7 cells were also tested for levels of the CD40, CD80, CD86 maturation markers, after infection with CD40-targeted vector. In the experiment shown in Fig. 2.6, RAW 264.7 cells also showed increase in the expression of the maturation marker CD40 when infected with the CD40-targeted Ad5-CMV-SV40 T-Ag compared with the untargeted Ad5-CMV-SV40 T-Ag. Between 9 and 10% of the uninfected RAW 264.7 cells and RAW 264.7 cells infected with untargeted Ad5-CMV-SV40 T-Ag showed expression of CD40. However, the percentage of RAW 264.7 cells expressing CD40 increased to about 39% when infected with CD40-targeted Ad5-CMV-SV40 T-Ag. Thus, compared with the untreated cells, RAW 264.7 cells infected with CD40-targeted Ad5-CMV-SV40 T-Ag demonstrated a similar elevation in the levels of the CD40 maturation marker as DCs. Interestingly, however, the CD80 and CD86 maturation markers maintained low levels of expression, despite infection with CD40-targeted Ad5-CMV-SV40 T-Ag.

2.3.8. Bio-Plex analysis of cytokines and chemokines secreted by dendritic cells infected with CD40-targeted Ad5-CMV-SV40 T-Ag. The activated, mature antigen presenting cells are known to produce and secrete inflammatory cytokines and chemokines. The type of the cytokines secreted will determine the nature of the immune response induced. Th-1 type cytokines (*e.g.,* IL-12) will induce a Th-1 type cell mediated immune response. Th-2 type cytokines (*e.g.,* IL-4) will induce a Th-2 type humoral immune response. To study the nature of the cytokines secreted by DCs upon infection by CD40-targeted adenovirus, a bipolar multiplex assay was performed to assess the levels of 23 different cytokines and chemokines. In this study, DCs were infected *in vitro* with Ad5-CMV-SV40 T-Ag complexed with 120 ng CFm40L/1 $\times$ 10^8 ifu virus at an m.o.i. of 100 ifu/cell. Likewise, DCs were infected with untargeted Ad5-CMV-SV40 T-Ag at an m.o.i. of 100 ifu/cell. Uninfected DCs were used as controls. At 48 h post-infection, the cell culture supernatants were harvested and analyzed.

As shown in Fig. 2.6, DCs infected with CD40-targeted Ad5-CMV-SV40 T-Ag demonstrated increased secretion of several inflammatory cytokines and chemokines, compared with DCs infected with untargeted Ad5-CMV-SV40 T-Ag or with uninfected DCs. DCs infected with untargeted Ad5-CMV-SV40 T-Ag also showed increased secretion of inflammatory cytokines and chemokine, but the increase was generally lower than DCs infected by CD40-targeted Ad5-CMV-SV40 T-Ag. The pattern of cytokines and chemokines whose secretion was up regulated was mixed, and included the Th-1 type cytokines, IL-1α, IL-1β, IL-3, IL-12 (p40), IL-12 (p70), IL-17 and TNF-α, as well as the Th-2 type cytokines, IL-4, IL-6, IL-13 and G-CSF, and chemokines such as MCP-1 and KC were also up regulated. The secretion of IL-3, IL-4, TNF-α, and MCP-1 were found to be maximal at 24 h post-infection infection with CD40-targeted Ad5-CMV-SV40 T-Ag. IL-1α, IL-1β, IL-13 and IL-17 were maximally secreted at 48 h post-infection, and IL-6, IL-12 (p40), IL-12 (p70) and KC were maximally secreted by the DCs at 72 h post-infection. Thus, DCs infected with CD40-targeted Ad5-CMV-SV40 T-Ag show increased expression of a wide range of cytokines and chemokines. Generally, we observed a mixed Th-1/Th-2-profile response.

2.3.9. Bio-Plex analysis of cytokines and chemokines secreted by RAW 264.7 cells infected with CD40-targeted Ad5-CMV-SV40 T-Ag. RAW 264.7 cells were again studied as another model of APCs for secretion of inflammatory cytokines and chemokines. The infection of RAW 264.7 cells was carried out like the infection of DCs at an m.o.i. of 100 viral particles/cell complexed with 120 ng of CFm40L. The CD40-targeted RAW 264.7 cells, as shown in Fig. 2.7, also demonstrated increased secretion of several inflammatory cytokines and chemokines compared with cells infected by untargeted Ad5-CMV-SV40 T-Ag or with uninfected RAW 264.7 cells. Similar to DCs, RAW 264.7 cells also showed increased secretion of the cytokines and chemokines when infected by untargeted Ad5-CMV-SV40 T-Ag. However, the increase was lower than that obtained by infection with CD40-targeted Ad5-CMV-SV40 T-Ag. The Th-1 cytokines whose secretion was increased, included IL-1A, IL-1B, IL-2, IL-3, IL-12 (p40), IL-12 (p70), IL-17, TNF-α, IFN-gamma and GM-CSF. The Th-2 cytokines whose secretion was increased, included IL-5, IL-6, IL-10 and G-CSF. The secretion of the chemokine KC was also up regulated. Most of the cytokines were maximally secreted by RAW 264.7 cells at 72 h post-infection. However, GM-CSF and IL-5 were maximally secreted at 48 h and IL-10 was maximally secreted at 24 h post-infection. These results using CD40-targeted RAW 264.7 cells, in contrast to DCs, show an increased secretion of primarily Th-1 cytokines and therefore exhibit mainly a Th-1 type cytokine response.

2.4. Discussion

The CD40-targeted adenovirus can infect DCs and macrophages more efficiently than untargeted adenovirus as shown by the result in Figs. 2.1, 2.2, 2.3 and 2.4. The titration experiment in which the DCs and RAW 264.7 cells were infected with Ad5-CMV-GFP in the presence of increasing concentrations of the CFm40L, helped to determine the ratio of virus and CFm40L to be used as a standard ratio for efficient

infection of the antigen presenting cells. The virus: CFm40L ratio of 10^8 ifu of virus: 30 ng of CFm40L infects approximately 28 - 32% of the DCs as well as RAW 264.7 cells. After this, any further increase in the amount of CFm40L used, did not cause any significant increase in the infection of DCs. To ensure the maximum infection of DCs, but prevent maturation induced cell-death because of over-stimulation, the ratio of 10^8 ifu of virus: 120 ng of CFm40L was chosen as the preferred ratio for infection of DCs and RAW 264.7 cells *in vitro* and for the *in vivo* immunization of animals. The results in Figs. 2.1 and 2.2 also show that even at maximum infectivity, only 28 - 32% of the cells were infected by CD40-targeted adenovirus. Thus, a large percentage of the DCs remain refractory to infection by CD40-targeted Ad5-CMV-SV40 T-Ag. One of the possibilities could have been that not a large percentage of bone marrow derived DCs and RAW 264.7 cells express CD40. While this may be true for RAW 264.7 cells, where approximately only 10% of the uninfected cells express CD40 (Fig. 2.6), but it is not true for bone marrow derived DCs cultured *in vitro*, where about 70% of the uninfected DCs express CD40 (Fig. 2.5). Even though approximately 70% of the DCs express CD40, only 28 - 32% were infected by CD40-targeted adenoviral vector, *i.e.,* about half of them remain uninfected. There can be many possibilities that would explain why this would happen, such as lowered uptake of foreign antigen (virus) by DCs because of maturation, or apoptosis of infected DCs on activation.

Nonetheless, the low efficiency of infection of DCs by CD40-targeted adenovirus is not an obstacle in the use of the virus for efficient immunization as few infected DCs are required to activate the antigen-specific lymphocytes. Even a few infected and mature DCs can activate a great number of antigen-specific lymphocytes and generate an effective immune response against the antigen [104]. Given that only 28 - 32% of DCs and RAW 264.7 cells were infected by CD40-targted adenovirus, the CD40-targeted adenovirus is still more efficient than the untargeted wild-type adenovirus at infecting both DCs and RAW 264.7 cells, as shown in Figs.2.3 and 2.4. The DCs and RAW 264.7 cells infected by CD40-targeted Ad5-CMV-SV40 T-Ag were more mature than the cells infected by untargeted Ad5-CMV-SV40 T-Ag as shown by the increased expression of maturation markers on their cell surface (Figs. 2.5 and 2.6). However, the DCs and RAW 264.7 cells show a difference in the type maturation markers, whose expression was increased on infection with CD40-targeted adenovirus. The DCs infected by CD40-targeted Ad5-CMV-SV40 T-Ag show increased expression of CD40 and CD86 compared to uninfected DCs and DCs infected by untargeted Ad5-CMV-SV40 T-Ag. While the RAW 264.7 cells infected by CD40-targeted Ad5-CMV-SV40 T-Ag showed increased expression of only CD40 and not that of CD80 and 86 compared to uninfected RAW 264.7 cells and RAW 264.7 cells infected by untargeted Ad5-CMV-SV40 T-Ag. This differential expression of maturation markers by DCs and cells of the macrophage cell line RAW 264.7 on infection by CD40-targeted Ad5-CMV-SV40 T-Ag may be indicative of a potential difference in the immune responses induced by DCs and RAW 264.7 cells against SV40 T-Ag.

The DCs and RAW 264.7 cells infected by CD40-targeted Ad5-CMV-SV40 T-Ag also showed enhanced secretion of inflammatory cytokines and chemokines than uninfected cells and cells infected by untargeted Ad5-CMV-SV40 T-Ag (Figs. 2.7 and 2.8). The DCs showed increased secretion of several cytokines of both, Th-1 as well as Th-2 type, such as IL-12 and IL-4. While the RAW 264.7 cells showed increased secretion of mainly Th-1 type cytokines such as IL-12 and TNF-α. Thus, on infection by CD40-targeted Ad5-CMV-SV40 T-Ag, DCs showed a mixed Th-1/Th-2 type cytokine response, while RAW 264.7 cells showed mainly a Th-1 type cytokine response. Another intriguing difference in the cytokine secretion by the two cell types lay in the IL-12 p40/70 ratio. IL-12 is a Th-1 type inflammatory cytokine that is made up of two subunits, IL-12 (p40) and IL-12 (p70). The DCs infected by CD40-targeted Ad5-CMV-SV40 T-Ag showed a higher IL-12 p40/p70 ratio, while the RAW 264.7 cells showed a lower IL-12 p40/p70 ratio. A higher IL-12 p40/p70 ratio has been associated with Th-2 type response, while a lower IL-12 p40/p70 with a Th-1 type response [108]. These differences in the profiles of cytokines secreted by DCs and cells of the macrophage cell line RAW 264.7 were again suggestive of potential difference in the nature of immune response induced by both cell types.

Thus, CD40-targeted adenovirus can efficiently infect DCs and RAW 264.7 cells. The DCs and RAW 264.7 cells infected by the CD40-targeted adenovirus show increased phenotypic maturation and enhanced secretion of inflammatory cytokines and chemokines compared with cells infected by untargeted adenovirus and uninfected cells.

3. Signal transduction pathways in CD40 ligand-induced dendritic cell activation

3.1. Introduction

The DCs infected by CD40-targeted Ad5-CMV-SV40 T-Ag show increased maturation and elevated secretion of inflammatory cytokines and chemokines compared with DCs infected by untargeted Ad5-CMV-SV40 T-Ag and uninfected DCs. Thus, the CD40-targeted Ad5-CMV-SV40 T-Ag must induce changes in the cell signaling pathways in the DCs to cause increased activation of the DCs. The study of the changes in cell

signaling would help to identify the specific pathways that are responsible for the maturation and activation of the DCs that occur upon infection with CD40-targeted adenovirus. The identification of the specific pathways that are activated in the DCs could be used to generate DCs with enhanced activation potential by *ex vivo* manipulation of the involved signaling pathways.

The interaction of a vector with cell surface receptors results in the initiation of multiple cascades of signal transduction pathways in the target cells. Many viruses as well as vectors bind to cell surface receptors, the cross-linking of which leads induction of NF-KappaB, ATF-2/c-Jun, interferon regulatory factors (IRFs), and MAP kinases (p38, ERK, JNK) [109]. These pathways finally activate a number of immunoregulatory genes in the nucleus, which includes IFNα/β, IFN-γ, IL-6 and IL-12 and the chemokines MIP-2, RANTES and IP-10 [109]. The different cell surface components of the vector are responsible for the activation of the different cell signaling pathways. Thus, the cell surface molecules play an important role in determining the pathways that will be activated and consequently the genes that will be regulated. The DC-targeted adenovirus that we have used is the adenovirus vector that is coated by the CFm40L bi-specific adaptor molecule. Coating the adenoviral vector with the adapter molecule would lead to masking of the native cell surface structures and display of new molecules on the surface. Thus, we expect that the binding of DC-targeted adenoviral vector with a target cell would induce cell signaling pathways in the cell that are different from that induced by untargeted adenoviral vector and hence as a result, lead to regulation of different immunoregulatory genes.

The changes in the signal transduction pathways in DCs infected by CD40-targeted Ad5-CMV-SV40 T-Ag were studied by analyzing the phosphorylation status of several protein kinases, transcription factors and expression of other cell signaling proteins, and comparing them with those in DCs infected by untargeted Ad5-CMV-SV40 T-Ag and uninfected DCs. The phosphorylation status and expression of 36 different signal transduction proteins in the DCs was studied using multi-antibody immunoblot analysis (Kinexus Bioinformatics, Vancouver, CA). In addition, the time-course of the phosphorylation of some of the cell signaling proteins was studied using Western blot analysis to determine the time at which the changes in the cell signaling proteins start to occur after infection.

3.2 . Materials and Methods

3.2.1. Isolation and culture of mouse Bone Marrow Derived Dendritic Cells (BMDCs). Bone marrow cells were isolated from the fibulas and femurs of 6-8 week old B6C3F1 mice. The cells were then cultured in complete media (RPMI-1640 containing 10% fetal bovine serum, 2 mM L-glutamine, 1% non-essential amino acids, 100 U/ml penicillin, 100 µg/ml streptomycin, 10 ng/ml GM-CSF and 10 ng/ml IL-4 for 5 days. On day 5, the BMDCs were harvested using versene and used for further experiments [103].

Analysis of phosphorylation of 36 cell signaling proteins in DCs infected by CD40-targeted adenovirus at 24 h after infection, by immunoblot analysis.

3.2.2. Infection of BMDCs. The cells were plated in 6-well dishes, with 1×10^6 cells plated per well. The cells were incubated in a humidified incubator at 37^0C, 5% CO_2 for 24 h after infection. The BMDCs were infected with Ad5-CMV-SV40 T-Ag and Ad5-CMV-SV40 T-Ag complexed with CFm40L. The multiplicity of infection that was used for the experiments was 100:1 (ifu:cell). The concentration of the ligand used was 120 ng per 10^8 viral particles. At the end of 24 h after infection, the cells were harvested and cell lysates were made.

3.2.3. Immunoblot analysis. For this analysis, the cells were infected as described above. The cells were harvested at the given time-point and lysates were prepared. Protein concentrations of each sample were determined using the Bradford method, and all lysates were normalized to 1 µg/µl. The phosphorylation status and expression of 36 different cell signaling proteins in the cell lysates of the infected DCs was determined by the Kinexus Bioinformatics company using the immunoblot analysis.

Time course analysis of induction of phosphorylation of cell signaling proteins in DCs infected by CD40-targeted adenovirus by Western blot.

3.2.4. Infection of BMDCs. The cells were plated in 6-well dishes, with 1×10^6 cells plated per well. The cells were incubated in a humidified incubator at 37^0C, 5% CO_2 for 0, 6, 12, 24 and 48 h after infection. At each time point, BMDCs were infected with Ad5-CMV-SV40 T-Ag complexed with CFm40L. The multiplicity of infection that was used for the experiments was 100:1 (ifu:cell). The concentration of the ligand used was 120 ng per 10^8 viral particles. At the above time-points, the cells were harvested and cell lysates were made.

3.2.5. Western blot Analysis. For this analysis, the cells were infected as described above. The cells were harvested at given time-points and lysates were prepared. Protein concentrations of each sample were determined using the Bradford method, and all lysates were normalized to the lowest concentration of protein. Samples were loaded onto 10% SDS-polyacrylamide gels, separated by electrophoresis, and transferred to nitrocellulose membranes (15 V for 15 min). Membranes were blocked for 1 h with 5% bovine

serum albumin in Tris-Cl buffered saline (TBS), followed by two 5 min washes with 1% Tween-20 in TBS (TTBS). The membranes were incubated for 1 h in TTBS containing the primary antibody. The primary antibodies used were polyclonal rabbit anti-mouse phospho-p38 MAP kinase [Thr 180/Tyr 182] (Cell Signaling, catalog # 9211), p38 MAP kinase (Cell Signaling, catalog # 9212), phospho-ERK1/ERK2 [Thr202/Tyr204] (Cell Signaling, catalog # 9101) , ERK1/ERK2 (Cell Signaling catalog # 9102), Phospho-STAT1 [Tyr 70] (Cell Signaling catalog # 9171), STAT1 (Cell Signaling catalog # 9172), phospho-AKT [Thr 308] (Cell signaling catalog # 9275) and AKT (Cell Signaling Catalog # 9272). After 1 h, the blots were washed three times for 30 min each with TTBS. Afterwards, the membranes were incubated for 1 h in TTBS containing a horseradish peroxidase-labeled goat anti-rabbit IgG antibody (Santa Cruz Biotechnology), and washed three times for 30 min each with TTBS. Finally the membranes were developed using the ECL substrate (Amersham), and exposed to x-ray film.

Analysis of phosphorylation of 36 cell signaling proteins in DCs infected by CD40-targeted adenovirus at 1 h after infection, by immunoblot analysis.

3.2.6. Infection of BMDCs. The cells were plated in 6-well dishes, with 1×10^6 cells plated per well. The cells were incubated in a humidified incubator at 37^0C, 5% CO_2 for 1 h after infection. The BMDCs were infected with Ad5-CMV-SV40 T-Ag and Ad5-CMV-SV40 T-Ag complexed with CFm40L. The multiplicity of infection that was used for the experiments was 100:1 (ifu:cell). The concentration of the ligand used was 120 ng per 10^8 viral particles. At the end of 1 h after infection, the cells were harvested and cell lysates were made.

3.2.7. Immunoblot analysis. For this analysis, the cells were infected as described above. The cells were harvested at the given time-point and lysates were prepared. Protein concentrations of each sample were determined using the Bradford method, and all lysates were normalized to 1 µg/µl. The phosphorylation status of 36 different cell signaling proteins in the cell lysates of the infected DCs was determined by the Kinexus Bioinformatics company using the immunoblot analysis.

3.3. Results

3.3.1. Semi-quantitative analysis of expression and phosphorylation of cell signaling proteins in DCs infected with Ad5-CMV-SV40 T-Ag at 24 h post-infection. DCs infected by CD40-targeted Ad5-CMV-SV40 T-Ag show increased expression of maturation markers on their cell surface and elevated secretion of inflammatory cytokines and chemokines into the supernatant. To explore the changes in signal transduction that were responsible for the increase in expression of maturation markers and secretion of inflammatory cytokines and chemokines, the infected DCs were analyzed for the expression and phosphorylation of several protein kinases and other cell signaling proteins. In this study, DCs were infected *in vitro* with Ad5-CMV-SV40 T-Ag complexed with 120 ng CFm40L/1×10^8 ifu virus at an m.o.i. of 100 ifu/cell. Likewise, DCs were infected with untargeted Ad5-CMV-SV40 T-Ag at an m.o.i. of 100 ifu/cell. Uninfected DCs were used as controls. At 24 h post-infection, the cells were harvested and cell lysates were made. The cell lysates were analyzed for the expression as well as phosphorylation of 36 different cell signaling proteins using a signal transduction protein profiling system (Kinexus, Vancouver, CA).

This system provided both qualitative and semi-quantitative analysis of the expression and phosphorylation states of protein kinases and cell signaling proteins in a multi-antibody immunoblot of cell samples. We chose to analyze alterations in a total of 36 different cell signaling proteins that potentially play a role in cytokine expression. Fig. 3.1 represents the immunoblot that features the first of 18 target signaling proteins in uninfected DCs, DCs infected with untargeted Ad5-CMV-SV40 T-Ag and DCs infected with CD40-targeted Ad5-CMV-SV40 T-Ag. The multi-antibody immunoblot analysis was specifically optimized to detect band shifts in signaling proteins on SDS-PAGE gels that may arise from their phosphorylation. The semi-quantitative analysis of the strength of the enhanced chemiluminescence signal of each target protein was determined by densitometric analysis (Fig. 3.2). Fig. 3.3 shows a chart of the same semi-quantitative analysis. As shown in Figs. 3.1, 3.2 and 3.3 there were changes, up-regulation as well as down-regulation, in the phosphorylation states of several protein kinases and expression of other cell signaling proteins. Fig. 3.4 represents the multi-antibody immunoblot that features a second set of 18 target signaling proteins signaling proteins in uninfected DCs, DCs infected with untargeted Ad5-CMV-SV40 T-Ag and DCs infected with CD40-targeted Ad5-CMV-SV40 T-Ag. Fig. 3.5 shows a chart that provides the semi-quantitative analysis of the phosphorylation status of each of the target proteins. Fig. 3.6 shows a chart of the same semi-quantitative analysis. The protein kinases, whose phosphorylation increased significantly in DCs infected with CD40-targeted Ad5-CMV-SV40 T-Ag compared with uninfected DCs at 24 h post-infection were: Erk1 [Thr 202 + Tyr 204], Erk2 [Thr 185 + Tyr 187], PKBα (Akt1) [Thr 308], STAT 1 [Tyr 701], B23 [Ser 4], MEK4 [Ser 257 + Thr 261], MEK1 [Ser 297], MEK1 [Thr 291], MEK [Thr 385], MAPKAPK2 [Thr 222] and Smad 1/5/9. The proteins whose expression increased markedly at 24 h post-infection were: Fas-L and Fas. The kinases, whose phosphorylation decreased significantly included: JNK [Thr 183 + Tyr 185], JUN

[Ser 73], p38 MAPK [Thr 180 + Thr 182], PKCα/β2 [Thr 538/Thr 641], STAT 3 [Ser 727], STAT 5 [Tyr 694], GSK3α [Ser 21], GSK3β [Ser 9], GSK3β [Tyr 216], MEK6 [Ser 207], MEK2 [Thr 394], Src [Tyr 418] and Src [Tyr 529]. Thus, a number of the target protein kinases showed changes, increase as well as decrease, in their phosphorylation states.

3.3.2. Western blot analysis of time-course of phosphorylation of cell signaling proteins in DCs infected with CD40-targeted Ad5-CMV-SV40 T-Ag. The immunoblot analysis of DCs infected with CD40-targeted Ad5-CMV-SV40 T-Ag, showed changes in the phosphorylation status and expression of several cell signaling proteins, compared with the DCs infected with untargeted Ad5-CMV-SV40 T-Ag and the uninfected DCs at 24 h post-infection. To confirm the multi-antibody immunoblot results and to determine the time frame of changes in phosphorylation and expression of the cell signaling proteins after infection, DCs were infected *in vitro* with Ad5-CMV-SV40 T-Ag complexed with 120 ng CFm40L/1 $\times$ 10^8 ifu virus at an m.o.i. of 100 ifu/cell. At 0, 1, 3, 6, 12, 24 and 48 h after infection, the cells were harvested, lysed and analyzed for changes in the phosphorylation states of several cell signaling proteins by Western blot. As shown in Fig. 3.7, phosphorylation of the p38 MAP kinase occurred within 1 h after infection with the CD40-targeted Ad5-CMV-SV40 T-Ag and the phosphorylation was maintained through 48 h post-infection. While there was significant increase in the phosphorylation of p38 within 1 h after infection, the levels of total p38 remained approximately the same. Likewise, the phoshporylation of **E**xtracellular **r**egulated protein-serine **k**inase 1(ERK1) and **E**xtracellular **r**egulated protein-serine **k**inase (ERK2), as shown in Fig. 3.8 markedly increased within 1 h and was sustained through 12 h after infection. **S**ignal **T**ransducer and **A**ctivator of **T**ranscription **1** (STAT1) is a transcription factor whose activity is regulated by both the p38 MAP kinase and ERK 1/2. The time-course studies, Fig. 3.9, showed that the phosphorylation of STAT1 was also induced between 1 and 3 h after infection. Protein-serine kinase B alpha (AKT 1) is an anti-apoptotic cell signaling protein., which inactivates several pro-apoptotic targets and increases cell survival. The phosphorylation of AKT1 in DCs infected by CD40-targeted Ad5-CMV-SV40 T-Ag, as shown in Fig. 3.10, was induced within 1 h after infection. However, the expression of AKT 1 was transient and was lost by 3 h post-infection. Thus, the changes in the phosphorylation status of the cell signaling proteins in DCs infected by CD40-targeted Ad5-CMV-SV40 T-Ag is complex, and start to occur early in time after the infection.

3.3.3. Semi-quantitative analysis of expression and phosphorylation of cell signaling proteins in DCs infected with Ad5-CMV-SV40 T-Ag at 1 h post-infection: As shown in Figs. 3.7-3.10, the changes in the cell signaling in DCs after infection with CD40-targeted Ad5 SV40T-Ag starts to occurred within 1 h. Thus, to study the changes in expression and phosphorylation status of several MAP kinases and cell signaling proteins, the DCs were infected *in vitro* with Ad5-CMV-SV40 T-Ag complexed with 120 ng CFm40L/1 $\times$ 10^8 ifu virus at an m.o.i. of 100 ifu/cell. Likewise, DCs were infected with untargeted Ad5-CMV-SV40 T-Ag at an m.o.i. of 100 ifu/cell. The DCs were also treated with just 120 ng of CFm40L. Uninfected DCs were used as controls. At 1 h post-infection, the cells were harvested and lysates were made. The cell lysates were analyzed for the changes in phosphorylation and expression of several cell signaling proteins by densitometry using the multi-antibody immunoblot analysis. Fig. 3.11 represents the immunoblot featuring the first 18 target signaling proteins in uninfected DCs, DCs treated with CFm40L, DCs infected with untargeted Ad5-CMV-SV40 T-Ag and DCs infected with CD40-targeted Ad5-CMV-SV40 T-Ag. Fig. 3.12 shows a chart that provides the semi-quantitative analysis of the phosphorylation status of each of the target protein. Fig. 3.13 shows a chart of the same semi-quantitative analysis. Fig. 3.14 represents the multi-antibody immunoblot featuring the second set of 18 target signaling proteins in uninfected DCs, DCs treated with CFm40L, DCs infected with untargeted Ad5-CMV-SV40 T-Ag and DCs infected with CD40-targeted Ad5-CMV-SV40 T-Ag. Fig. 3.15 is a chart that provides the semi-quantitative analysis of the phosphorylation status of each of the target protein. Fig. 3.16 shows a chart of the same semi-quantitative analysis.

Again, several of the target protein kinases showed changes, increase as well as decrease, in their phosphorylation states and expression at 1 h post-infection. The protein kinases, whose phosphorylation increased in DCs infected with CD40-targeted Ad5-CMV-SV40 T-Ag compared with uninfected DCs at 1 h post-infection were: ERK1 [Thr 202 + Tyr 204], ERK2 [Thr 185 + Tyr 187], p38 MAPK [Thr 180 + Tyr 182], GSK3β [Tyr 216], MEK6 [Ser 257+Thr 251], MEK1 [Ser 207], MEK1 [Ser 291], MEK 1/2 [Thr 385], MAPKAPK2 [Thr 394] and Src [Tyr 418]. The protein whose expression increased markedly at 1 h after infection was Fas-L. The protein kinases, whose phophorylation went down significantly in DCs at 1 h post-infection were: JKKα [Ser 180], JNK [Thr 183/Tyr 185], Jun [Thr 183 + Tyr 185], PKBα (AKT 1) [Ser 473], PKCα/β2 [Thr 638/Thr 641], STAT2 [Ser 690], FAS, FOS [Thr 232], GSK3β [Ser 9], NF kappa B [Thr 334], and Smad 1/5/9. These results confirmed that the changes in cell signaling in DCs after infection with either untargeted or CD40-targeted adenovirus start to occur early in time after the infection.

3.4. Discussion

The Western blot analysis of BMDCs infected with CD40-targeted Ad5-CMV-SV40 T-Ag, done by the company Kinexus, showed changes in the phosphorylation and expression of several cell signaling proteins, compared with the BMDCs infected with untargeted Ad5-CMV-SV40 T-Ag and the uninfected DCs. Of the three main types of MAP kinases (ERK 1/2, p38 MAPK and SAPK/JNK), phosphorylation of ERK1/2 and p38 MAPK was found to occur in DCs

infected with CD40-targeted Ad5-CMV-SV40 T-Ag. STAT1 is a transcription factor whose activity is controlled by both, ERK1/2 as well as p38MAPK. Phosphorylation of STAT 1 was also found to occur in the BMDCs infected with CD40 targeted Ad5-CMV-SV40 T-Ag. The analysis of time-course of phosphorylation of ERK 1/2, p38 MAPK and STAT1 revealed that phosphorylation of ERK1/2 and p38 occurred within 1 h post-infection and phosphorylation of STAT1 occurred between 1 and 3 h after infection. The phosphorylation of AKT1, which is an anti-apoptotic protein, also occurs within 1 h of infection using CD40-targeted Ad5-CMV-SV40 T-Ag. Thus, several changes in the signal transduction pathways occur in DCs on infection with CD40-targeted Ad5-CMV-SV40 T-Ag, and these changes start to occur early in time, starting within 1 h after infection.

The changes in the signal transduction pathways probably lead to the activation of DCs, which is marked by elevated expression of maturation markers such as CD40, CD80 and CD86 on the DC cell surface and increased secretion of inflammatory cytokines and chemokines by DCs. As part of future studies, it would be interesting to correlate the cell signaling pathways with the expression of phenotypic maturation markers and secretion of the inflammatory cytokines and chemokines. Inhibitors of protein kinases can be used to block the different protein kinase pathways in the DCs and the changes in the secretion of inflammatory cytokines and expression of activation markers on cell surface can be determined. The results will help to identify the cell signaling proteins and pathways that are responsible for the increased expression of co-stimulatory maturation markers and enhanced secretion of cytokines and chemokines.

4. In situ administration of a CD40 targeted Ad5-CMV-SV40 T-Ag

4.1. Introduction

The *in vitro* results showed that dendritic cells could be efficiently infected by CD40-targeted adenovirus. Infection by CD40-targeted adenovirus induced DC maturation as well as secretion of inflammatory cytokines and chemokines by DCs. The next goal was to determine the potency of the CD40-targeted adenoviral vaccine *in vivo*, *i.e.,* to determine if CD40-targeted adenovirus expressing the tumor antigen can infect dendritic cells *in vivo* and induce a tumor antigen-specific immune response. The gold standard for determining the efficacy of an anti-tumor vaccine in animal models is the disease free or increased survival of animals on challenge with tumor cells and/ or improved survival of tumor bearing animals. However, before moving to the survival studies, it is important to measure the immune response generated in the animals upon vaccination, because even though the immune response may have been effectively induced, the tumor cells may adopt mechanisms to evade detection and killing by the activated immune effector cells, thereby making it difficult to cause an improvement in the survival of the immunized animals [110]. The induced immune response can be quantified or monitored by several methods [111].

The lytic activity of activated CD8 positive T-cells can be measured by the cytotoxicity assays. *In vivo*, it is the killing activity of the CD8 positive Cytotoxic T-cells that leads to the clearance of the tumor and survival of the animal. Thus, to measure the lytic activity of the CTLs is a relevant assay to measure the anti-tumor immune response. The *in vitro* CTL assay involves mixing of the splenocytes or purified CD8 positive T-cells from the immunized animals and the target tumor cells that have been labeled with chromium (^{51}Cr) *in vitro*. This assay requires the stimulation and expansion of the T-cells *in vitro*. In addition, the target cells are killed by the CTLs *in vitro* [112]. However, the *in vivo* cytotoxicity assay measures the lysis of the target cells that are killed by the CTLs *in vivo [113]*.

Both, the *in vitro* and the *in vivo* CTL assays were used to measure the cytolytic activity of the CTLs, induced by the CD40-targeted adenoviral vaccine expressing the target tumor antigen in the immunized mice. The B6C3F1 mice were chosen as the model system to evaluate the induced CTL responses. B6C3F1 mice are immunocompetent mice. The use of mice with an intact immune system is critical for understanding progression and treatment of the disease and to evaluate new therapeutic approaches. SV40 T-Ag was the chosen model tumor antigen because it is highly immunogenic, inducing both antibody and cytotoxic T lymphocyte (CTL) responses [114] . The target cell line chosen for the *in vitro* CTL assay is MOVCAR-2 because it is a mouse ovarian cancer cell line derived from the B6C3F1 mice that expresses the SV40 T Ag [115]. To test the validity of the use of MOVCAR-2 cells as target cells for cytotoxicity assay, expression of the target SV40 T-Ag in the MOVCAR-2 parental cell line and retention of this expression by MOVCAR-2 cells in tumors *in vivo* was confirmed by Western blot analysis. The expression of other components of the antigen processing and presentation pathway, such as MHC class I and **T**ransporter of **A**ntigenic **P**eptides-1 (TAP-1) was also confirmed in the MOVCAR-2 cells.

4.2. Materials and Methods

***In vitro* Cytotoxic T Lymphocyte assay.**

4.2.1. Assay of Tumorigenicity. B6C3F1 mice were injected with MOVCAR-2 cells. 1×10^8 MOVCAR-2 cells were injected intraperitoneally into each B6C3F1 mouse. The mice were then monitored for tumor formation.

4.2.2. Analysis of SV40 T-Ag expression in MOVCAR-2 tumor cells by Western blot. The MOVCAR-2 cell line and tumor cells cultured from the ascites and solid tumor collected from B6C3F1 mice injected with the MOVCAR-2 cell line were analyzed for expression of the tumor antigen, SV40 T-Ag. The cells were harvested and lysates were prepared. Protein concentrations of each sample were determined using the Bradford method, and all lysates were normalized to the lowest concentration of protein. Samples were loaded onto 10% SDS-polyacrylamide gels, separated by electrophoresis, and transferred to nitrocellulose membranes (15 V for 15 min). Membranes were blocked for 1 h with 5% bovine serum albumin in Tris-Cl buffered saline (TBS), followed by two 5 min washes with 1% Tween-20 in TBS (TTBS). The membranes were incubated for 1 h in TTBS containing a primary mouse anti-mouse SV40 T-Ag antibody (BD Biosciences, clone PAb101), and washed three times for 30 min each with TTBS. Afterwards, the membranes were incubated for 1 h in TTBS containing a horseradish peroxidase-labeled goat anti-mouse IgG antibody, and washed three times for 30 min each with TTBS. Finally the membranes were developed using the ECL substrate (Amersham), and exposed to x-ray film.

4.2.3. Analysis of expression of MHC class I in MOVAR-2 cell line and MOVCAR-2 tumor cells by flow cytometry. MOVCAR-2 cell line and tumor cells cultured from the ascites and solid tumor collected from B6C3F1 mice injected with the MOVCAR-2 cell line were analyzed for expression of MHC class I. The MOVCAR-2 cells activated by addition of recombinant mouse IFN-gamma (R&D Systems) were used as the positive control. After 48 h of incubation *in vitro*, the cells were harvested and stained, and 5×10^5 cells were stained per well for MHC class I, *i.e.,* the H-2K^b (BD Biosciences clone AF6-88.5) and H-2K^k(BD Biosciences clone 36-7-5) haplotypes of MHC class I. The antibodies were used at 1 µg/ml. Labeled antibody were added to the cells of interest and incubated in the dark for 20 min at 4^0C. Isotype control antibodies were also used to set up compensation. The cells were fixed in 1% paraformaldehyde for 5 min in the dark, washed twice and resuspended in 200 µl of FACS buffer. The cells were analyzed using a FACScan flow cytometer (Becton Dickinson).

4.2.4. Analysis of expression of TAP 1 in MOVAR-2 cell line and MOVCAR-2 tumor cells by Western blot. MOVCAR-2 cell line and tumor cells cultured from the ascites and solid tumor collected from B6C3F1 mice injected with the MOVCAR-2 cell line were analyzed for expression of TAP 1. The MOVCAR-2 cells activated by addition of recombinant mouse IFN-gamma (R&D Systems) were used as the positive control. After 48 h of incubation *in vitro*, the cells were harvested and lysates were prepared. Protein concentrations of each sample were determined using the Bradford method, and all lysates were normalized to the lowest concentration of protein. Samples were loaded onto 10% SDS-polyacrylamide gels, separated by electrophoresis, and transferred to nitrocellulose membranes (15V for 15 min). Membranes were blocked for 1 h with 5% bovine serum albumin in Tris-Cl buffered saline (TBS), followed by two 5 min washes with 1% Tween-20 in TBS (TTBS). The membranes were incubated for 1 h in TTBS containing a primary mouse anti-mouse TAP 1 (Santa Cruz Biotechnology catalog # 11465), and washed three times for 30 min each with TTBS. Afterwards, the membranes were incubated for 1 h in TTBS containing a horseradish peroxidase-labeled goat anti-mouse IgG antibody, and washed three times for 30 min each with TTBS. Finally the membranes were developed using the ECL substrate (Amersham), and exposed to x-ray film.

4.2.5. Generation Of Cytotoxic T-Lymphocytes (CTLs). CTLs were generated by immunizing B6C3F1 mice with Ad5-CMV-SV40 T-Ag complexed with CFm40L and Ad5-CMV-SV40 T-Ag alone. Each mouse was injected with 10^9 ifu of Ad5-CMV-SV40 T-Ag alone and 10^9 ifu of Ad5-CMV-SV40 T-Ag complexed with 1200 ng of CFm40L. A second dose was administered two weeks later. At ten days after the second immunization, the mice were sacrificed and spleens were collected. Splenocytes containing the CTLs were co-cultured with a synthetic peptide (CKGVNKEYL) that corresponds to an epitope of SV40 T-Ag for 5 days.

4.2.6. Chromium Release Assay. The cytotoxicity of the generated CTLs was determined in a standard 4-h chromium release assay. The target MOVCAR-2 cells (Interferon-gamma treated as well as untreated) and CMT.64 cell line (negative control) were labeled with 100 □Ci of $Na_2{}^{51}CrO4$ for 1.5 h. 1×10^3 labeled target cells were then co-cultured with different numbers of effector T-cells in a 96-well (v-bottom plates) for 4 h. At the end of the culture, 100 □l of supernatants were collected and radioactivity was measured on a gamma-counter. Maximum and spontaneous release of ^{51}Cr was obtained from the supernatants of the target cells in 1% Nonidet P-40 and in medium alone respectively. All experiments were set up in triplicate wells. Percent Specific lysis was calculated by the following formula [112]:

% specific lysis = (Experimental c.p.m. - Spontaneous c.p.m.) / (Maximal c.p.m. - Spontaneous c.p.m.) × 100.

***In vivo* Cytotoxic T Lymphocyte assay.**

4.2.7. Generation of Cytotoxic T-Lymphocytes (CTLs). CTLs were generated by immunizing B6C3F1 mice with different doses of Ad5-CMV-SV40 T-Ag and Ad5-CMV-SV40 T-Ag complexed with CFm40L. Different doses of Ad5-CMV-SV40 T-Ag used for the immunization were as follows: 1×10^9, 1×10^8, 1×10^7, 1×10^6, 1×10^5, 1×10^4, 1×10^3 and 1×10^2. 1×10^9 ifu of Ad5-CMV-SV40 T-Ag was complexed with 1200 ng of CFm40L, 1×10^8 ifu with 120 ng, 1×10^7 ifu with 12 ng, 1×10^6 ifu with 1.2ng, 1×10^5 ifu with 0.12 ng, 1×10^4 ifu with 0.012 ng, 1×10^3 ifu with 0.0012 ng and 1×10^2 ifu with 0.00012 ng of CFm40L. Mice that only received saline were used as the negative control. The mice received the same second dose of immunization, with the same virus, two weeks later. At 10 days after the second immunization, the mice were used for the *in vivo* CTL assay.

4.2.8. *In vivo* CTL assay. Target cells for the *in vivo* CTL assay were prepared by making splenocytes from the spleens of naïve B6C3F1 mice. The erythrocytes were lysed from the splenocytes by using the ACK lysis buffer. The spleen cells were then divided into two populations. One population was pulsed with peptides (CKGVNKEYL and VVYDFLKC) corresponding to the antigenic epitopes of SV40 T-Ag by co-incubating the cells and each peptide (2.5 µg/ml in the culture medium) at 37^0C for 90 min. The second control population was not pulsed with any peptide. The pulsed splenocytes were labeled with a high concentration of CFSE (5 µM) and the non-pulsed splenocytes were labeled with a low concentration of CFSE (0.5 µM). The pulsed and the non-pulsed splenocytes were then mixed 1:1 and injected intravenously into B6C3F1 mice that were already immunized using Ad5-CMV-SV40 T-Ag. Mice that received only saline were used as the control mice. 2×10^7 cells were injected in each mouse in 500 µl of PBS. After 5 h., the mice were sacrificed and their spleens were harvested. The spleen cells were analyzed by flow cytometry and the two cell populations were detected by their different CFSE fluorescence intensities. The percentage of specific cell lysis was calculated using the following formulas [113]:

Ratio = (percentage of $CFSE^{low}$/ percentage of $CFSE^{high}$)

Percentage specific lysis = [1- (ratio unprimed/ratio primed) $\times$ 100]

4.3. Results

4.3.1. Analysis of SV40 T-Ag expression in MOVCAR-2. MOVCAR-2 is a mouse ovarian carcinoma cell line that expresses SV40 T-Ag and forms tumors in syngeneic immunocompetent B6C3F1 mice. Prior to using MOVCAR-2 cells as target cells to measure the induced cytotoxic T-cell response against SV40 T-Ag, it was important to confirm the expression of SV40 T-Ag in the parental cell line and in tumors formed *in vivo*. Thus, to determine expression of SV40 T-Ag, in MOVCAR-2 tumors, 1×10^8 cells were injected i.p. into B6C3F1 mice. The mice were monitored for tumor growth; after approximately 8 weeks, the mice started to show signs of tumor growth and were sacrificed and examined histopathologically. The MOVCAR-2 cells formed both ascites as well as solid tumors *in vivo*. The cells from the ascites as well as solid tumors were cultured *in vitro* and tested for the expression of SV40 T-Ag. As shown in Figure 5.1, the tumor cells cultured from both, the solid tumors (lane 1) and ascites (lane 2) showed expression of SV40 T-Ag. The parental MOVCAR-2 cell line (lane 3) expresses SV40 T-Ag and was used as the positive control. Thus, MOVCAR-2 cells from parental cell line as well as *in vivo* tumors demonstrate expression of SV40 T-Ag as shown by Western blot analysis.

4.3.2. Analysis of cell-surface expression of MHC Class I in MOVCAR-2. Along with expression of target tumor antigen, it was also important to determine expression of cell surface MHC class I and other components of the antigen processing and presentation pathway. Down-modulation of these molecules is one of the methods adopted by tumor cells to evade the immune system. Target tumor antigens can only be recognized by the activated lymphocytes if they are presented on the cell surface of the tumor cells along with MHC molecules. The appropriate cell surface presentation of the tumor antigen requires processing and presentation of the antigen along with MHC by the cellular antigen processing and presentation pathway. Expression of MHC as well as other components of the antigen processing pathway can be induced in the cells by exposure to IFN-gamma. Expression of MHC class I on MOVCAR-2 cells, from parental cell line as well as cells cultured from ascites and solid tumors was determined by flow cytometry. These cells were also treated *in vitro* with IFN-gamma to measure the induction of MHC class I after exposure to IFN-gamma.

At 48 h after treatment with IFN-gamma, the cells were harvested and analyzed for induction of MHC class I expression on the cell surface. As shown in Fig. 4.2, only 10% of the cells from the parental MOVCAR-2 cell line were positive for the K^b-haplotype of MHC class I. However, the expression of this haplotype increased to 89% when the cells were treated with IFN-gamma. In addition, only 12% of the cells were positive for the K^k-haplotype of MHC class I. The expression of K^k-haplotype, similar to of K^b-haplotype, increased to 87% when the cells were treated with IFN-gamma. As shown in Fig. 4.3, there was no detectable expression

of both, the K^b as well as K^k haplotype on MOVCAR-2 cells cultured from the ascites. However, the expression of the K^b-haplotype increased to 79% of the cells and that of K^b-haplotype increased to 84% of cells after exposure to IFN-gamma. The MOVCAR-2 cells cultured from the solid tumors, as shown in Fig. 4.4, also showed no detectable expression of the K^b and K^k-haplotypes of the MHC class I. However, there was significant induction in the expression of MHC class I after treatment with IFN-gamma, as 86% of the treated cells were K^b-haplotype positive and 91% of the treated cells were K^k-haplotype positive. Thus, MOVCAR-2 cells themselves, either from parental cell line or from *in vivo* tumors, did not show significant expression of MHC class I. However, the expression of MHC class I in these cells could be induced by treatment with IFN-gamma. Hence, these results suggest that the MOVCAR-2 cells can be used as a target in the cytotoxicity assays, but only after treatment with IFN-gamma.

4.3.3. Analysis of TAP-1 expression in MOVCAR-2. The MOVCAR-2 cells were also tested for expression of TAP-1 protein before and after treatment with IFN-gamma. The TAP (**T**ransporter **A**ssociated with antigen **P**rocessing) proteins belong to the ABC group of membrane transporters and are responsible for transporting peptides derived from antigens expressed in the cytosol to the endoplasmic reticulum, where they are assembled along with MHC, before being exported to the Golgi apparatus, to be finally inserted into the plasma membrane. Thus, down-modulation in the expression of TAP proteins leads to blockade in the processing and presentation of the tumor antigens on the cell surface. Expression of TAP-1 protein the MOVCAR-2 cells was determined by Western blot analysis. As shown in Fig. 4.5, MOVCAR-2 cells, from parental cell line (lane 1), cells cultured from ascites (lane 3), and cells cultured from solid tumor (lane 5) did not show detectable expression of TAP-1. However, upon treatment with IFN-gamma, the MOVCAR-2 cells from parental cell line (lane 2), cells cultured from ascites (lane 4), and cells cultured from solid tumor (lane 6) showed induction in the expression of TAP-1. The cells from the MOVCAR-2 parental cell line showed greater induction in the expression of TAP-1 than the MOVCAR-2 cells cultured from the ascites and solid tumor upon exposure to IFN-gamma. Thus, like MHC class I, the MOVCAR-2 cells, either from cell line or from tumors, did not show detectable expression of TAP-1. However, the expression was significantly induced upon treatment with IFN-gamma as shown by Western blot analysis. This confirms the results suggesting that MOVCAR-2 cells can be used as target cells for cytotoxicity assays, but only after treatment with IFN-gamma.

4.3.4. Assessment of CTL activity by ^{51}Cr Release Assay. The anti-tumor immune response induced by the CD40-targeted adenoviral vaccine in B6C3F1 mice was quantified by measuring the killing of target cells that express the tumor antigen *in vitro*, by activated tumor antigen-specific cytotoxic T-cells (CTLs) generated *in vivo*. Fig. 4.1 showed that MOVCAR-2 cells do express the target tumor antigen, SV40 T-Ag, and thus can be used as target in the cytotoxicity assay. However, Figs. 4.2, 4.3, 4.4 and 4.5 show that MOVCAR-2 cells can be used as target only after treatment with IFN-gamma, since without exposure to IFN-gamma the cells by themselves, do not express significant amounts of MHC class I and TAP-1, which are necessary for the efficient processing and presentation of the tumor antigen on the cell surface. Thus, IFN-gamma treated MOVCAR-2 cells were chosen as the target cells to measure the lytic activity of the activated antigen-specific CTLs. As shown in Fig. 4.6, the splenocytes isolated from B6C3F1 mice immunized using the CD40-targeted Ad5-CMV-SV40 T-Ag showed increased killing of the target cell line, MOVCAR-2, than the splenocytes isolated from mice immunized using untargeted Ad5-CMV-SV40 T-Ag at all target cell:effector cell (T:E) ratios used. The increase in killing obtained when CD40-targeted adenoviral vector was used was approximately 20% greater than that obtained by untargeted adenovirus at all T:E ratios. Untreated naïve MOVCAR-2 cells that did not express significant levels of MHC class I and TAP-1 was used as a negative control. Likewise, the CMT.64 cell line that does not express SV40 T-Ag, was also used as a negative control. There was minimal killing of both control cell types, with approximately 22 - 24% killing at T:E ratio of 1:100, by the splenocytes isolated from mice immunized using CD40-targeted as well as untargeted Ad5-CMV-SV40 T-Ag. Thus, the chromium release based cytotoxicity assay suggests that CD40-targeted adenovirus expressing tumor antigen can activate antigen-specific T-cells and induce a greater cytotoxic T lymphocyte response than untargeted adenovirus expressing the same antigen.

4.3.5. Assessment of CTL Activity by CFSE-based *in vivo* CTL Assay. The anti-tumor immune response induced by CD40-targeted adenovirus was also determined by measuring the killing of target cells *in vivo* by activated CTLs using the CFSE-based *in vivo* cytolytic assay. The target cells in this assay were splenocytes pulsed with peptides that correspond to the antigenic epitopes of SV40 T-Ag. Unpulsed splenocytes were used as negative control cells. Both, target and control splenocyte populations were mixed 1:1 and injected intravenously in the B6C3F1 mice immunized using CD40-targeted Ad5-CMV-SV40 T-Ag, 1×10^9 ifu of Ad5-CMV-SV40 T-Ag complexed with 2400 ng of cFm40L and untargeted 1×10^9 ifu of Ad5-CMV-SV40 T-Ag. As shown in Fig. 4.7, mice immunized using CD40-targeted Ad5-CMV-SV40 T-Ag showed similar

killing of the target splenocytes as the mice immunized using untargeted Ad5-CMV-SV40 T-Ag. The target cell lysis observed, was approximately between 78-90%. These results were markedly different from those obtained using the *in vitro* CTL assay in which CD40-targeted adenovirus induced a greater cytotoxic T lymphocyte response than untargeted adenovirus expressing the same antigen. These results could be explained by the possibility that the immune system maybe saturated at this high dose, 2×10^9 ifu of virus resulting in a lack of difference in between the induced cytotoxic T-cell response between the two groups.

To explore this possibility, lower doses of the virus were used for immunization. The lower doses of Ad5-CMV-SV40 T-Ag used were 2×10^8, 2×10^7, 2×10^6, 2×10^5, 2×10^4, 2×10^3 and 2×10^2 ifu per mouse. The amount of CFm40L complexed with the above doses of virus for targeting to CD40, were 240, 24, 2.4, 0.24, 0.024, 0.0024 and 0.00024 ng, respectively. As shown in Fig. 4.8, the percentage of specific killing obtained by CD40-targeted Ad5-CMV-SV40 T-Ag was similar to that obtained by untargeted Ad5-CMV-SV40 T-Ag at all the doses of virus used. The CD40-targeted Ad5-CMV-GFP (2×10^8 ifu of Ad5-CMV-GFP complexed with 240 ng of CFm40L) and untargeted Ad5-CMV-GFP were also used as controls for immunization. As shown in the representative histograms of Fig. 4.9, there was no lysis of the target splenocyte population, that pulsed with peptides corresponding to the antigenic epitopes of SV40 T-Ag (peak M2), in B6C3F1 mice immunized using CD40-targeted Ad5-CMV-GFP and untargeted Ad5-CMV-GFP. In addition, there was no lysis of the control splenocyte population (peak M1) that was not pulsed with any peptide, in mice immunized using CD40-targeted as well as untargeted adenoviral vectors. Thus, these results suggest the killing of target splenocyte population observed in B6C3F1 mice immunized using CD40-targeted and untargeted Ad5-CMV-SV40 T-Ag was mediated by cytotoxic T-cells (CTLs) that are specific for SV40 T-Ag. The results from the CFSE-based *in vivo* cytolytic assay suggest that the cytotoxic T lymphocyte response induced by CD40-targeted Ad5-CMV-SV40 T-Ag was similar to that induced by untargeted Ad5-CMV-SV40 T-Ag.

4.4. Discussion

The result from the Western blot analysis of MOVCAR-2 cells in Fig. 4.1 confirms the expression of the target tumor antigen, SV40 T-Ag, in the parental MOVCAR-2 cell line and also demonstrates the tumors formed *in vivo* by the MOVCAR-2 cells, retain expression of the SV40 T-Ag. It was important to know the expression of the target antigen was retained *in vivo* by the tumor cells because the activated CTLs are specific for target tumor antigen, *i.e.,* they will kill only those cells that express the targeted tumor antigen. Thus, loss or down-modulation of expression of the tumor antigen *in vivo* by tumor cells will render them resistant to killing by the activated antigen-specific lymphocytes. Therefore, the Western blot result (Fig. 4.1) supports the choice of using MOVCAR-2 cells as targets to measure the anti-tumor immune response induced against SV40 T-Ag. The flow cytometric analysis of the target MOVCAR-2 cells, Figs. 4.2, 4.3 and 4.4, reveal that MOVCAR-2 cells do not express significant amount of MHC class I. In fact, the level of expression, which was at least between 10 - 12% in the parental MOVCAR-2 cell line, decreases to undetectable levels in tumor cells *in vivo*. Thus, loss or down-modulation of MHC expression may be one of the mechanisms by which the MOVCAR-2 cells evade the immune system and form tumors. However, fortunately the expression of MHC class I in MOVCAR-2 parental cell line as well as tumor cells isolated from ascites and solid tumors can be up-regulated significantly by treatment with IFN-gamma as shown in Figs. 4.2, 4.3 and 4.4. This demonstrated the loss or decrease in expression of MHC class I by MOVCAR-2 was because of changes in regulation of the expression and not because of genetic alteration, and the expression can be up-regulated by exposure to inflammatory agents such as IFN-gamma. Likewise, as shown in Fig. 4.5, there was no detectable expression of TAP-1, which is one of the important components of the antigen processing and presentation pathway, in MOVCAR-2 cells. However, this expression was up-regulated by treating the MOVCAR-2 cells with IFN-gamma. Thus, results from Figs. 4.1-4.5 suggest that MOVCAR-2 cells can be used as target cells in cytotoxicity assays to measure the induced anti-tumor CTL response, but only after treatment with IFN-gamma.

The results from the cytotoxicity assays demonstrate the CD40-targeted adenovirus expressing the tumor antigen SV40 T-Ag does induce an SV40 T-Ag specific cytotoxic T lymphocyte response, *i.e.,* it does induce activation and proliferation of the antigen-specific cytotoxic T lymphocytes *in vivo*. However, the results from the *in vitro* CTL assay differ from that of the *in vivo* CTL assay. The *in vitro* CTL assay, Fig. 4.6, suggests the CTL response induced by the CD40-targeted Ad5-CMV-SV40 T-Ag, as measured by the killing of the target tumor cell line, MOVCAR-2, which expresses SV40 T-Ag, was greater than that induced by untargeted Ad5-CMV-SV40 T-Ag. The CTL response detected was specific for SV40 T-Ag as there was minimal killing of the negative control, cell line CMT.64, which does not express SV40 T-Ag. However, the *in vivo* CTL assay, Figs. 4.7, 4.8 and 4.9, suggest the CTL response induced by the CD40-targeted Ad5-CMV-SV40 T-Ag, as measured by the killing of target splenocytes pulsed with peptides corresponding to antigenic epitopes of SV40 T-Ag, was approximately similar to that induced by the untargeted Ad5-CMV-SV40 T-Ag. Again, the killing activity was

specific for cells that express SV40 T-Ag as there was no decrease in the population of the negative control cells, splenocytes that were not pulsed with SV40 T-Ag peptides. In addition, there was no killing of splenocytes observed in mice immunized using CD40-targeted as well as untargeted adenovirus expressing GFP (Ad5-CMV-GFP). Thus although the killing activity observed in both cases was tumor antigen-specific, there was a discrepancy in between the results of the two cytotoxicity assays.

This discrepancy could be because of various factors. The most obvious one is the killing of the target cells takes place *in vitro* in the chromium release assay and *in vivo* in the *in vivo* CTL assay. The difference in the milieu could result in the difference observed in killing. The target cells used in both assays were also different. The *in vitro* CTL assay uses a tumor cell line or primary tumor cells as the target, whereas the *in vivo* CTL assay uses splenocytes as the target cells. The tumor cell line or cells express the tumor antigen endogenously whereas the splenocytes were pulsed *in vitro* with peptides corresponding to the antigenic epitopes of the target tumor antigen. Thus, the tumor cells will express, process and display several epitopes of the tumor antigen on its cell surface, while the splenocytes will only display the epitopes of the antigen that it has been pulsed with. Also, the antigen density on the target cells that are used in both assays is different, and could contribute to the difference in the results obtained from both assays. Thus, the differences in the results could be attributed to the differences in the experimental protocol and/or the target cells used.

The lytic activity observed using the *in vivo* CTL assay may be more representative of the T-lymphocyte mediated killing of the tumor in animals because of the *in vivo* nature of the assay. In addition, the *in vivo* CTL assay involves injecting both populations of splenocytes, the ones that have not been pulsed with any peptide (negative control) and splenocytes that have been pulsed with peptides corresponding to the target antigen (test), in the same animal and thus there is an internal negative control of the same cellular origin for every mice that was tested for the CTL activity. However, the target cells that were used in the *in vitro* CTL assay, *i.e.,* tumor cell line or tumor cells are the actual target cells that the immune cells will encounter in cancer patients or tumor-bearing animals. Therefore, both assays have their pros and cons. Our hypothesis is that CD40-targeted adenovirus should infect DCs more efficiently than untargeted adenovirus and thus, should be able to elicit a greater CTL immune response than the untargeted vector. Thus, although the results from the *in vitro* chromium release assay were in accordance with our hypothesis, it is difficult to determine which assay is more reliable and to determine whether the CTL response induced by CD40-targeted adenoviral vector is greater than or similar to the CTL response triggered by the untargeted adenovirus. Nonetheless, both assays point the CD40-targeted adenovirus expressing tumor antigen does induce an antigen-specific CTL response, similar, if not greater than that induced by untargeted adenovirus expressing the same tumor antigen. Thus, the CD40-targeted adenoviral vaccine is a potent vaccine.

5. Liver Toxicity and biodistribution studies

5.1. Introduction

Liver toxicity is one of the main obstacles in the use of first-generation adenoviral vectors for application as therapeutic vectors in gene therapy. Ad5 is one of the most commonly used vectors in gene therapy. The natural tropism of wild-type Ad5 is for the liver and thus systemic administration of this virus leads to its accumulation in the liver, producing pathogenic effects in the liver [116]. The host immune response to adenovirus is responsible for mediating the toxic effects in the liver [117, 118].

The immune response to adenovirus can be divided into two phases [119]. The first phase occurs between day 1 and 4 after infection. It is characterized by an acute inflammatory response which involves the release of certain inflammatory cytokines (IL-6, TNF-α, IL-8, *etc.*) and the recruitment of immune effector cells in the liver. Chemokine expression is induced in the liver within one h after infection and is responsible for the recruitment of neutrophils. The recruitment of neutrophils and other immune effector cells is responsible for mediating the hepatic injury. The second phase begins between 5 to 7 days after infection. The second phase is characterized by an adaptive immune response specific for viral or transgene products. The initial innate and the subsequent adaptive immune response to adenoviral or transgene products are responsible for inducing the toxic effects in the liver.

The sequestration of the adenovirus particles in the liver leads to hepatotoxicity and, the effective dose of adenovirus that can enter the systemic circulation and find its target cell is decreased, reducing the therapeutic effect. The approaches adopted to reduce adenovirus induced toxicity include attempts to reduce the immunogenicity of the virus and to de-target virus from the liver. The attempts to reduce immunogenicity of adenovirus vectors include: 1) deletion of viral genes to reduce the number of viral proteins synthesized [120-122], *e.g.,* gutless adenovirus, and 2) modification of the capsid proteins, genetic as well as non-genetic, such that they are less immunogenic [123]. The approaches used to de-target the adenovirus from the liver are: 1)

modification, both genetic as well as non-genetic, of the fiber or fiber knob domain, such that it does not bind to CAR [124, 125], and 2) use of bi-specific adapter molecules [126].

Bi-specific adapter molecules can be chemically conjugated targeting moieties or recombinant fusion proteins that can bind to adenovirus fiber knob on one side and to the target cell on the other, serving as a bridge between the adenovirus and the target cell. The use of bi-specific adapter molecule generates adenoviruses which are de-targeted from the liver as the fiber knob domain of the virus is blocked by the adapter molecule. Genetic modification of adenovirus may reduce its production capacity. Non-genetic modification, such as PEGylation [125] can reduce the uptake of the virus by the liver, but does not increase its targeting to the target cell. Thus, the use of bi-specific molecules appear to be the most efficient, safe, viable and cost-effective approach to generate targeted adenovirus.

We generated a dendritic cell targeted adenoviral vector in our laboratory by using a bi-specific adapter molecule called CFm40L. This molecule has the CAR domain on one end and the CD40 binding ligand domain on the other end. This molecule can bind to the fiber knob of the adenovirus by its CAR domain. It can also bind to all cell types expressing the CD40 receptor by its CD40-binding ligand domain. Dendritic cells express CD40 receptor on their cell surface. Thus, when the adenovirus and the CFm40L adapter molecule are mixed together, the adapter molecule binds to the adenovirus by its CAR domain. The adenovirus that is coated by the CFm40L adapter molecule, can infect any cell that expresses CD40 receptor, which includes dendritic cells.

We expected the use of CFm40L adapter molecule will de-target the adenovirus from the liver and re-target it to dendritic cells which express CD40. De-targeting from the liver would lead to reduced liver toxicity and thus more efficient and safer use of adenovirus for immunotherapy. We checked the de-targeting of CD40-targeted adenovirus from the liver by measuring the amount of adenoviral DNA in the livers of mice, after immunization with the virus. We also determined expression of the transgene in the livers of mice after immunization. We also looked for secretion of the liver toxicity enzyme, alanine aminotransferase (ALT), and inflammatory cytokines in the serum of the immunized mice, and performed histological studies of the liver after immunization.

5.2. Materials and Methods

5.2.1. Quantitative Real-Time PCR. B6C3F1 mice were immunized using Ad5-CMV-SV40 T-Ag or Ad5-CMV-SV40 T-Ag complexed with CFm40L as described above. One day after the second immunization the mice were sacrificed and the liver, spleen, and kidney tissues were removed. Total DNA was extracted from 50 mg of liver and kidney and 20 mg of spleen using the QIAamp DNA mini kit (Valencia, CA) according to the manufacturer's instructions. Quantification of adenoviral DNA was performed using Real-Time PCR for E4 gene. The primers and probe sequences were as follows:

forward primer sequence
5'-GGAGTGCGCCGAGACAAC-3',
reverse primer sequence
5'-ACTACGTCCGGCGTTCCAT-3',
probe sequence
5'-6FAM-TGGCATGACACTACGACCAACACGATCT-TAMRA-3'.

The probe was labeled with a reporter fluorescent dye (6-carboxy-fluorescein) at the 5' end and a quencher fluorescent dye TAMRA (6-carboxy-tetramethyl-rhodamine) at the 3' end. Samples were equalized for DNA input using standard primers against mouse GAPDH. The real-time PCR reactions were performed in 50 μl volumes containing 500 ng of total DNA, 100 μM forward primer, 100 μM reverse primer, 50 μM probe and 1X PCR Master Mix (EuroGentec). The following thermal cycling parameters were optimized for adenoviral E4 gene quantification: 2 min at 50°C, 10 min at 95°C, followed by 40 cycles of 1 min at 95°C and 1 min at 60°C.

5.2.2. *Bio-Plex* cytokine assay. The serum samples were collected from immunized mice one day after the second immunization. The concentrations of Th-2 type cytokines such as IL-5 and IL-13 were analyzed by the *Bio-Plex* multiplex mouse cytokine assay kit (Bio-Rad laboratories, Hercules, CA) and the cytokine reagent kit (Bio-Rad) according to the manufacturer's protocol. Briefly, 50 μl of diluted standards or serum samples were added to a 96-well plate coated with beads that have antibodies specific for the above cytokines conjugated to them. Thus, the cytokines present in the serum will bind to the antibodies that are coupled to the beads. The reaction was incubated at RT by vortexing at 300 rpm for 30 min. The plate was then washed thrice to remove any unbound protein. A mixture of biotinylated antibodies specific for a different epitope on the cytokines was then added to the beads. The reaction was incubated again at RT by vortexing at 300 rpm for 30 min After three washes, Streptavidin-phycoerythrin (streptavidin-PE) was added to the reaction containing biotinylated antibodies bound to the cytokines in a sandwich. The reaction was incubated

at RT by vortexing at 300 rpm for 10 min. After three washes, the data from the reaction was collected and analyzed using the *Bio-Plex* suspension array system (Bio-Rad, Hercules, CA).

5.2.3. Histological examination of liver. B6C3F1 mice were immunized using Ad5-CMV-SV40 T-Ag or Ad5-CMV-SV40 T-Ag complexed with CFm40L as described above. One day after the second immunization, the mice were sacrificed and the livers were removed. The liver tissues were immersion-fixed in 4% buffered formaldehyde, embedded in paraffin, sectioned, and stained with hematoxylin-eosin and Romanoswki's stain.

5.2.4. Analysis of Serum Alanine aminotransferase (ALT) levels. The quantification of ALT levels in the mice serum was done by Charles River Laboratories using ELISA.

5.2.5. MicroPET Analysis of Adenovirus Biodistribution. The B6C3F1 mice were immunized using Ad5-CMV-TK complexed with CFm40L and Ad5-CMV-TK alone. Each mice was injected with 10^9 ifu of Ad5-CMV-TK alone and complexed with 120 ng of CFm40L. Two days after the immunization, the mice were injected in the tail vein with 150 μCi of [^{18}F]-FHBG. After 60 min, the animals were imaged in a microPET scanner, and image data were acquired for 15 min. MicroPET images were reconstructed by using an iterative reconstruction technique.

5.3. Results

5.3.1. Quantification of adenovirus DNA in livers of mice immunized using CD40-targeted and untargeted Ad5-CMV-SV40 T-Ag by Real-time PCR analysis. Binding of the targeting ligand, CFm40L, to the adenovirus masks the CAR-binding fiber knob domain of the adenovirus and targets the virus to cells expressing CD40. Since the CD40-targeted adenoviral vector was retargeted away from cells expressing CAR to cells expressing CD40, we hypothesized the natural liver tropism of the adenovirus would be altered. The potential of CD40-targeted adenovirus to target and infect the liver cells was tested by determining the amount of adenoviral DNA present in the livers of B6C3F1 mice injected with either CD40-targeted or untargeted adenovirus. The adenovirus E4 gene copy number, a surrogate marker for adenovirus infectivity, was quantified by real-time PCR in the livers of the immunized mice. As shown in Fig. 5.1, there was a 6-fold decrease in adenoviral E4 DNA in the livers of mice immunized using the CD40-targeted Ad5-CMV-SV40 T-Ag than in livers of mice immunized using untargeted Ad5-CMV-SV40 T-Ag. Thus, CD40-targeted Ad5-CMV-SV40 T-Ag showed reduced liver infection than untargeted Ad5-CMV-SV40 T-Ag.

5.3.2. Quantification of transgene expression in livers of mice immunized using CD40-targeted and untargeted adenovirus by microPET scan analysis. The results from Fig. 5.1 demonstrated that CD40 targeting of an adenovirus resulted in decreased liver infection than untargeted adenovirus. To confirm this approach of targeting an adenovirus and limiting liver infectivity, HSV-Tk expression was examined by microPET scanning, using [^{18}F]-FHBG as a substrate. In the experiment shown in Fig. 5.2, three mice were imaged as described in the 'Materials and Methods' section. Image data from the control mouse injected i.p. with 0.5 ml saline (A) showed background accumulation of the [^{18}F]-FHBG substrate in the large intestine as well as urinary excretion in the bladder. Clinical toxicity of the Ad vector was primarily hepatic, based on the tropism of the virus to the liver. Intraperitoneal injection of a mouse with 1×10^9 ifu of untargeted Ad-CMV-HSV-Tk resulted in strong expression of HSV-Tk in the liver as demonstrated by accumulation of the [^{18}F]-FHBG (B). Importantly, intraperitoneal injection of a mouse with 1×10^9 ifu of DC40-targeted Ad-CMV-HSV-Tk showed almost no expression in the liver (C). These results clearly show a differential expression between untargeted Ad-CMV-HSV-Tk and CD40-targeted Ad-CMV-HSV-Tk in normal liver, and demonstrate that CD40 targeting can reduce liver infectivity.

5.3.3. Analysis of inflammatory cytokines in the serum of mice immunized using CD40-targeted and untargeted Ad5-CMV-SV40 T-Ag by *Bio-Plex* Cytokine assay. Liver toxicity induced by adenovirus was initiated by an inflammatory response to the adenovirus present in the liver. Thus, adenovirus-induced liver toxicity was accompanied by an increase in the levels of pro-inflammatory cytokines in the blood. Since results from Figs. 5.1 and 5.2 showed that CD40-targeted adenovirus reduced targeting and infection of the liver, we hypothesized there was an accompanying decrease in inflammatory response to the modified virus. The inflammatory response induced by the CD40-targeted adenovirus was determined by analyzing the serum of the immunized mice for the presence of inflammatory cytokines using the Bio-Plex cytokine assay. The results of this assay in Fig. 5.3, showed an increase in the Th-2-type cytokines IL-5 and IL-13 in the serum of mice immunized using untargeted Ad5-CMV-SV40 T-Ag compared with control naïve mice. In addition, there was a 4.5-fold increase in the amount of IL-5 and a 1.6-fold increase in the amount of IL-13 in the serum samples compared with control naïve mice. Importantly however, there was no significant change in the amounts of IL-5 and IL-13 in the serum of the mice immunized using CD40-targeted Ad5-CMV-SV40 T-Ag compared with control naïve mice or with mice immunized using CFm40L targeting ligand alone. Thus, the

amount of the Th-2-type cytokines, IL-5 and IL-13, present in the sera of the mice immunized using CD40-targeted Ad5-CMV-SV40 T-Ag was comparable to that present in the control naïve mice. These results show reduced inflammation in mice immunized using CD40-targeted Ad5-CMV-SV40 T-Ag than mice that received the untargeted Ad5-CMV-SV40 T-Ag.

5.3.4. Histological examination of Liver tissue from mice immunized using CD40-targeted Ad5-CMV-SV40 T-Ag and untargeted Ad5-CMV-SV40 T-Ag. The results from Fig. 5.3 showed there was decrease in the amount of Th-2-type inflammatory cytokines, IL-5 and IL-13, in the sera of mice immunized using CD40-targeted Ad5-CMV-SV40 T-Ag compared with the mice immunized using untargeted Ad5-CMV-SV40 T-Ag. Both IL-5 and IL-13, have been shown to induce inflammation by increasing infiltration of neutrophils and eosinophils. To determine if up-regulation in the amounts of IL-5 and IL-13 led to increased local inflammation, histological examination of the livers of mice immunized using CD40-targeted Ad5-CMV-SV40 T-Ag and untargeted Ad5-CMV-SV40 T-Ag was performed by using hematoxylin and eosin and Romanowski staining. As shown in Fig. 5.4, the hematoxylin and eosin staining of liver sections revealed increased infiltration of immune cells in the livers of mice immunized using untargeted Ad5-CMV-SV40 T-Ag than the control naïve mice. The livers of mice immunized using CD40-targeted Ad5-CMV-SV40 T-Ag showed an absence of infiltration by immune cells, similar to control naïve mice. The Romanowski staining of the liver sections revealed there was increased inflammation of the capsule of the liver (capsulitis), observed in the livers of the mice immunized using the untargeted Ad5-CMV-SV40 T-Ag compared with the livers of the control naïve mice. There was also increased infiltration of leukocytes and lymphocytes in the capsule and in the peri-sinusoidal spaces of the livers of mice immunized using untargeted Ad5 SV450 T-Ag. The livers of mice that received CD40-targeted Ad5-CMV-SV40 T-Ag showed a normal capsule and little infiltration of leukocytes and lymophocytes. Thus, these results demonstrate there was reduced inflammation in the livers of mice immunized using CD40-targeted Ad5-CMV-SV40 T-Ag than mice immunized using untargeted Ad5-CMV-SV40 T-Ag.

5.3.5. Analysis of Alanine Aminotransferase (ALT), in serum of mice immunized using CD40-targeted and untargeted Ad5-CMV-SV40 T-Ag. Another test for determining liver toxicity assessment of serum ALT levels. ALT is an enzyme that plays a role in protein metabolism, and is found mainly in the liver, but also in smaller amounts in the kidneys, heart, muscles, and pancreas. ALT is measured clinically to determine if the liver is damaged or diseased. Low levels of ALT are normally found in the blood. However, when the liver is damaged or diseased, it releases ALT into the bloodstream. Most increases in ALT levels are caused by liver damage. The amount of the liver toxicity enzyme, ALT, in the sera of the immunized mice was measured by ELISA. The results, Fig. 5.5, showed there was an approximately 2.5-fold increase in the amount of the liver toxicity enzyme present in the serum of mice immunized using untargeted Ad5-CMV-SV40 T-Ag compared with control naïve mice. However, the amount of ALT present in the serum of mice immunized using CD40-targeted Ad5-CMV-SV40 T-Ag was similar to the control naïve mice. These results demonstrate there was reduced liver toxicity in mice immunized using CD40-targeted Ad5-CMV-SV40 T-Ag compared with the mice immunized using untargeted Ad5-CMV-SV40 T-Ag.

5.4. Discussion

One of the goals in targeting adenovirus was to de-target from the liver, as accumulation of adenoviral particles in the liver induces an acute innate inflammatory response followed by an adaptive immune response to viral proteins and transgenes, which result in liver toxicity [119]. Our results show that CD40-targeted adenovirus vector resulted in reduced liver infection and toxicity than the untargeted adenovirus as shown by: 1) decreased amount of adenoviral DNA in the liver, as measured by real-time PCR, 2) reduced expression of the transgene , *thymidine kinase*, in livers of mice injected with CD40-targeted Ad-TK than the mice injected with untargeted Ad-TK, as measured by PET, 3) decreased amount of Th-2-type inflammatory cytokines such as IL-5 and IL-13 in the serum, and 4) reduced infiltration of lymphocytes and leukocytes in the liver. Thus, our results show that by decreasing infection of liver cells, the CD40-targeted adenoviral vector reduced acute inflammatory response and subsequent adaptive immune response, leading to lower liver toxicity.

The Coxsackie and Adenovirus Receptor (CAR), αv-integrins and heparin sulfate glycosaminoglycans and blood factors (Factor IX and C4 Binding Protein) are molecules that bind to adenovirus and determine the tropism of the adenoviral vector *in vivo* [127]. The fiber-knob domain of Ad5 binds to CAR and blood factors. The penton base of the adenoviral particle binds to the αv-integrins. The fiber shaft of the adenovirus binds to Heparin Sulfate Glycosaminoglycans. Studies by Vigne *et al.,* [128] suggest that simultaneous ablation of CAR and αv-integrin binding, by introducing mutations in the fiber knob domain and deleting the RGD motif in the penton base respectively, fails to reduce Ad5 liver tropism. While studies by Kim JH *et al.,* [129] suggest that ablation of CAR binding, by introducing mutation in the β sheet of the fiber knob, reduces adenovirus liver

tropism and toxicity. Our results supports the results of Kim JH *et al.,* and suggests the fiber-knob domain of the adenoviral particle does play an important role in infecting liver cells, as it is this domain that is masked by the CFm40L adapter molecule in the CD40-targeted adenoviral vector. Our findings support the hypothesis that binding of fiber-knob domain to its receptor plays an important role in determining the tropism of Ad5 vector to the liver.

There are various mechanisms of hepatotoxicity [130]. Some of them are: 1) Bile acid induced hepatocyte apoptosis, 2) inflammatory liver injury, 3) cytochrome P4502E1 dependent toxicity, 4) peroxynitrite induced hepatotoxicity, and 5) hepatotoxicity due to mitochondrial dysfunction. Our results suggest the mechanism of liver toxicity induced in our study, by use of untargeted adenovirus, is the inflammatory liver injury. Nonetheless, we cannot exclude the other possibilities since we have not tested for them. We saw increased infiltration of leukocytes and lymphocytes in the capsule and around the peri-sinusoidal regions of the liver. There was also increased production of inflammatory cytokines such as IL-5 and IL-13. Both IL5 and IL-13 have been shown to play a role in hepatitis induced liver damage by recruitment of leukocytes in the liver and inducing a Th-2 type immune response (Wynn *et al.)*. Our results support this hypothesis.

The CFm40L adapter molecule de-targets the adenovirus from the liver, leading to reduced infection of the liver by CD40-targeted adenovirus. The reduced infection of the liver by the virus leads to a decreased immune response, *i.e.,* production of inflammatory cytokines and chemokines and infiltration of the liver by immune cells, and thus reduced liver toxicity. The fact that CFm40L adapter molecule can successfully de-target the adenovirus from the liver also supports the binding between the adapter molecule and adenovirus was stable *in vivo*.

6. Immunization of mice and tumor challenge experiments

6.1. Introduction

The anti-tumor efficacy of any pre-clinical therapy needs to be evaluated using a reliable marker of tumor inhibition. The most relevant marker is reduction in tumor growth and increase in survival of treated animals. Thus, survival studies are the gold standard in evaluating the efficacy of anti-cancer therapies. However, by focusing only on the end-point, one misses out on the changes in tumor growth that occur between. The changes in the kinetics of tumor growth that occur in response to anti-tumor therapy can be monitored by regularly measuring the size of the growing tumors. However, this is only possible with superficially growing tumors and not with tumors that are not superficial, *e.g.,* visceral tumors, metastatic and disseminated tumors. In addition, the small changes in tumor mass are missed, when only the gross tumor dimensions are measured. The changes in tumor mass can be monitored by weighing the animals. However, in the early stages of tumor growth, weight is not a reliable marker since it can be influenced by many other factors. Thus, monitoring the proliferation of the tumor cells *in vivo* with the changes in weight of the animals would be a good approach to monitor tumor progression in the animals.

Bioluminescent imaging was chosen to monitor the growth of tumor cells *in vivo* in our studies. Bioluminescence is the production of visible light during an enzymatic reaction. The enzyme responsible for the production of light is luciferase and the substrate that it acts upon is luciferin. The most commonly used luciferase enzyme and its substrate, luciferin are produced by the firefly *Photinus pyralis*. Introducing the firefly *luciferase* gene in mammalian cells can provide a bio-marker to visualize the cells when luciferin is added. When these cells with the *luciferase* gene are injected into animals, they can be visualized *in vivo* when luciferin is injected into the animals. Luciferin is non-toxic to animals. Bioluminescent imaging was chosen to monitor tumor growth as it is a non-invasive approach and it has a greater intensity than fluorescent imaging to image visceral tumors [131].

Ovarian cancer cell lines, IG10 and HM-3, were stably transfected with a plasmid that encoded for the SV40 T-Ag protein, since that is the target tumor antigen against which the immune response is raised. HM-3 is a sub line of OV2944 which is a ovarian tumor cell line of B6C3F1 origin [132]. IG10 is a mouse ovarian cancer cell line of C57BL/6 origin [133]. Cell lines (IG10 and HM-3) that did not originally express SV40 T-Ag were chosen as they would serve as excellent negative controls, since they would be the same as the target cells, but, without the target SV40 T-Ag. This would provide a good pair of target (IG10-SV40 and HM-3-SV40) and control (IG10 and HM-3) cells, both essentially from the same parental cell line, but one with the target tumor antigen (SV40 T-Ag) and one without. These cells were then stably transfected with a plasmid that encoded for the firefly luciferase so the growth of these cells *in vivo* in B6C3F1 mice can be visualized by imaging. The tumor-forming potential of the transfected cell lines was tested by injecting the cells in B6C3F1 mice, and the rate of tumor growth was monitored by bioluminescent imaging. The status of expression of the components of the antigen processing and presentation pathway, such as TAP-1 and MHC class I, in the

transfected cell lines was determined to evaluate the efficacy of these cells to be recognized by the activated tumor antigen-specific lymphocytes.

After evaluation of the tumor cell lines for their tumorigenicity, expression of tumor antigen and MHC-I, the IG10-SV40 cell line were used in tumor challenge experiments. The efficacy of the protective anti-tumor immunity generated by CD40-targeted and untargeted Ad5-CMV-SV40 T-Ag was evaluated by immunizing the immunocompetent B6C3F1 mice with the respective viral vectors, and challenging them the tumor cells. The challenged mice were then monitored every week for change in body weight and survival.

6.2. Materials and Methods

6.2.1. Cell culture of IG10 and HM-3 cells. The IG10 cells were purchased from the ATCC and maintained in Dulbecco's modified Eagle's medium (DMEM) containing 10% Fetal bovine Serum (FBS) (Gemini BioProducts) and 1% antibiotic antimycotic (Invitrogen). The HM-3 mouse ovarian cancer cell line was provided by Dr. K. Yokoro, Department of Biophysics, Faculty of Science, Kyoto University [132]. The HM-3 cells were also maintained in Dulbecco's modified Eagle's medium (DMEM) containing 10% Fetal bovine Serum (FBS) (Gemini BioProducts) and 1% antibiotic antimycotic (Invitrogen).

6.2.2. Stable transfection of SV40 T-Ag and Luciferase in IG10 and HM-3 cells. The cDNA encoding SV40 T antigen (2600 bp) was cloned into the pZIP-Neo SV(X)1 mammalian expression vector (Addgene, MA). The recombinant plasmid was then stably transfected into IG10 and HM-3 cells using lipofectamine plus^{TM} (Invitrogen, CA). The IG10 and HM-3 cells expressing SV40 T antigen were isolated by selection of the neomycin resistant cells in DMEM media containing 500 µg/ml of neomycin. The cDNA encoding luciferase was cloned into the pSELECT-Hyg expression vector (Invivogen, CA). The recombinant plasmid containing the luciferase gene was stably transfected into IG10 and HM-3 cells expressing SV40 T-Ag as well as parental IG10 and HM-3 cells, using lipofectamine plus^{TM} (Invitrogen, CA). The IG10 and HM-3 cells expressing luciferase, IG10-Luc and HM-3-Luc, were isolated by selection of the hygromycin resistant cells in DMEM media containing 200 µg/ml of hygromycin. The IG10 and HM-3 cells expressing both SV40 T-Ag and luciferase, IG10-SV40-Luc and HM-3-SV40-Luc, were isolated by selection of the neomycin and hygromycin resistant cells in DMEM media containing 500 µg/ml of neomycin and 200 µg/ml of hygromycin.

6.2.3. Analysis of SV40 T-Ag expression in IG10-SV40-Luc and HM-3-SV40-Luc cells. The IG10-SV40-Luc, HM-3-SV40-Luc, IG10-Luc and HM-3-Luc cells were cultured *in vitro*. The cells were harvested when 70% confluency was achieved and lysates were prepared. Protein concentrations of each sample were determined using the Bradford method, and all lysates were normalized to the lowest concentration of protein. Samples were loaded onto 10% SDS-polyacrylamide gels, separated by electrophoresis, and transferred to nitrocellulose membranes (15V for 15 min). Membranes were blocked for 1 h with 5% bovine serum albumin in Tris-Cl buffered saline (TBS), followed by two 5 min washes with 1% Tween-20 in TBS (TTBS). The membranes were incubated for 1 h in TTBS containing a primary mouse anti-mouse SV40 T-Ag antibody (CBD Biosciences clone PAb101), and washed three times for 30 min each with TTBS. Afterwards, the membranes were incubated for 1 h in TTBS containing a horseradish peroxidase-labeled goat anti-mouse IgG antibody, and washed three times for 30 min each with TTBS. Finally the membranes were developed using the ECL substrate (Amersham), and exposed to x-ray film.

6.2.4. Analysis of tumorigenicity of IG10 and HM-3 cells stably transfected with plasmid encoding SV40 T-Ag. IG10-SV40-Luc and IG10-Luc as well as HM-3-SV40-Luc and HM-3-Luc cells were injected in B6C3F1 mice. Three B6C3F1 mice were injected intraperitoneally per cell line at the rate of 1×10^7 cells per mouse. The mice were then monitored for tumor growth by measuring the expression of luciferase *in vivo* by bioluminescent imaging of the mice using the IVIS scan. The mice were scanned weekly until the time they showed obvious tumor growth and had to be sacrificed.

6.2.5. *In vitro* assay of growth curve of HM-3 cells: HM-3 and HM-3-SV40 cells were plated separately in 100 mm tissue culture dishes.1×10^5 cells were plated in each dish. The cells of each cell line were harvested each day after plating, until 7 days and the number of viable cells of each cell type was determined by using the Vi-Cell cell viability analyzer (Beckman Coulter). The Vi-Cell automates the widely accepted trypan blue exclusion method to determine the viability of cells.

6.2.6. Analysis of expression of MHC class I in IG10-Luc, IG10-SV40-Luc, HM-3-Luc and HM-3-SV40-Luc cells by flow cytometry. The cell lines were analyzed for expression of H-2K^b haplotype of MHC class I, on their cell-surface. The cells were also activated by addition of recombinant mouse IFN-gamma (R&D Systems) to measure the induction of MHC class I. After 48 h of incubation *in vitro*, the cells were harvested and stained, and 5×10^5 cells of each cell line were stained per well for H-2K^b of MHC class I (BD Biosciences clone AF6-88.5). The antibodies were used at 1 µg/ml. Labeled antibody were added to the cells of interest and incubated in the dark for 20 min at 4^0C. Isotype control antibodies were also used to set up

compensation. The cells were fixed in 1% paraformaldehyde for 5 min in the dark, washed twice and resuspended in 200 µl of FACS buffer. The cells were analyzed using a FACScan flow cytometer (Becton Dickinson).

6.2.7. Analysis of expression of TAP 1 in IG10-Luc, IG10-SV40-Luc, HM-3-Luc and HM-3-SV40-Luc cells by Western blot. The cell lines were analyzed for expression of TAP 1. The cells activated by addition of recombinant mouse IFN-gamma (R&D Systems) were used as the positive control. After 48 h of incubation *in vitro*, the cells were harvested and lysates were prepared. Protein concentrations of each sample were determined using the Bradford method, and all lysates were normalized to the lowest concentration of protein. Samples were loaded onto 10% SDS-polyacrylamide gels, separated by electrophoresis, and transferred to nitrocellulose membranes (15V for 15 min). Membranes were blocked for 1 h with 5% bovine serum albumin in Tris-Cl buffered saline (TBS), followed by two 5 min washes with 1% Tween-20 in TBS (TTBS). The membranes were incubated for 1 h in TTBS containing a primary mouse anti-mouse TAP-1 (Santa Cruz Biotechnology, catalog # 11465), and washed three times for 30 min each with TTBS. Afterwards, the membranes were incubated for 1 h in TTBS containing a horseradish peroxidase-labeled goat anti-mouse IgG antibody, and washed three times for 30 min each with TTBS. Finally the membranes were developed using the ECL substrate (Amersham), and exposed to x-ray film.

6.2.8. Analysis of SV40 T-Ag expression in IG10-SV40-Luc and HM-3-SV40-Luc tumor cells by Western blot. IG10-SV40-Luc as well as HM-3-SV40-Luc were injected in B6C3F1 mice. Three B6C3F1 mice were injected intraperitoneally per cell line at the rate of 1×10^7 cells per mouse. The mice were then monitored for tumor growth. The mice were sacrificed when they showed obvious tumor growth and ascites as well as solid tumors were collected from these mice. The tumor cells cultured from the ascites and solid tumor collected from B6C3F1 mice injected with the cell lines were analyzed for expression of the tumor antigen, SV40 T-Ag. The cells were harvested and lysates were prepared. Protein concentrations of each sample were determined using the Bradford method, and all lysates were normalized to the lowest concentration of protein. Samples were loaded onto 10% SDS-polyacrylamide gels, separated by electrophoresis, and transferred to nitrocellulose membranes (15V for 15 min). Membranes were blocked for 1 h with 5% bovine serum albumin in Tris-Cl buffered saline (TBS), followed by two 5 min washes with 1% Tween-20 in TBS (TTBS). The membranes were incubated for 1 h in TTBS containing a primary mouse anti-mouse SV40 T-Ag antibody (BD Biosciences, clone PAb101), and washed three times for 30 min each with TTBS. Afterwards, the membranes were incubated for 1 h in TTBS containing a horseradish peroxidase-labeled goat anti-mouse IgG antibody, and washed three times for 30 min each with TTBS. Finally the membranes were developed using the ECL substrate (Amersham), and exposed to x-ray film.

6.2.9. Prophylactic adenoviral immunization. B6C3F1 mice were immunized with the CD40-targeted and untargeted adenovirus. Each mouse received either 10^8 ifu of Ad5-CMV-SV40 T-Ag complexed with 1200ng of CFm40L or 10^8 ifu of Ad5-CMV-SV40 T-Ag by itself, intraperitoneally. Mice that received only PBS, CD40-targeted Ad5-null (10^8 ifu of virus complexed with 1200 ng of CFm40L per mouse), untargeted Ad5-null (10^8 ifu of virus per mouse) and CFm40L (1200 ng per mouse) were used as controls. The mice received a booster dose of the same immunization two weeks later. 10 mice were used per immunization group. Ten days after the booster immunization, the mice were challenged with tumor cells.

6.2.10. Tumor challenge. The IG10(SV40) cells were activated by addition of recombinant mouse IFN-gamma (R&D Systems). After 48 hr of incubation *in vitro*, the cells were harvested from cell culture flasks using 1% trypsin and washed with PBS. The cells were injected into the B6C3F1 mice immunized as described above. Each mouse received 10^7 cells intraperitonealy at day 10 after the boost immunization.

6.2.11. Survival studies. The tumor challenged mice were monitored weekly for changes in tumor growth. The change in bodyweight of the mice was used as an indicator of tumor growth and was measured every week until 11 weeks after challenge with the tumor cells. Mice that exhibited significant tumor burden or pain and distress were euthanized by asphyxiation with CO_2 according to the guidelines of the Institutional Animal Care and Research Advisory Committee at Louisiana State University Health Sciences Center, Shreveport, LA.

6.3. Results

6.3.1. Tumorigenicity of IG10 cells. The anti-tumor efficacy of the CD40-targeted Ad5-CMV-SV40 T-Ag vaccine can be determined by measuring the growth of tumor cells expressing the SV40 T-Ag *in vivo*. Bioluminescent imaging is one of the ways by which tumor progression can be monitored *in vivo*. IG10 cells stably transfected with plasmids encoding SV40T-Ag and luciferase was used as the target tumor cell since it expresses SV40 T-Ag (Fig. 6.1). IG10 cells stably transfected with plasmid encoding for luciferase was used as negative control since it does not express SV40 T-Ag. To confirm the tumor forming potential of the IG10

cells in B6C3F1 mice and to measure the growth of these tumor cells in the mice, three B6C3F1 mice were injected with IG10 cells expressing luciferase (IG10-Luc) at 5×10^7 cells per mouse and *in vivo* bioluminescent imaging of luciferase was used to monitor tumor progression. The mice were scanned for luciferase expression using the IVIS imaging system 24 h after injecting the tumor cells. The mice were then scanned weekly for change in expression of luciferase to monitor the growth of the IG10 tumor cells in B6C3F1 mice. As shown in Fig. 6.2, the mice show marked increase in the expression of luciferase at 1 week post-injection compared with 1 day after injection, indicating increase in growth of the IG10-Luc tumor cells *in vivo*. This is the proof-of-principle that growth of IG10 tumor cells can be monitored by *in vivo* bioluminescent imaging. Survival studies were also done on these animals. The survival time of these non-immunized B6C3F1 mice was approximately 4 weeks post-injection.

6.3.2. Analysis of cell-surface expression of MHC Class I in IG10. Expression of MHC class I on IG10-Luc and IG10-SV40-Luc cells was determined by flow cytometry. These cells were also treated *in vitro* with IFN-gamma to measure the induction of MHC class I after exposure to IFN-gamma. At 48 h after treatment with IFN-gamma, the cells were harvested and analyzed for induction of MHC class I expression on the cell surface. As shown in Fig. 6.3, the MHC class I expression was undetectable by flow cytometry in the naïve IG10-Luc and IG10-SV40-Luc cells. However, the expression of MHC class I increased to 88% in IG10-Luc cells and to 94% in IG10-SV40-Luc cells, when these cells were treated with IFN-gamma. Thus, IG10-Luc and IG10-SV40-Luc cells themselves do not show significant expression of MHC class I. However, the expression of MHC class I in these cells can be induced by treatment with IFN-gamma. Hence, these results suggest that both IG10-SV40-Luc and IG10-Luc cells can be used as target and negative control cells respectively, to measure the induced anti-SV40 T-Ag immune response, but only after treatment with IFN-gamma.

6.3.3. Analysis of TAP-1 expression in IG10. The IG10 cells were also tested for expression of TAP-1 protein before and after treatment with IFN-gamma by Western blot analysis. As shown in Fig. 6.4, IG10-Luc cells (lane 1) and IG10-SV40-Luc cells (lane 3) do not show detectable expression of TAP-1. However, upon treatment with IFN-gamma, both IG10-Luc cells (lane 2) and IG10-SV40-Luc (lane 4) show induction in the expression of TAP-1. Thus, like MHC class I, the IG10-Luc and IG10-SV40-Luc cells, do not show detectable expression of TAP-1. However, the expression was significantly induced upon treatment with IFN-gamma as shown by Western blot analysis. This confirms the results suggesting that IG10-SV40-Luc and IG10-Luc cells can be used as target and negative control cells respectively, to measure the induced anti-SV40 T-Ag immune response, but only after treatment with IFN-gamma.

6.3.4. Analysis of SV40 T-Ag expression in IG10-SV40 tumors. Prior to using IG10-SV40 cells as target cells to measure the induced immune response against SV40 T-Ag, it was important to confirm that the expression of SV40 T-Ag was retained in tumors formed *in vivo*. Thus, to determine expression of SV40 T-Ag, in IG10-SV40 tumors, 5×10^7 IG10-SV40 cells were injected i.p. into B6C3F1 mice. The mice were monitored for tumor growth; after approximately 4 weeks, the mice started to show signs of tumor growth and were sacrificed and examined histopathologically. The IG10-SV40 cells formed both ascites as well as solid tumors *in vivo*. The cells from the ascites as well as solid tumors were cultured *in vitro* and tested for the expression of SV40 T-Ag. As shown in Figure 6.5, the tumor cells cultured from both, the ascites (lane 1) and solid tumor (lane 2) showed expression of SV40 T-Ag. Thus, IG10-SV40 cells retain expression of the target tumor antigen, SV40 T-Ag, in tumors *in vivo*.

6.3.5. Analysis of HM-3 cells stably transfected by expression plasmid encoding SV40 T-Ag for expression of SV40 T-Ag. The HM-3 cells were stably transfected with an expression vector encoding the SV40 T-Ag. The expression of SV40 T-Ag in the stably transfected HM-3 cells was confirmed by Western blot analysis. As shown in Fig. 6.6, the HM-3 cells that were stably transfected with the plasmid encoding SV40 T-Ag (lane 2), did show expression of the SV40 T-Ag. The parental HM-3 cells (lane 1) do not express SV40 T-Ag and was used as the negative control. Thus, the stably transfected HM-3-SV40 cells do express the target tumor antigen, *i.e.,* SV40 T-Ag, and thus can be used as target cells to measure the immune response induced against SV40 T-Ag in B6C3F1 mice.

6.3.6. Tumorigenicity of HM-3 cells. The anti-tumor efficacy of the CD40-targeted Ad5-CMV-SV40 T-Ag vaccine in B6C3F1 mice can be determined by measuring the growth of tumor cells expressing the target SV40 T-Ag in immunized mice. HM-3 cells stably transfected with plasmids encoding SV40T-Ag and luciferase, HM-3-SV40-Luc, were used as the target tumor cells since they expresses SV40 T-Ag (Fig. 6.6). HM-3 cells stably transfected with plasmid encoding for luciferase only, HM-3-Luc, were used as negative control since they do not express SV40 T-Ag. To confirm the tumor-forming potential of HM3(SV40)-Luc and HM-3-Lu cells, three B6C3F1 mice were injected with HM-3-SV40-Luc cells and three mice were injected with

HM-3-Luc cells at 5×10^7 cells per mouse and *in vivo* bioluminescent imaging of luciferase was used to monitor tumor progression. The mice were scanned for luciferase expression using the IVIS imaging system 24 h after injecting the tumor cells. The mice were then scanned weekly for change in expression of luciferase to monitor the growth of the HM-3-SV40-Luc and HM-3-Luc tumor cells in B6C3F1 mice.

At 4 weeks post-injection, the mice injected with HM-3-SV40-Luc cells showed tumor growth and as shown in Fig. 6.7, they also showed marked increase in the expression of luciferase compared with 1day after injection with tumor cells. At 7 weeks post-injection, the B6C3F1 mice injected with HM-3-Luc cells showed signs of tumor growth and also, as shown in Fig. 6.8, increased expression of luciferase compared with day 1 after injection with the tumor cells. This is the proof-of-principle that growth of HM-3-SV40 and HM-3 tumor cells in B6C3F1 mice can be monitored by *in vivo* bioluminescent imaging.

6.3.7. Determination of growth curve of HM-3 cells *in vitro*. The *in vivo* bioluminescent imaging of HM-3 cells in B6C3F1 mice suggested that HM-3-SV40 cells grow and multiply faster than HM-3 cells. To confirm this observation, an *in vitro* assay to determine the growth curve of the HM-3 cells was done. 1×10^5 HM-3 and HM-3-SV40 cells were plated in 100 mm Petri-dishes. The cells were harvested and the number of viable cells of each cell line was counted everyday until 7 days after plating the cells. The growth curve of each cell line was plotted by plotting the total number of viable cells obtained on each day after seeding, against the number of days after plating, at which the cells were counted. The growth curve of HM-3-SV40 cells was higher than the growth curve of HM-3 cells, indicating that HM-3-SV40 proliferates faster than the HM-3 cells. The difference in between the growth rates of the two cell lines was most significant at 6 days after plating the cells, when the total number of viable HM-3-SV40 cells was approximately 7.5×10^6, while it was approximately 3.0×10^6 for HM-3 cells.

6.3.8. Analysis of cell-surface expression of MHC Class I in HM-3. Expression of MHC class I on HM-3-Luc and HM-3-SV40-Luc cells was determined by flow cytometry. These cells were also treated *in vitro* with IFN-gamma to measure the induction of MHC class I after exposure to IFN-gamma. At 48 h after treatment with IFN-gamma, the cells were harvested and analyzed for induction of MHC class I expression on the cell surface. As shown in Fig. 6.10, the MHC class I expression was extremely low in the naïve cells. 1.7 % of HM-3-Luc was MHC class I-positive and 2.3 % of HM-3-SV40-Luc cells were MHC class I-positive before IFN-gamma treatment. However, the expression of MHC class I increased to 88% in HM-3-Luc cells and to 94% in HM-3-SV40-Luc cells, when these cells were treated with IFN-gamma. Thus, HM-3-Luc and HM-3-SV40-Luc cells themselves show insignificant expression of MHC class I. However, the expression of MHC class I in these cells can be induced by treatment with IFN-gamma. Hence, these results suggest that both HM-3-SV40-Luc and HM-3-Luc cells can be used as target and negative control cells respectively, to measure the induced anti-SV40 T-Ag immune response, but only after treatment with IFN-gamma.

6.3.9. Analysis of TAP-1 expression in HM-3. The HM-3 cells were also analyzed for expression of TAP-1 protein before and after treatment with IFN-gamma by Western blot analysis. As shown in Fig. 6.11, HM-3-Luc cells (lane 1) and HM-3-SV40-Luc cells (lane 3) do not show detectable expression of TAP-1. However, upon treatment with IFN-gamma, both HM-3-Luc cells (lane 2) and HM-3-SV40-Luc (lane 4) show marked induction in the expression of TAP-1. Thus, similar to expression of MHC class I, the HM-3-Luc and HM-3-SV40-Luc cells, do not show detectable expression of TAP-1. However, like MHC class I expression again, the expression of TAP-1 was significantly induced upon treatment with IFN-gamma as shown by Western blot analysis. This confirms the results suggesting that HM-3-SV40-Luc and HM-3-Luc cells can be used as target and negative control cells respectively, to measure the induced anti-SV40 T-Ag immune response, but only after treatment with IFN-gamma.

6.3.10. Analysis of SV40 T-Ag expression in HM-3-SV40 tumors. Before using HM-3-SV40 cells as target cells to measure the induced immune response against SV40 T-Ag, it was important to confirm that the expression of SV40 T-Ag was retained in tumors formed *in vivo*. Thus, to determine expression of SV40 T-Ag, in HM-3-SV40 tumors, 5×10^7 HM-3-SV40 cells were injected i.p. into B6C3F1 mice. The mice were monitored for tumor growth; after approximately 4 weeks, the mice started to show signs of tumor growth and were sacrificed and examined histopathologically. The HM-3-SV40 cells formed both ascites as well as solid tumors *in vivo*. The cells from the ascites as well as solid tumors were cultured *in vitro* and tested for the expression of SV40 T-Ag. As shown in Figure 6.12, the tumor cells cultured from both, the ascites (lane 1) and solid tumor (lane 2) showed expression of SV40 T-Ag. Thus, HM-3-SV40 cells retain expression of the target tumor antigen, SV40 T-Ag, in tumors *in vivo*.

6.3.11. Survival studies and analysis of tumor growth in mice immunized with CD40-targeted Ad5-CMV-SV40 T-Ag. The gold standard for the evaluation of an anti-tumor vaccine is the survival studies of the immunized mice upon challenge with the tumor cells. The B6C3F1 mice were immunized with CD40-targeted

as well as untargeted Ad5-CMV-SV40 T-Ag. Mice that received CD40-targeted Ad5-null, untargeted Ad5-null, CFm40L and PBS were used as controls. The immunized and control mice were challenged with IFN-γ treated IG10-SV40 tumor cells. A survival study was performed on these mice. Also, the tumor growth in these mice was analyzed by measuring change in their bodyweight every week.

As shown in figure 6.13, the mice immunized with CD40-targeted Ad5-CMV-SV40 T-Ag as well as untargeted Ad5-CMV-SV40 T-Ag showed 100% survival till 11 weeks after challenge with the tumor cells. While the control mice that received untargeted Ad5-null, CD40-targeted Ad5-null, CFm40L and PBS showed reduced survival rates of 50%, 65%, 78% and 57% respectively, at 11 weeks post-challenge. Likewise, the mice immunized with CD40-targeted and untargeted Ad5-CMV-SV40 T-Ag donot show change in their bodyweight, as significant as that shown by the control mice (figure 6.13). As shown in figure 6.13, at 11 weeks after challenge with the tumor cells, the mice immunized with CD40-targeted and untargeted Ad5-CMV-SV40 T-Ag showed an increase of only 20% in their body weight. While at 11 weeks, the mice that received only PBS showed the highest increase in their bodyweight, of approximately 86%. The animals that were immunized with untargeted Ad5-null, CD40-targeted Ad5-null and the CFm40L alone showed an increase in bodyweight of approximately 70%, 56% and 54%, respectively.

Thus, immunization with both CD40-targeted and untargeted Ad5-CMV-SV40 T-Ag confers protective immunity to B6C3F1 mice against tumor cells expressing SV40 T-Ag, leading to reduced tumor growth and enhanced survival of the tumor challenged mice. The immune response induced by immunization with CD40-targeted Ad5-CMV-SV40 T-Ag is similar to that induced by untargeted Ad5-CMV-SV40 T-Ag, as shown by their similar survival rates and changes in body weight upon challenge with tumor cells expressing SV40 T-Ag. Also, the anti-tumor immune response induced is specific for SV40-T-Ag, as immunization with CD40-targeted and untargeted Ad5-null doesnot confer the same protective response against IG10-SV40 cells. Thus, CD40-targeted adenoviral vector expressing tumor antigen can successfully be used to generate antigen-specific prophylactic anti-tumor immunity in mice.

6.4. Discussion

The IG10 and HM-3 tumor cells were both successfully transfected with plasmids encoding SV40 T-Ag and luciferase as shown by the expression of SV40 T-Ag using Western blot analysis (Figs. 6.1 and 6.6) and expression of luciferase by bioluminescent imaging (Figs. 6.2, 6.7 and 6.8). SV40 T-Ag was the chosen target tumor antigen. Luciferase is an enzyme that acts on a substrate called luciferin and in the enzymatic reaction visible light is emitted. Introducing the *luciferase* gene in the tumor cells enables their visualization by bioluminescent imaging. The tumor forming potential of the stably transfected cells was confirmed in B6C3F1 mice injected with the stably transfected tumor cells.

The B6C3F1 mice injected with IG10-SV40 and IG10-Luc cells showed obvious signs of tumor growth at 4 weeks post-injection. The progression of tumor growth in the mice was also monitored by using bioluminescent imaging. As shown in Fig. 6.2, there was increase in the expression of luciferase in the B6C3F1 mice injected with IG10-Luc cells at 1 week post-injection compared with 1 day after injection, indicating proliferation of the IG10-Luc cells *in vivo* within the first week after injection. Thus, bioluminescent imaging can be used to follow the cell proliferation of IG10-Luc tumor cells in B6C3F1 mice. The IG10-SV40 and IG10-Luc cells formed both, ascites as well as solid tumors in B6C3F1 mice. The retention of SV40 T-Ag expression in tumors formed in mice injected with IG10-SV40 cells was confirmed by Western blot analysis as show in Fig. 6.5. The expression of the components of the antigen processing and presentation pathway such as MHC class I and TAP-1 was also determined to test the efficacy of the IG10-SV40 and IG10-Luc cells to serve as the target and control cells respectively. As shown in Figs. 6.3 and 6.4, both IG10-SV40 and IG10-Luc cells do not show significant expression of MHC class I and TAP-1 by themselves. However, both cell types show significant increase in the expression of both molecules on treatment with IFN-gamma. Thus, IG10-SV40 and IG10-Luc cells can be used as target tumor cells and control tumor cells respectively, but only on treatment with IFN-gamma.

The B6C3F1 mice injected with HM-3-Luc cells showed obvious tumor growth at 7 weeks post-injection. While the mice injected with HM-3-SV40-Luc cells showed obvious tumor growth at 4 weeks after injection. As shown in Fig. 6.7, there was significant increase in the expression of luciferase in B6C3F1 mice injected with HM-3-Luc cells at 7 weeks post-injection compared with 1 day after injection. While, as shown in Fig. 6.8, the mice injected with HM-3-SV40-Luc cells showed significant increase in the expression of luciferase at just 4 weeks after injection. Thus, with the demonstratio that bioluminescent imaging could be used to visualize and monitor the growth of HM-3-SV40-Luc and HM-3-Luc cells in B6C3F1 mice, these results also suggested the rate of growth of HM-3-SV40-Luc cells was greater than that of HM-3-Luc cells.

The *in vitro* analysis of the rate of growth of HM-3-SV40-Luc and HM-3-Luc cells confirmed the rate of proliferation of HM-3-SV40-Luc was greater than that of HM-3-Luc cells. This was not surprising as SV40 T-Ag is known to transform and confer proliferative advantage to cells when introduced into primary cells and established cell lines [134, 135]. The SV40 T-Ag disrupts cell growth control mechanisms primarily by binding to and inactivating the tumor suppressor proteins p53 and pRB family proteins [134]. The fact that HM-3-SV40-Luc cells form tumors faster than HM-3-Luc cells in B6C3F1 mice was considered when doing the survival studies in B6C3F1 mice on immunization with CD40-targeted and untargeted Ad5-CMV-SV40 T-Ag.

Both HM-3-SV40-Luc and HM-3-Luc cells, can be used as the target tumor cells and control tumor cells in the survival studies, but only on treatment with inflammatory agents such as IFN-gamma. As shown in Figs. 6.9 and 6.10, the cells by themselves do not express significant MHC class I and TAP-1, however, there was significant induction in the expression of both of these molecules upon treatment with IFN-gamma. Both MHC class I and TAP-1 are essential for the efficient processing and presentation of tumor antigens on the cell-surface. Fig. 6.11 confirms the retention of expression of the target SV40 T-Ag in the tumors formed by HM-3-SV40-Luc cells in B6C3F1 mice. Thus, IFN-gamma treated HM-3-SV40-Luc cells and HM-3-Luc cells form a good pair of target tumor and control tumor cells respectively, to evaluate the anti-SV40 T-Ag immune response induced in B6C3F1 mice by CD40-targeted Ad5-CMV-SV40 T-Ag. In addition, the tumor progression of these cells can be followed *in vivo* by using bioluminescent imaging. However, the increase in bioluminescence was not consistent with increase in tumor growth at all time points and thus, changes in the weight of the animals should be monitored with bioluminescent imaging to follow the progression of tumor growth of these cell types in the B6C3F1 mice.

The IG10-SV40 tumor cells were used in the tumor challenge studies. The mice immunized with CD40-targeted Ad5-CMV-SV40 T-Ag and untargeted Ad5-CMV-SV40 T-Ag both showed increased survival and reduced tumor growth compared to the control mice. The increase in survival and reduction in tumor growth elicited by CD40-targeted Ad5-CMV-SV40 T-Ag was comparable to that induced by untargeted Ad5-CMV-SV40 T-Ag. Thus, the prophylactic anti-tumor immune response induced by CD40-targeted Ad5-CMV-SV40 T-Ag is similar to that generated by untargeted Ad5-CMV-SV40 T-Ag.

KEY RESEARCH ACCOMPLISHMENTS:

Task 1

- We have characterized the phenotypic changes in vitro in isolated dendritic cells and RAW 264.7 cells after infection with a CD40-targeted Ad vector compared to an untargeted Ad.
- We have demonstrated dramatically enhanced gene transfer using the CD40-targeted Ad5-(SV40 T-Ag)-CFm40L vector
- Infection with the CD40-targeted Ad5-(SV40 T-Ag)-CFm40L vector induced phenotypical maturation and up-regulated cytokine expression.
- We have characterized the phenotypic changes in p38 MAPK, ERK, and Akt signaling pathway activation in vitro in isolated dendritic cells after infection with a CD40-targeted Ad vector compared to an untargeted Ad.

Task 2

- We have established and characterized a syngeneic immunotherapy model of ovarian cancer using the MOVCAR-2 mouse ovarian tumor cell line.
- We have determined the ability of dendritic cells infected with Ad5-(SV40 T-Ag)-CFm40L ex vivo and transferred to host animals, to activate CTLs in vivo against MOVCAR cells.
- We have established and characterized a syngeneic immunotherapy model of ovarian cancer using the IG10 mouse ovarian tumor cell line.
- We have determined the ability of dendritic cells infected with Ad5-SV40 TAg + CFm40L ex vivo and transferred to host animals, to activate CTLs in vivo against IG10 cells.
- We have characterized the induction of MHC II, TAP1 and TAP2 in IG10 cells after treatment with IFN-γ.
- We have determined the ability of dendritic cells infected with Ad5-SV40 TAg + CFm40L in vivo, to activate CTLs against IG10 cells.
- We have demonstrated enhance CTL killing of IG10 target cells by treatment with IFN-γ.

Task 3

- We have established determined the biodistribution in vivo of Ad5-SV40 TAg + CFm40L compared to untargeted Ad5-SV40 TAg.
- We showed that IFN-gamma treated HM-3-SV40-Luc cells and HM-3-Luc cells form a good pair of target tumor and control tumor cells respectively, to evaluate the anti-SV40 T-Ag immune response induced in B6C3F1 mice by CD40-targeted Ad5-CMV-SV40 T-Ag. In addition, the tumor progression of these cells can be followed in vivo by using bioluminescent imaging. However, the increase in bioluminescence was not consistent with increase in tumor growth at all time points and thus, changes in the weight of the animals should be monitored with bioluminescent imaging to follow the progression of tumor growth of these cell types in the B6C3F1 mice.
- We found that the prophylactic anti-tumor immune response induced by CD40-targeted Ad5-CMV-SV40 T-Ag is similar to that generated by untargeted Ad5-CMV-SV40 T-Ag.
- The IG10 and HM-3 tumor cells were both successfully transfected with plasmids encoding SV40 T-Ag and luciferase as shown by the expression of SV40 T-Ag using Western blot analysis and expression of luciferase by bioluminescent imaging.
- The B6C3F1 mice injected with IG10-SV40 and IG10-Luc cells showed obvious signs of tumor growth at 4 weeks post-injection. The progression of tumor growth in the mice was also monitored by using bioluminescent imaging. There was increase in the expression of luciferase in the B6C3F1 mice injected with IG10-Luc cells at 1 week post-injection compared with 1 day after injection, indicating proliferation of the IG10-Luc cells in vivo within the first week after injection.
- We confirmed the retention of SV40 T-Ag expression in tumors formed in mice injected with IG10-SV40 cells y Western blot analysis. The expression of the components of the antigen processing and presentation pathway such as MHC class I and TAP-1 was also determined to test the efficacy of the IG10-SV40 and IG10-Luc cells to serve as the target and control cells respectively. Both IG10-SV40 and IG10-Luc cells do not show significant expression of MHC class I and TAP-1 by themselves. However, both cell types show significant increase in the expression of both molecules on treatment with IFN-gamma.

- The B6C3F1 mice injected with HM-3-Luc cells showed obvious tumor growth at 7 weeks post-injection. While the mice injected with HM-3-SV40-Luc cells showed obvious tumor growth at 4 weeks after injection. As shown in Fig. 4.7, there was significant increase in the expression of luciferase in B6C3F1 mice injected with HM-3-Luc cells at 7 weeks post-injection compared with 1 day after injection. While, as shown in Fig. 4.8, the mice injected with HM-3-SV40-Luc cells showed significant increase in the expression of luciferase at just 4 weeks after injection.
- We confirmed the in vitro analysis of the rate of growth of HM-3-SV40-Luc and HM-3-Luc cells confirmed the rate of proliferation of HM-3-SV40-Luc was greater than that of HM-3-Luc cells. This was not surprising as SV40 T-Ag is known to transform and confer proliferative advantage to cells when introduced into primary cells and established cell lines. The SV40 T-Ag disrupts cell growth control mechanisms primarily by binding to and inactivating the tumor suppressor proteins p53 and pRB family proteins. The fact that HM-3-SV40-Luc cells form tumors faster than HM-3-Luc cells in B6C3F1 mice was considered when doing the survival studies in B6C3F1 mice on immunization with CD40-targeted and untargeted Ad5-CMV-SV40 T-Ag.
- We demonstrated that both HM-3-SV40-Luc and HM-3-Luc cells, can be used as the target tumor cells and control tumor cells in the survival studies, but only on treatment with inflammatory agents such as IFN-gamma. The cells by themselves do not express significant MHC class I and TAP-1, however, there was significant induction in the expression of both of these molecules upon treatment with IFN-gamma. Both MHC class I and TAP-1 are essential for the efficient processing and presentation of tumor antigens on the cell-surface.
- We confirmed the retention of expression of the target SV40 T-Ag in the tumors formed by HM-3-SV40-Luc cells in B6C3F1 mice.
- We used the IG10-SV40 tumor cells in tumor challenge studies. The mice immunized with CD40-targeted Ad5-CMV-SV40 T-Ag and untargeted Ad5-CMV-SV40 T-Ag both showed increased survival and reduced tumor growth compared to the control mice. The increase in survival and reduction in tumor growth elicited by CD40-targeted Ad5-CMV-SV40 T-Ag was comparable to that induced by untargeted Ad5-CMV-SV40 T-Ag.
- The results from the survival studies of the B6C3F1 mice showed that the tumor protective effect induced by CD40-targeted Ad5-CMV-SV40 T-Ag was almost equivalent to that induced by untargeted Ad5-CMV-SV40 T-Ag.

Conclusions

- Western blot analysis of the antigen presenting cells (APCs) showed that the APCs can be successfully transduced using a CD40 targeted adenoviral vector. The expression of the transgene, SV40 T-Ag, as shown by the western blot analysis, occured only in cells that have been transduced with a CD40-targeted adenoviral vector (Ad5-SV40 T-Ag).
- Flow cytometric analyses of the APCs showed an increase in the expression of the cell surface activation marker CD40 in dendritic cells and untreated RAW cells that have been transduced with the CD40-targeted adenoviral vector compared to the cells that were untransduced or transduced with the adenoviral vector alone.
- Bio-plex cytokine assay showed an increased secretion of cytokines by the APCs that have been transduced with the CD40-targeted adenoviral vector compared to the cells that were untransduced or transduced with adenoviral vector alone.
- These results demonstrate that APCs can be successfully transduced using a CD40-targeted adenoviral vector and these transduced APCs show promise as candidates for use in tumor immunotherapy.
- We have demonstrated that direct immunization of mice in situ with a CD40-targeted Ad together with IFN-g treatment of target cells is effective in inducing an antigen-specific CTL response to SV40 T-Ag.
- Western blot analysis of the phosphorylated forms of p38 MAPK, ERK, and Akt demonstrate activation of these signaling pathways by infection of dendritic cells with Ad5-SV40 TAg + CFm40L.
- Characterization of the IG10 cell line in syngeneic mice demonstrate that it can provide a useful model for peritoneal carcinomatosis which is similar to the advanced stages of ovarian cancer in humans.
- Western blot analysis of IG10 clones demonstrate stable transfection of the SV40 TAg.
- Splenocytes from mice in the vaccination group receiving DCs transduced with Ad5-SV40 TAg exhibited specific lysis against IG10 clones expressing SV40 TAg, but not against parental IG10 cells or IG10 clone 2 expressing GFP. However, administration of the SV40 TAg alone is not sufficient to stimulate a strong immune response.

- Pre-treatment with an adenoviral vector expressing the murine interferon-gamma (Ad-IFN-γ) enhances CTL lysis of IG10 target cells.
- Flow cytometric results demonstrate up-regulation of MHC II by pre-treatment with IFN-γ.
- Western blot assays demonstrate up-regulation of TAP1 and TAP2 by pre-treatment with IFN-γ.
- Splenocytes from mice in the vaccination group receiving Ad5-SV40 TAg +CFm40L exhibited specific lysis against IG10 clones expressing SV40 TAg, but not against parental IG10 cells or IG10 clone 2 expressing GFP.
- Pre-treatment with an adenoviral vector expressing the murine interferon-gamma (Ad-IFN-γ) enhances CTL lysis of IG10 target cells.
- Biodistribution of Ad5-SV40 TAg +CFm40L in vivo compared to untargeted Ad5-SV40 TAg demonstrated significantly lower liver transduction.
- Bioluminescent imaging can be used to follow the cell proliferation of IG10-Luc tumor cells in B6C3F1 mice. The IG10-SV40 and IG10-Luc cells formed both, ascites as well as solid tumors in mice
- IG10-SV40 and IG10-Luc cells can be used as target tumor cells and control tumor cells respectively, but only on treatment with IFN-gamma. B6C3F1 mice.
- With the demonstratio that bioluminescent imaging could be used to visualize and monitor the growth of HM-3-SV40-Luc and HM-3-Luc cells in B6C3F1 mice, these results also suggested the rate of growth of HM-3-SV40-Luc cells was greater than that of HM-3-Luc cells.
- The results from the survival studies was not in accordance with our hypothesis that CD40-targeted Ad5-CMV-SV40 T-Ag would infect DCs more efficiently than untargeted Ad5-CMV-SV40 T-Ag, and will thus induce a greater SV40 T-Ag specific anti-tumor immune response in mice than untargeted Ad5-CMV-SV40 T-Ag. One possibility is that SV40 T-Ag is a highly immunogenic antigen and thus even minimal infection that may be achieved by untargeted Ad5-CMV-SV40 T-Ag is sufficient to induce an immune response as strong as that induced by CD40-targeted Ad5-CMV-SV40 T-Ag. Another possibility is that though there was no difference observed in the immunization potential of CD40-targeted and untargeted Ad5-CMV-SV40 T-Ag in the prophylactic tumor model, a therapeutic model could reveal a difference in between the immune responses. It is much more difficult to achieve therapeutic immunity than it is to achieve protective immunity by anti-cancer vaccines because the tumor cells have already evolved and adopted various strategies to avoid elimination by the immune system, such as down-modulation of MHC expression, induction of regulatory T-cells, etc. A third possibility is that although CD40-targeted Ad5-CMV-SV40 T-Ag generated a the tumor protective effect similar to that induced by untargeted Ad5-CMV-SV40 T-Ag in naïve B6C3F1 mice, it may generate an enhanced immune response compared to the untargeted Ad5-CMV-SV40 T-Ag in mice pre-exposed to adenovirus. Mice pre-exposed to adenovirus develop neutralizing antibodies to adenovirus, which dampen the efficacy of the adenoviral gene therapy. Prior exposure to adenovirus has primed most humans with rapid neutralizing antibody against re-exposure to adenovirus.

REPORTABLE OUTCOMES:

Genetic Immunotherapy Targeted to Antigen Presenting Cells Using a CD40-Targeted Adenoviral Vector (2005) Disha A. Mody, Larry Smart, Yoshinobu Odaka, Xiao L. Li, Cigdem E. Yilmaz, Alexander V. Pereboev, J. Michael Mathis American Society of Gene Therapy Eighth Annual Meeting. Abstract 274.

Changes in Maturation Profiles of Dendritic Cells Transduced with a CD40-Targeted Adenoviral Vector (2006) Disha A. Mody, Alexander V. Pereboev, Don A. Sibley, David T. Curiel, J. Michael Mathis American Society of Gene Therapy Ninth Annual Meeting. Abstract 836.

CD40-Targeted Adenoviral Vector Transduction of Dendritic Cells (2007) Disha Mody, Yoshinobu Odaka, Jagat Poduturri, Xiao L. Li, David T. Curiel, Alexander V. Pereboev, and J. Michael Mathis. American Society of Gene Therapy Tenth Annual Meeting. May 30 - June 3. Abstract 33.

CD40-Targeted Adenoviral Vector Transduction of Dendritic Cells (2007) Disha A. Mody, Yoshinobu Odaka, Jagat Podduturi, Xiao L. Li, David T. Curiel, Alexander V. Pereboev, and J. Michael Mathis. European Society of Cell and Gene Therapy Fifteenth Annual Meeting. October 27 - 30. Abstract 257.

Evaluation of Target Antigen Immunogenicity In Vivo Using a CD40-Targeted Adenovirus Model Disha Mody, Bing Cheng, Jagat Podduturi, Don A. Sibley, Yoshinobu Odaka, Larry Smart, Xiao L. Li, David T. Curiel, Alexander Pereboev, J. Michael Mathis. (2008). American Society of Gene Therapy Eleventh Annual Meeting. Abstract 554.

Irina D. Florea, Disha Mody, Tina C. Lavranos, Disha Mody, Stephen B. Pruett, and J. Michael Mathis (2009) “characterization of a mouse ovarian carcinoma cell line: a syngeneic model for the development of novel cancer therapeutics”, Manuscript in preparation.

Irina D. Florea, Disha Mody, Tina C. Lavranos, Susan Boling, Stephen B. Pruett, and J. Michael Mathis. Characterization of the effects of interferon-gamma delivered via an adenoviral vector on a mouse ovarian carcinoma cell line. 2009. Manuscript in preparation.

Disha A. Mody, Yoshinobu Odaka, Jagat Podduturi, Xiao L. Li, David T. Curiel, Alexander V. Pereboev, and J. Michael Mathis. CD40-Targeted Adenoviral Vector Transduction of Dendritic Cells. 2009. Manuscript in preparation.

Disha A. Mody, Yoshinobu Odaka, Jagat Podduturi, Xiao L. Li, David T. Curiel, Alexander V. Pereboev, and J. Michael Mathis. Dendritic Cell-Based Genetic Immunotherapy for Ovarian Cancer. 2009. Manuscript in preparation.

CONCLUSION:

Our results show that CD40-targeted Ad5-CMV-SV40 T-Ag successfully elicits a protective SV40 T-Ag specific anti-tumor immune response in mice and induces reduced liver toxicity compared to untargeted Ad5-CMV-SV40 T-Ag. To the best of our knowledge, this is the first study to show a modified Ad5 vector to be both, potent and safe. Several studies have demonstrated either potency or reduced liver toxicity of modified adenoviral vectors, but not both. Curiel et al have shown tumor targeting and hepatic untargeting by a Coxackie/Adenovirus receptor (sCAR) ectodomain anti-carcinoembryonic antigen (MFE) bispecific adaptor [126]. However, our results have not only shown successful DC-targeting and hepatic untargeting, but also successful induction of anti-tumor immune response and reduced liver inflammation by CD40-targeted adenovirus compared to untargeted adenovirus. According to our knowledge, our study is the first to demonstrate potency as well as safety of a therapeutic targeted adenoviral vector *in vivo*.

The goal was to target antigen presenting cells like DCs using adenoviral vector and express tumor antigens in them to elicit an anti-tumor immune response. However, adenovirus cannot efficiently infect DCs because of deficiency of CAR on DC cell surface. Thus, we used a bispecific adapter molecule called CFm40L, to target adenovirus to cells that express CD40, which includes DCs. CD40-targeted adenoviral vectors are known to infect DCs and induce antigen specific anti-tumor immune response more efficiently than untargeted adenovirus [103]. Our results also showed that DCs were more efficiently infected by CD40-targeted Ad5-CMV-SV40 T-Ag than untargeted Ad5-CMV-SV40 T-Ag. The DCs infected by CD40-targeted Ad5-CMV-SV40 T-Ag showed increased potential for activating lymphocytes that was marked by elevated phenotypic expression of co-stimulatory molecules and enhanced secretion of inflammatory cytokines and chemokines by infected DCs. Thus, our results demonstrated that CD40-targeted Ad5-CMV-SV40 T-Ag can efficiently infect APCs *in vitro* and increase their activation potential by increasing their maturation status.

Our results also showed an antigen-specific CTL response and a prophylactic anti-tumor immune response in B6C3F1 mice immunized with CD40-targeted Ad5-CMV-SV40 T-Ag. The results from both, the *in vivo* CTL assay and survival studies of the B6C3F1 mice showed that the anti-SV40 T-Ag immune response induced by CD40-targeted Ad5-CMV-SV40 T-Ag was almost equivalent to that induced by untargeted Ad5-CMV-SV40 T-Ag. This was not in accordance with our hypothesis that CD40-targeted Ad5-CMV-SV40 T-Ag would infect DCs more efficiently than untargeted Ad5-CMV-SV40 T-Ag, and will thus induce a greater SV40 T-Ag specific anti-tumor immune response in mice than untargeted Ad5-CMV-SV40 T-Ag. One possibility is that SV40 T-Ag is a highly immunogenic antigen and thus even minimal infection that may be achieved by untargeted Ad5-CMV-SV40 T-Ag is sufficient to induce an immune response as strong as that induced by CD40-targeted Ad5-CMV-SV40 T-Ag. And thus, there was no difference observed in the killing of target cells by CTLs in the *in vivo* CTL assay, and in the survival of tumor-challenged B6C3F1 mice immunized by CD40-targeted and untargeted Ad5-CMV-SV40 T-Ag. Another possibility is that though there was no difference observed in the immunization potential of CD40-targeted and untargeted Ad5-CMV-SV40 T-Ag in the prophylactic model, the therapeutic model could reveal the probable difference in between the immune responses. It is much more difficult to achieve therapeutic immunity than it is to achieve protective immunity by anti-cancer vaccines because the tumor cells have already evolved and adopted various strategies to avoid elimination by the immune system, such as down-modulation of MHC expression, induction of regulatory T-cells, *etc.* Therefore, though there was no difference in the protective immunity induced by CD40-targeted and untargeted Ad5-CMV-SV40 T-Ag, it cannot be ruled out there might be a difference in their potential to induce therapeutic immunity. A third possibility is that although CD40-targeted Ad5-CMV-SV40 T-Ag generated an anti-SV40 T-Ag specific immune response similar to that induced by untargeted Ad5-CMV-SV40 T-Ag in naïve B6C3F1 mice, it may generate an enhanced immune response compared to the untargeted Ad5-CMV-SV40 T-Ag in mice pre-exposed to adenovirus. Mice pre-exposed to adenovirus develop neutralizing antibodies to adenovirus, which dampen the efficacy of the adenoviral gene therapy. Prior exposure to adenovirus has primed most humans with rapid neutralizing antibody against re-exposure to adenovirus.

The presence of Ad5-specific neutralizing antibody is one of the major obstacles in the use Ad5 serotype for systemic gene therapy. Various approaches used to overcome this obstacle include: 1) deletion of viral genes to reduce the number of viral proteins synthesized [120-122], *e.g.,* gutless adenovirus, and 2) modification of the capsid proteins, genetic as well as non-genetic, such that they are less immunogenic [123]. The CD40-targeted adenovirus is coated with the CFm40L bi-specific adaptor molecule and thus the antigenic fiber knob domain of the virus and other cell surface structures are masked. As a result, CD40-targeted adenovirus may be able to sustain longer *in vivo* than untargeted adenovirus in the presence of Ad-specific neutralizing antibodies, and thus have a higher therapeutic index. Studies by Huang et al, which show that

neutralizing antibodies had no inhibitory effects on CFm40L mediated Ad-luc transduction of human DCs *in vitro*, supports this possibility [136]. Regardless of all possibilities, there is no doubt that the CD40-targeted Ad5-CMV-SV40 T-Ag is an effective adenoviral vaccine, whose potency is as good as that of untargeted Ad5-CMV-SV40 T-Ag, if not better.

We also observed reduced liver toxicity in B6C3F1 mice immunized with CD40-targeted Ad5-CMV-SV40 T-Ag compared with mice immunized with untargeted Ad5-CMV-SV40 T-Ag. Our hypothesis was that by targeting adenovirus to CD40, the natural hepato-tropism of the adenovirus is altered, leading to hepatic un-targeting and reduced liver toxicity. Our results showed there was reduced infection and inflammation of the liver in B6C3F1 mice immunized with CD40-targeted Ad5-CMV-SV40 T-Ag than those immunized with untargeted Ad5-CMV-SV40 T-Ag. Thus, our results support our hypothesis that targeting adenovirus to CD40, de-targets it from the liver, resulting in reduced liver inflammation compared with untargeted adenovirus. Therefore, our studies demonstrate that CD40-targeted Ad5-CMV-SV40 T-Ag is a safer vaccine than untargeted Ad5-CMV-SV40 T-Ag.

The generation of an effective anti-tumor immunity consists of two components: a) successful induction of anti-tumor immune response, and b) effective killing of the tumor cells mediated by activated immune cells, *i.e.,* a successful effector phase. Defects in the induction of the immune response due to poor-presentation of the tumor antigens by tumor cells, can be overcome with CD40-targeted adenoviral vector as it targets expression of tumor antigens to professional antigen presenting cells like the DCs. However, other factors or defects that render the tumor cells invisible to the immune system or resistant to killing by the immune cells, such as expression of poorly immunogenic antigens, down-modulation or loss of expression of MHC by tumor cells, secretion of immunosuppressive cytokines or induction of regulatory T-cells, etc. cannot be overcome by using the CD40-targeted adenoviral vaccine by itself [110]. In that situation other adjuvants, like cytokine therapy to increase the inflammation in the tumor milieu, neutralizing antibodies for immunosuppressive cytokines such as IL-10 and TGF-β or depletion of regulatory T-cells along with induction of immune response using CD40-targeted adenoviral vaccine will be necessary for the successful elimination of tumor cells. Another possible approach to overcome the above problems would be to use highly immunogenic antigens not expressed by the tumor cells to immunize the diseased animals using CD40-targeted adenoviral vaccine, and then use tumor targeted vectors to express the immunogenic antigen specifically in the tumor cells. This would mimic the prophylactic model of immunization where the antigen-specific immune response is already induced and active before the antigen is expressed in the tumor cells and thus the infected tumor cells will be more sensitive to killing by the activated immune cells. This approach would have several advantages such as exploitation of known immunogenic antigens to induce a strong antigen specific immune response, expression of the antigens specifically by the tumor cells, thus avoiding the possibility of an autoimmune response. This strategy would also help to overcome the strategies used by the tumor cells to avoid immune-mediated killing, such as down-modulation of expression of the tumor specific antigen, induction of antigen specific regulatory T-cells, *etc.* The CTLs and other immune cells which are already activated, will detect and kill the tumor cells expressing the antigen, before they have had a chance to evolve and adopt these strategies, taking advantage of the prophylactic mode of immunization.

Apart from its immunization potential, CD40-targeted adenoviral vector can also be used in evaluating immunogenicity of newly identified tumor antigens. The major challenge in making efficient vaccines against tumor antigens is identifying immunogenic antigens against which an effective immune response can be induced. Thus, selecting highly immunogenic antigens will greatly increase the prospects of making an effective anti-tumor vaccine. The current process of evaluating the target antigens for their potential use in vaccination is time-consuming, cumbersome and less efficient [137]. CD40-targeted adenoviral vectors expressing target antigen can be used to infect APCs *in vivo* and induce an antigen-specific immune response. The induced immune responses can then be measured and compared with compare the immunogenicity of different target antigens. This method has the advantage of using the APC machinery to address questions about antigen processing and HLA binding, rather than trying to reconstitute antigen processing *in vitro*, predicting and then testing the binding of peptides to MHC molecules *in vitro*. In addition, this is an *in vivo* model, which is less likely to be influenced by external factors.

Thus, the ability of CD40-targeted adenovirus expressing target antigen to induce protective antigen-specific immunity *in vivo* without causing significant liver toxicity makes it an attractive candidate for use as anti-tumor vaccine. Future studies involve pre-clinical evaluation of CD40-targeted Ad vectors to induce specific therapeutic immunity using clinically relevant ovarian tumor antigens, such as MUC-1.

REFERENCES:

1. Waldmann, T.A., *Immunotherapy: past, present and future.* Nat Med, 2003. 9(3): p. 269-77.
2. Coley, W.B., *The treatment of malignant tumors by repeated inoculations of erysipelas. With a report of ten original cases. 1893.* Clin Orthop Relat Res, 1991(262): p. 3-11.
3. Herr, H.W. and A. Morales, *History of bacillus Calmette-Guerin and bladder cancer: an immunotherapy success story.* J Urol, 2008. 179(1): p. 53-6.
4. Park, H.W., *Germs, hosts, and the origin of Frank Macfarlane Burnet's concept of "self " and "tolerance," 1936-1949.* J Hist Med Allied Sci, 2006. 61(4): p. 492-534.
5. Dunn, G.P., et al., *Cancer immunoediting: from immunosurveillance to tumor escape.* Nat Immunol, 2002. 3(11): p. 991-8.
6. Blattman, J.N. and P.D. Greenberg, *Cancer immunotherapy: a treatment for the masses.* Science, 2004. 305(5681): p. 200-5.
7. Urban, J.L. and H. Schreiber, *Tumor antigens.* Annu Rev Immunol, 1992. 10: p. 617-44.
8. Boon, T., et al., *Tumor antigens recognized by T lymphocytes.* Annu Rev Immunol, 1994. 12: p. 337-65.
9. Boon, T. and P. van der Bruggen, *Human tumor antigens recognized by T lymphocytes.* J Exp Med, 1996. 183(3): p. 725-9.
10. Rosenberg, S.A., *A new era for cancer immunotherapy based on the genes that encode cancer antigens.* Immunity, 1999. 10(3): p. 281-7.
11. Melief, C.J., et al., *Strategies for immunotherapy of cancer.* Adv Immunol, 2000. 75: p. 235-82.
12. Fenton, R.G. and D.L. Longo, *Genetic instability and tumor cell variation: implications for immunotherapy.* J Natl Cancer Inst, 1995. 87(4): p. 241-3.
13. Stoler, D.L., et al., *The onset and extent of genomic instability in sporadic colorectal tumor progression.* Proc Natl Acad Sci U S A, 1999. 96(26): p. 15121-6.
14. Rosenberg, S.A., *Cancer vaccines based on the identification of genes encoding cancer regression antigens.* Immunol Today, 1997. 18(4): p. 175-82.
15. Chen, L., *Immunological ignorance of silent antigens as an explanation of tumor evasion.* Immunol Today, 1998. 19(1): p. 27-30.
16. Melief, C.J. and W.M. Kast, *Cytotoxic T lymphocyte therapy of cancer and tumor escape mechanisms.* Semin Cancer Biol, 1991. 2(5): p. 347-54.
17. Maudsley, D.J. and J.D. Pound, *Modulation of MHC antigen expression by viruses and oncogenes.* Immunol Today, 1991. 12(12): p. 429-31.
18. Solana, R., et al., *MHC class I antigen expression is inversely related with tumor malignancy and ras oncogene product (p21ras) levels in human breast tumors.* Invasion Metastasis, 1992. 12(3-4): p. 210-7.
19. Garrido, F., et al., *Natural history of HLA expression during tumour development.* Immunol Today, 1993. 14(10): p. 491-9.
20. Zheng, P., et al., *Two mechanisms for tumor evasion of preexisting cytotoxic T-cell responses: lessons from recurrent tumors.* Cancer Res, 1999. 59(14): p. 3461-7.
21. Johnsen, A.K., et al., *Deficiency of transporter for antigen presentation (TAP) in tumor cells allows evasion of immune surveillance and increases tumorigenesis.* J Immunol, 1999. 163(8): p. 4224-31.
22. Gobbi, G., et al., *Expression of HLA class I antigen and proteasome subunits LMP-2 and LMP-10 in primary vs. metastatic breast carcinoma lesions.* Int J Oncol, 2004. 25(6): p. 1625-9.
23. Kamarashev, J., et al., *TAP1 down-regulation in primary melanoma lesions: an independent marker of poor prognosis.* Int J Cancer, 2001. 95(1): p. 23-8.
24. St-Pierre, Y., *Organizing a tete-a-tete between cell adhesion molecules and extracellular proteases: a risky business that could lead to the survival of tumor cells.* Front Biosci, 2005. 10: p. 1040-9.
25. Pistoia, V., et al., *Soluble HLA-G: Are they clinically relevant?* Semin Cancer Biol, 2007. 17(6): p. 469-79.
26. Witter, R.L., E.J. Smith, and L.B. Crittenden, *Tolerance, viral shedding, and neoplasia in chickens infected with non-defective reticuloendotheliosis viruses.* Avian Dis, 1981. 25(2): p. 374-94.
27. Durda, P.J., et al., *Induction of "antigen silencing" in melanomas by oncostatin M: down-modulation of melanocyte antigen expression.* Mol Cancer Res, 2003. 1(6): p. 411-9.
28. Thomas, D.A. and J. Massague, *TGF-beta directly targets cytotoxic T cell functions during tumor evasion of immune surveillance.* Cancer Cell, 2005. 8(5): p. 369-80.
29. Beckebaum, S., et al., *Increased levels of interleukin-10 in serum from patients with hepatocellular carcinoma correlate with profound numerical deficiencies and immature phenotype of circulating dendritic cell subsets.* Clin Cancer Res, 2004. 10(21): p. 7260-9.

30. Krishnakumar, S., et al., *Expression of Fas ligand in retinoblastoma.* Cancer, 2004. 101(7): p. 1672-6.
31. Li, S.Y., et al., *Influence of FasL gene expression on hepatic metastasis of colorectal carcinoma.* Hepatobiliary Pancreat Dis Int, 2004. 3(2): p. 226-9.
32. Rivoltini, L., et al., *Immunity to cancer: attack and escape in T lymphocyte-tumor cell interaction.* Immunol Rev, 2002. 188: p. 97-113.
33. Liyanage, U.K., et al., *Increased prevalence of regulatory T cells (Treg) is induced by pancreas adenocarcinoma.* J Immunother (1997), 2006. 29(4): p. 416-24.
34. Elpek, K.G., et al., *CD4+CD25+ T regulatory cells dominate multiple immune evasion mechanisms in early but not late phases of tumor development in a B cell lymphoma model.* J Immunol, 2007. 178(11): p. 6840-8.
35. Nencioni, A., et al., *Anticancer vaccination strategies.* Ann Oncol, 2004. 15 Suppl 4: p. iv153-60.
36. Scanlan, M.J., et al., *Cancer/testis antigens: an expanding family of targets for cancer immunotherapy.* Immunol Rev, 2002. 188: p. 22-32.
37. Banchereau, J. and R.M. Steinman, *Dendritic cells and the control of immunity.* Nature, 1998. 392(6673): p. 245-52.
38. Steinman, R.M., et al., *Antigen capture, processing, and presentation by dendritic cells: recent cell biological studies.* Hum Immunol, 1999. 60(7): p. 562-7.
39. Albert, M.L., B. Sauter, and N. Bhardwaj, *Dendritic cells acquire antigen from apoptotic cells and induce class I-restricted CTLs.* Nature, 1998. 392(6671): p. 86-9.
40. Ridge, J.P., F. Di Rosa, and P. Matzinger, *A conditioned dendritic cell can be a temporal bridge between a CD4+ T-helper and a T-killer cell.* Nature, 1998. 393(6684): p. 474-8.
41. Schoenberger, S.P., et al., *T-cell help for cytotoxic T lymphocytes is mediated by CD40-CD40L interactions.* Nature, 1998. 393(6684): p. 480-3.
42. Bennett, S.R., et al., *Help for cytotoxic-T-cell responses is mediated by CD40 signalling.* Nature, 1998. 393(6684): p. 478-80.
43. McArthur, J.G. and R.C. Mulligan, *Induction of protective anti-tumor immunity by gene-modified dendritic cells.* J Immunother (1997), 1998. 21(1): p. 41-7.
44. Zitvogel, L., et al., *Therapy of murine tumors with tumor peptide-pulsed dendritic cells: dependence on T cells, B7 costimulation, and T helper cell 1-associated cytokines.* J Exp Med, 1996. 183(1): p. 87-97.
45. Mayordomo, J.I., et al., *Bone marrow-derived dendritic cells pulsed with synthetic tumour peptides elicit protective and therapeutic antitumour immunity.* Nat Med, 1995. 1(12): p. 1297-302.
46. Ribas, A., et al., *Genetic immunization for the melanoma antigen MART-1/Melan-A using recombinant adenovirus-transduced murine dendritic cells.* Cancer Res, 1997. 57(14): p. 2865-9.
47. De Veerman, M., et al., *Retrovirally transduced bone marrow-derived dendritic cells require CD4+ T cell help to elicit protective and therapeutic antitumor immunity.* J Immunol, 1999. 162(1): p. 144-51.
48. Okada, H., et al., *Bone marrow-derived dendritic cells pulsed with a tumor-specific peptide elicit effective anti-tumor immunity against intracranial neoplasms.* Int J Cancer, 1998. 78(2): p. 196-201.
49. Tuting, T., et al., *Autologous human monocyte-derived dendritic cells genetically modified to express melanoma antigens elicit primary cytotoxic T cell responses in vitro: enhancement by cotransfection of genes encoding the Th1-biasing cytokines IL-12 and IFN-alpha.* J Immunol, 1998. 160(3): p. 1139-47.
50. Ossevoort, M.A., et al., *Dendritic cells as carriers for a cytotoxic T-lymphocyte epitope-based peptide vaccine in protection against a human papillomavirus type 16-induced tumor.* J Immunother Emphasis Tumor Immunol, 1995. 18(2): p. 86-94.
51. Celluzzi, C.M. and L.D. Falo, Jr., *Physical interaction between dendritic cells and tumor cells results in an immunogen that induces protective and therapeutic tumor rejection.* J Immunol, 1998. 160(7): p. 3081-5.
52. Celluzzi, C.M., et al., *Peptide-pulsed dendritic cells induce antigen-specific CTL-mediated protective tumor immunity.* J Exp Med, 1996. 183(1): p. 283-7.
53. Brossart, P., et al., *Virus-mediated delivery of antigenic epitopes into dendritic cells as a means to induce CTL.* J Immunol, 1997. 158(7): p. 3270-6.
54. Boczkowski, D., et al., *Dendritic cells pulsed with RNA are potent antigen-presenting cells in vitro and in vivo.* J Exp Med, 1996. 184(2): p. 465-72.
55. De Bruijn, M.L., et al., *Immunization with human papillomavirus type 16 (HPV16) oncoprotein-loaded dendritic cells as well as protein in adjuvant induces MHC class I-restricted protection to HPV16-induced tumor cells.* Cancer Res, 1998. 58(4): p. 724-31.

56. Fields, R.C., K. Shimizu, and J.J. Mule, *Murine dendritic cells pulsed with whole tumor lysates mediate potent antitumor immune responses in vitro and in vivo.* Proc Natl Acad Sci U S A, 1998. 95(16): p. 9482-7.
57. Gong, J., et al., *Induction of antigen-specific antitumor immunity with adenovirus-transduced dendritic cells.* Gene Ther, 1997. 4(10): p. 1023-8.
58. Gong, J., et al., *Induction of antitumor activity by immunization with fusions of dendritic and carcinoma cells.* Nat Med, 1997. 3(5): p. 558-61.
59. Paglia, P., et al., *Murine dendritic cells loaded in vitro with soluble protein prime cytotoxic T lymphocytes against tumor antigen in vivo.* J Exp Med, 1996. 183(1): p. 317-22.
60. Porgador, A. and E. Gilboa, *Bone marrow-generated dendritic cells pulsed with a class I-restricted peptide are potent inducers of cytotoxic T lymphocytes.* J Exp Med, 1995. 182(1): p. 255-60.
61. Song, W., et al., *Dendritic cells genetically modified with an adenovirus vector encoding the cDNA for a model antigen induce protective and therapeutic antitumor immunity.* J Exp Med, 1997. 186(8): p. 1247-56.
62. Toes, R.E., et al., *Protective anti-tumor immunity induced by vaccination with recombinant adenoviruses encoding multiple tumor-associated cytotoxic T lymphocyte epitopes in a string-of-beads fashion.* Proc Natl Acad Sci U S A, 1997. 94(26): p. 14660-5.
63. Wan, Y., et al., *Dendritic cells transduced with an adenoviral vector encoding a model tumor-associated antigen for tumor vaccination.* Hum Gene Ther, 1997. 8(11): p. 1355-63.
64. Tjoa, B.A., et al., *Evaluation of phase I/II clinical trials in prostate cancer with dendritic cells and PSMA peptides.* Prostate, 1998. 36(1): p. 39-44.
65. Hsu, F.J., et al., *Vaccination of patients with B-cell lymphoma using autologous antigen-pulsed dendritic cells.* Nat Med, 1996. 2(1): p. 52-8.
66. Nestle, F.O., et al., *Vaccination of melanoma patients with peptide- or tumor lysate-pulsed dendritic cells.* Nat Med, 1998. 4(3): p. 328-32.
67. Tjandrawan, T., et al., *Autologous human dendriphages pulsed with synthetic or natural tumor peptides elicit tumor-specific CTLs in vitro.* J Immunother (1997), 1998. 21(2): p. 149-57.
68. van Elsas, A., et al., *Peptide-pulsed dendritic cells induce tumoricidal cytotoxic T lymphocytes from healthy donors against stably HLA-A*0201-binding peptides from the Melan-A/MART-1 self antigen.* Eur J Immunol, 1996. 26(8): p. 1683-9.
69. Abdel-Wahab, Z., et al., *Human dendritic cells, pulsed with either melanoma tumor cell lysates or the gp100 peptide(280-288), induce pairs of T-cell cultures with similar phenotype and lytic activity.* Cell Immunol, 1998. 186(1): p. 63-74.
70. Ashley, D.M., et al., *Bone marrow-generated dendritic cells pulsed with tumor extracts or tumor RNA induce antitumor immunity against central nervous system tumors.* J Exp Med, 1997. 186(7): p. 1177-82.
71. Arthur, J.F., et al., *A comparison of gene transfer methods in human dendritic cells.* Cancer Gene Ther, 1997. 4(1): p. 17-25.
72. Nair, S.K., et al., *Induction of primary carcinoembryonic antigen (CEA)-specific cytotoxic T lymphocytes in vitro using human dendritic cells transfected with RNA.* Nat Biotechnol, 1998. 16(4): p. 364-9.
73. Aicher, A., et al., *Successful retroviral mediated transduction of a reporter gene in human dendritic cells: feasibility of therapy with gene-modified antigen presenting cells.* Exp Hematol, 1997. 25(1): p. 39-44.
74. Bello-Fernandez, C., et al., *Efficient retrovirus-mediated gene transfer of dendritic cells generated from CD34+ cord blood cells under serum-free conditions.* Hum Gene Ther, 1997. 8(14): p. 1651-8.
75. Reeves, M.E., et al., *Retroviral transduction of human dendritic cells with a tumor-associated antigen gene.* Cancer Res, 1996. 56(24): p. 5672-7.
76. Henderson, R.A., et al., *Retroviral expression of MUC-1 human tumor antigen with intact repeat structure and capacity to elicit immunity in vivo.* J Immunother (1997), 1998. 21(4): p. 247-56.
77. Butterfield, L.H., et al., *Generation of melanoma-specific cytotoxic T lymphocytes by dendritic cells transduced with a MART-1 adenovirus.* J Immunol, 1998. 161(10): p. 5607-13.
78. Tillman, B.W., et al., *Adenoviral vectors targeted to CD40 enhance the efficacy of dendritic cell-based vaccination against human papillomavirus 16-induced tumor cells in a murine model.* Cancer Res, 2000. 60(19): p. 5456-63.
79. Wang, J., et al., *Eliciting T cell immunity against poorly immunogenic tumors by immunization with dendritic cell-tumor fusion vaccines.* J Immunol, 1998. 161(10): p. 5516-24.
80. Gong, J., et al., *Reversal of tolerance to human MUC1 antigen in MUC1 transgenic mice immunized with fusions of dendritic and carcinoma cells.* Proc Natl Acad Sci U S A, 1998. 95(11): p. 6279-83.

81. Cranmer, L.D., K.T. Trevor, and E.M. Hersh, *Clinical applications of dendritic cell vaccination in the treatment of cancer.* Cancer Immunol Immunother, 2004. 53(4): p. 275-306.
82. Wilson, H.L. and H.C. O'Neill, *Murine dendritic cell development: difficulties associated with subset analysis.* Immunol Cell Biol, 2003. 81(4): p. 239-46.
83. Chattergoon, M.A., et al., *Targeted antigen delivery to antigen-presenting cells including dendritic cells by engineered Fas-mediated apoptosis.* Nat Biotechnol, 2000. 18(9): p. 974-9.
84. Reddy, S.T., et al., *In vivo targeting of dendritic cells in lymph nodes with poly(propylene sulfide) nanoparticles.* J Control Release, 2006. 112(1): p. 26-34.
85. Esslinger, C., et al., *In vivo administration of a lentiviral vaccine targets DCs and induces efficient CD8(+) T cell responses.* J Clin Invest, 2003. 111(11): p. 1673-81.
86. Bonifaz, L., et al., *Efficient targeting of protein antigen to the dendritic cell receptor DEC-205 in the steady state leads to antigen presentation on major histocompatibility complex class I products and peripheral CD8+ T cell tolerance.* J Exp Med, 2002. 196(12): p. 1627-38.
87. Hart, J.P., M.D. Gunn, and S.V. Pizzo, *A CD91-positive subset of CD11c+ blood dendritic cells: characterization of the APC that functions to enhance adaptive immune responses against CD91-targeted antigens.* J Immunol, 2004. 172(1): p. 70-8.
88. Tacken, P.J., et al., *Effective induction of naive and recall T-cell responses by targeting antigen to human dendritic cells via a humanized anti-DC-SIGN antibody.* Blood, 2005. 106(4): p. 1278-85.
89. Carter, R.W., et al., *Preferential induction of CD4+ T cell responses through in vivo targeting of antigen to dendritic cell-associated C-type lectin-1.* J Immunol, 2006. 177(4): p. 2276-84.
90. Altin, J.G., C.L. van Broekhoven, and C.R. Parish, *Targeting dendritic cells with antigen-containing liposomes: antitumour immunity.* Expert Opin Biol Ther, 2004. 4(11): p. 1735-47.
91. Schjetne, K.W., A.B. Fredriksen, and B. Bogen, *Delivery of antigen to CD40 induces protective immune responses against tumors.* J Immunol, 2007. 178(7): p. 4169-76.
92. Korokhov, N., et al., *A single-component CD40-targeted adenovirus vector displays highly efficient transduction and activation of dendritic cells in a human skin substrate system.* Mol Pharm, 2005. 2(3): p. 218-23.
93. Izumi, M., et al., *In vivo analysis of a genetically modified adenoviral vector targeted to human CD40 using a novel transient transgenic model.* J Gene Med, 2005. 7(12): p. 1517-25.
94. Belousova, N., et al., *Genetically targeted adenovirus vector directed to CD40-expressing cells.* J Virol, 2003. 77(21): p. 11367-77.
95. Stam, A.G., et al., *CD40-targeted adenoviral GM-CSF gene transfer enhances and prolongs the maturation of human CML-derived dendritic cells upon cytokine deprivation.* Br J Cancer, 2003. 89(7): p. 1162-5.
96. Brandao, J.G., et al., *CD40-targeted adenoviral gene transfer to dendritic cells through the use of a novel bispecific single-chain Fv antibody enhances cytotoxic T cell activation.* Vaccine, 2003. 21(19-20): p. 2268-72.
97. de Gruijl, T.D., et al., *Prolonged maturation and enhanced transduction of dendritic cells migrated from human skin explants after in situ delivery of CD40-targeted adenoviral vectors.* J Immunol, 2002. 169(9): p. 5322-31.
98. Pereboev, A.V., et al., *Coxsackievirus-adenovirus receptor genetically fused to anti-human CD40 scFv enhances adenoviral transduction of dendritic cells.* Gene Ther, 2002. 9(17): p. 1189-93.
99. Tillman, B.W., et al., *Maturation of dendritic cells accompanies high-efficiency gene transfer by a CD40-targeted adenoviral vector.* J Immunol, 1999. 162(11): p. 6378-83.
100. Tatsis, N. and H.C. Ertl, *Adenoviruses as vaccine vectors.* Mol Ther, 2004. 10(4): p. 616-29.
101. Santosuosso, M., S. McCormick, and Z. Xing, *Adenoviral vectors for mucosal vaccination against infectious diseases.* Viral Immunol, 2005. 18(2): p. 283-91.
102. Souza, A.P., et al., *Recombinant viruses as vaccines against viral diseases.* Braz J Med Biol Res, 2005. 38(4): p. 509-22.
103. Pereboev, A.V., et al., *Enhanced gene transfer to mouse dendritic cells using adenoviral vectors coated with a novel adapter molecule.* Mol Ther, 2004. 9(5): p. 712-20.
104. O'Neill, D.W., S. Adams, and N. Bhardwaj, *Manipulating dendritic cell biology for the active immunotherapy of cancer.* Blood, 2004. 104(8): p. 2235-46.
105. Berzofsky, J.A., et al., *Progress on new vaccine strategies for the immunotherapy and prevention of cancer.* J Clin Invest, 2004. 113(11): p. 1515-25.

106. Stockwin, L.H., et al., *Engineered expression of the Coxsackie B and adenovirus receptor (CAR) in human dendritic cells enhances recombinant adenovirus-mediated gene transfer.* J Immunol Methods, 2002. 259(1-2): p. 205-15.
107. Zhang, H.G., et al., *Induction of specific T-cell tolerance by adenovirus-transfected, Fas ligand-producing antigen presenting cells.* Nat Biotechnol, 1998. 16(11): p. 1045-9.
108. Piazzolla, G., et al., *Interleukin-12 p40/p70 ratio and in vivo responsiveness to IFN-alpha treatment in chronic hepatitis C.* J Interferon Cytokine Res, 2001. 21(7): p. 453-61.
109. Chen, D., et al., *Adaptive and innate immune responses to gene transfer vectors: role of cytokines and chemokines in vector function.* Gene Ther, 2003. 10(11): p. 991-8.
110. Rabinovich, G.A., D. Gabrilovich, and E.M. Sotomayor, *Immunosuppressive strategies that are mediated by tumor cells.* Annu Rev Immunol, 2007. 25: p. 267-96.
111. Lyerly, H.K., *Quantitating cellular immune responses to cancer vaccines.* Semin Oncol, 2003. 30(3 Suppl 8): p. 9-16.
112. He, X.S., et al., *Costimulatory protein B7-1 enhances the cytotoxic T cell response and antibody response to hepatitis B surface antigen.* Proc Natl Acad Sci U S A, 1996. 93(14): p. 7274-8.
113. Coles, R.M., et al., *Progression of armed CTL from draining lymph node to spleen shortly after localized infection with herpes simplex virus 1.* J Immunol, 2002. 168(2): p. 834-8.
114. Kennedy, R.C., et al., *CD4+ T lymphocytes play a critical role in antibody production and tumor immunity against simian virus 40 large tumor antigen.* Cancer Res, 2003. 63(5): p. 1040-5.
115. Connolly, D.C., et al., *Female mice chimeric for expression of the simian virus 40 TAg under control of the MISIIR promoter develop epithelial ovarian cancer.* Cancer Res, 2003. 63(6): p. 1389-97.
116. Stone, D., et al., *Comparison of adenoviruses from species B, C, E, and F after intravenous delivery.* Mol Ther, 2007. 15(12): p. 2146-53.
117. Morral, N., et al., *Immune responses to reporter proteins and high viral dose limit duration of expression with adenoviral vectors: comparison of E2a wild type and E2a deleted vectors.* Hum Gene Ther, 1997. 8(10): p. 1275-86.
118. Lieber, A., et al., *The role of Kupffer cell activation and viral gene expression in early liver toxicity after infusion of recombinant adenovirus vectors.* J Virol, 1997. 71(11): p. 8798-807.
119. Worgall, S., et al., *Innate immune mechanisms dominate elimination of adenoviral vectors following in vivo administration.* Hum Gene Ther, 1997. 8(1): p. 37-44.
120. Morral, N., et al., *High doses of a helper-dependent adenoviral vector yield supraphysiological levels of alpha1-antitrypsin with negligible toxicity.* Hum Gene Ther, 1998. 9(18): p. 2709-16.
121. Morsy, M.A., et al., *An adenoviral vector deleted for all viral coding sequences results in enhanced safety and extended expression of a leptin transgene.* Proc Natl Acad Sci U S A, 1998. 95(14): p. 7866-71.
122. Schiedner, G., et al., *Genomic DNA transfer with a high-capacity adenovirus vector results in improved in vivo gene expression and decreased toxicity.* Nat Genet, 1998. 18(2): p. 180-3.
123. Cheng, C., et al., *Mechanism of ad5 vaccine immunity and toxicity: fiber shaft targeting of dendritic cells.* PLoS Pathog, 2007. 3(2): p. e25.
124. Shayakhmetov, D.M., et al., *Analysis of adenovirus sequestration in the liver, transduction of hepatic cells, and innate toxicity after injection of fiber-modified vectors.* J Virol, 2004. 78(10): p. 5368-81.
125. De Geest, B., et al., *Elimination of innate immune responses and liver inflammation by PEGylation of adenoviral vectors and methylprednisolone.* Hum Gene Ther, 2005. 16(12): p. 1439-51.
126. Li, H.J., et al., *Adenovirus tumor targeting and hepatic untargeting by a coxsackie/adenovirus receptor ectodomain anti-carcinoembryonic antigen bispecific adapter.* Cancer Res, 2007. 67(11): p. 5354-61.
127. Nicol, C.G., et al., *Effect of adenovirus serotype 5 fiber and penton modifications on in vivo tropism in rats.* Mol Ther, 2004. 10(2): p. 344-54.
128. Martin, K., et al., *Simultaneous CAR- and alpha V integrin-binding ablation fails to reduce Ad5 liver tropism.* Mol Ther, 2003. 8(3): p. 485-94.
129. Yun, C.O., et al., *Coxsackie and adenovirus receptor binding ablation reduces adenovirus liver tropism and toxicity.* Hum Gene Ther, 2005. 16(2): p. 248-61.
130. Jaeschke, H., et al., *Mechanisms of hepatotoxicity.* Toxicol Sci, 2002. 65(2): p. 166-76.
131. Lucignani, G., et al., *Molecular imaging of cell-mediated cancer immunotherapy.* Trends Biotechnol, 2006. 24(9): p. 410-8.
132. Hashimoto, M., et al., *Unstable expression of E-cadherin adhesion molecules in metastatic ovarian tumor cells.* Jpn J Cancer Res, 1989. 80(5): p. 459-63.

133. Roby, K.F., et al., *Development of a syngeneic mouse model for events related to ovarian cancer.* Carcinogenesis, 2000. 21(4): p. 585-91.
134. Butel, J.S. and J.A. Lednicky, *Cell and molecular biology of simian virus 40: implications for human infections and disease.* J Natl Cancer Inst, 1999. 91(2): p. 119-34.
135. Butel, J.S., D.L. Jarvis, and S.A. Maxwell, *SV40 T-antigen as a dual oncogene: structure and function of the plasma membrane-associated population.* Ann N Y Acad Sci, 1989. 567: p. 104-21.
136. Huang, D., et al., *Significant alterations of biodistribution and immune responses in Balb/c mice administered with adenovirus targeted to CD40(+) cells.* Gene Ther, 2008. 15(4): p. 298-308.
137. Viatte, S., P.M. Alves, and P. Romero, *Reverse immunology approach for the identification of CD8 T-cell-defined antigens: advantages and hurdles.* Immunol Cell Biol, 2006. 84(3): p. 318-30.

APPENDICES:

274. Genetic Immunotherapy Targeted to Antigen Presenting Cells Using a CD40-Targeted Adenoviral Vector Disha A. Mody[1], Larry Smart[1], Yoshinobu Odaka[1], Xiao L. Li[1], Cigdem E. Yilmaz[1], Alexander V. Pereboev[2] and J. Michael Mathis[1]

[1]Cellular Biology and Anatomy, LSU Health Sciences Center, Shreveport, LA
[2]Division of Human Gene Therapy, University of Alabama at Birmingham, Birmingham, AL

Introduction: Antigen Presenting Cells (APCs) specialize in capturing foreign antigens, displaying them on their cell surface along with MHC molecules to the lymphocytes and providing activation signals for their differentiation and proliferation. The main cell types that serve as APCs are dendritic cells and macrophages. They can capture, process and present antigens in association with MHC class I and class II molecules to na|[iuml]|ve CD8+ (cytotoxic) and CD4+ (helper) T lymphocytes, respectively. Through this process, specific cytotoxic T lymphocytes for that antigen are activated and they can recognize a target cell and kill it. The goal of this study was to determine the transducion efficiency of APCs using a CD40-targeted adenoviral vector expressing a tumor antigen. A second goal was to characterize transduced APCs to determine if APCs are suitable for use in tumor immunotherapy. Recently, we characterized a new model using a mouse ovarian carcinoma cell line (MOVCAR) that expresses the SV40 large T-Ag and forms tumors in syngeneic immunocompetent B6C3F1 mice. The SV40 large T-Ag is highly immunogenic, inducing both antibody and cytotoxic T lymphocyte (CTL) responses. Since this antigen is synthesized in MOVCAR cells, the SV40 large T-Ag is an attractive candidate as a model system for the development of a DC-targeted cancer vaccine. We hypothesize that transduction of APCs in vitro using a CD40-targeted Ad vector expressing SV40 T-Ag (Ad5-SV40-TAg) will result in a high level of transgene expression, and be effective in inducing an antigen-specific CTL response in vivo.
Methods: Primary cultures of mouse dendritic cells and cultures of the mouse RAW 264.7 cell line treated with lipopylysaccharide (LPS) were used as sources of APCs. To target Ad5-SV40-TAg to APCs, we utilized a recombinant adapter protein consisting of extracellular portion of the native adenovirus receptor, CAR, fused to a trimerization motif of a 71 amino acid domain from the pactriophage T4 fibritin protein, and linked to the extracellular domain of the mouse CD40 ligand. The APCs were treated with untargeted and CD40-targeted Ad5-SV40-TAg using increasing multiplicities of infection. Western blot analysis was used to determine the level of expression of the SV40 T-Ag in the transduced APCs, and flow cytometric analysis was used to determine the changes in the expression of the cell surface markers on the transduced APCs.
Results: Cells that were transduced with the CD40-targeted Ad5-SV40-TAg vector showed increased expression of transgene at 48 hours post-infection compared to cells tranduced with untargeted Ad5-SV40-TAg vector. In addition, APCs transduced with the CD40-targeted Ad5-SV40-TAg vector also showed increased expression of co-stimulatory molecules compared to untransduced APCs or to APCs tranduced with untargeted Ad5-SV40-TAg.
Conclusions: The results demonstrate that the APCs can be successfully transduced using a CD40 targeted adenoviral vector and that transduced APCs show increased expression of cell surface activation markers.

836. Changes in Maturation Profiles of Dendritic Cells Transduced with a CD40-Targeted Adenoviral Vector Disha A. Mody[1], Alexander V. Pereboev[2], Don A. Sibley[1], David T. Curiel[2] and J. Michael Mathis[1]

[1]Cellular Biology and Anatomy, LSU Health Sciences Center, Shreveport, LA
[2]Division of Human Gene Therapy, University of Alabama at Birmingham, Birmingham, AL

Introduction: Adenovirus (Ad)-mediated transduction of dendritic cells (DCs) is inefficient because of the lack of the primary Ad receptor, CAR. CD40 is a surface marker expressed by DCs that plays a crucial role in their maturation and subsequent stimulation of T cells. DC infection with Ad targeted to the CD40 results in increased gene transfer. Recently, we characterized a new model using a mouse ovarian carcinoma cell line (MOVCAR) that expresses the SV40 large T-Ag and forms tumors in syngeneic immunocompetent B6C3F1 mice. The SV40 large T-Ag is highly immunogenic, inducing both antibody and cytotoxic T lymphocyte (CTL) responses. Since this antigen is synthesized in MOVCAR cells, the SV40 large T-Ag is an attractive candidate

as a model system for the development of a DC-targeted cancer vaccine. We describe the further characterization of the CD40-targeting approach using an adapter molecule that bridges the fiber of the Ad5 to CD40 on mouse DC. This adapter molecule, CFm40L, consists of the ectodomain of CAR genetically linked via a trimerization motif to the extracellular domain of mouse CD40 ligand. We have demonstrated that DCs transduced with a CD40-targeted Ad vector expressing SV40 T-Ag (Ad5-SV40-TAg) showed an increased expression of cell surface activation markers and were effective in inducing an antigen-specific CTL response. To examine CD maturation induced by transduction with the CD40-targeted Ad vector, we examined changes in a panel of cytokines and chemokines. In addition, we examined the kinase signalling pathways involved in cytokine regulation.
Methods: We used a Bio-Plex assay was performed on supernatants from untransduced DCs and DCs transduced with untargeted Ad and CD40-targeted Ad5 to determine changes in production of a panel of 23 cytokines and chemokines at 24, 48, and 72 hours post infection. We uses a Kinexus phospho-antibody screening system on cell lysates from untransduced DCs and DCs transduced with untargeted Ad and CD40-targeted Ad to examine changes in phosphorylation / activation of 34 different protein phospho-kinases.
Results: DCs transduced with a CD40-targeted Ad showed increased secretion of the cytokines IL-1A, IL-1B, IL-6, and IL-12, as well as chemokines MIP-1A and RANTES compared to untransduced DCs or DCs transduced with untargeted Ad. Similarly, DCs transduced with a CD40-targeted Ad showed a decreased secretion of cytokine KC. DCs transduced with a CD40-targeted Ad showed increased phosphorylation of MEK1, Erk1, Erk, and STAT1(T385), and decreased phosphorylation of Akt1, compared to untransduced DCs or DCs transduced with untargeted Ad. In contrast, DCs transduced with a CD40-targeted Ad showed an inhibition of Src, Gsk3a, Gsk3b, and STAT1(S727) phosphorylation compared to DCs transduced with untargeted Ad.
Conclusions: We demonstrated Ad-mediated CD40-targeted gene transfer to murine DCs using an adapter molecule CFm40L promotes DC maturation with induction of a complex signaling cascade accompanied by characteristic changes in cytokine production.

33. CD40-Targeted Adenoviral Vector Transduction of Dendritic Cells Disha Mody[1], Don A. Sibley[1], Yoshinobu Odaka[1], Jagat Poduturri[1], Xiao L. Li[1], David T. Curiel[2], Alexander Pereboev[2], and J. Michael Mathis[1]

[1]Cellular Biology and Anatomy, Gene Therapy Program, LSU Health Sciences Center, Shreveport, LA
[2]Division of Human Gene Therapy, Departments of Medicine, Obstetrics and Gynecology, Pathology, and Surgery, and the Gene Therapy Center, University of Alabama at Birmingham, Birmingham, AL

Introduction: Dendritic cells (DCs) are professional antigen presenting cells of the immune system. Targeting DCs with tumor antigens can result in DC-mediated presentation of the tumor antigen to the immune system and elicit tumor-specific immune response. DCs are difficult to transduce by using an adenovirus (Ad) vector because of the scarcity of CAR on the DC cell surface. CD40 is a cell surface marker expressed by DCs, is crucial for their maturation and the subsequent activation of the immune system by the DCs. We have explored the possibility of targeting DCs using Ad vector via CD40. We have used CFm40L, a bispecific adaptor molecule with ectodomain of CAR one end end linked genetically by a trimerization motif to the extracellular domain of mouse CD40 ligand on the other end. CFm40L bridges the fiber knob domain of Ad to CD40 on mouse DC. The SV40 T-Ag is known to be a highly immunogenic protein. We used SV40 T-Ag as a model antigen to test the efficacy of CD40-targeted Ad vaccine to tranduce DCs and generate an effective immune response against tumor cells bearing SV40 T-Ag.
Methods: Western blot analysis was used to detect expression of SV40 T-Ag in the DCs transduced with CD40-targeted and untargeted Ad-SV40 T-Ag. Chromium release assays were used to test the Cytotoxic T Lymphocyte response generated in the immunized B6C3F1 mice against cells bearing SV40 T-Ag. Morphological and histological examination of the liver was performed to compare the liver toxicity induced in B6C3F1 mice by CD40-targeted Ad-SV40 TAg and untargeted Ad-SV40 T-Ag. Real-time PCR analysis of Ad DNA in the liver samples was used to assess targeting of liver in B6C3F1 mice by the untargeted and CD40-targeted Ad. PET scans were performed to measure the expression of the transgene TK (thymine kinase) in the livers of B6C3F1 mice immunized with CD40-targeted and untargeted Ad expressing TK.
Results: 1) DCs transduced by using CD40-targeted Ad-SV40 T-Ag showed increased expression of SV40 T-Ag compared to untargeted Ad-SV40 T-Ag. 2) The B6C3F1 mice immunized with CD40-targeted Ad-SV40 T-

Ag showed a greater Cytotoxic T Lymphocyte response than mice immunized with untargeted Ad-SV40 T-Ag. 3) There was reduced liver toxicity in B6C3F1 mice that were immunized with CD40-targeted Ad-SV40 T-Ag than the mice immunized with untargeted Ad-SV40 T-Ag as per morphological and histological examination. 4) CD40-targeted Ad vectors showed lower transduction of liver cells as compared to untargeted Ad vectors as shown by real-time PCR analysis of Ad DNA and expression of transgene (TK) in liver samples of both groups.
Conclusion: These results demonstrated that CD40-targeted Ad vaccine is a more potent and a safer vaccine than the untargeted Ad vaccine.

554. Evaluation of Target Antigen Immunogenicity *In Vivo* Using a CD40-Targeted Adenovirus Model

Disha Mody,1 Bing Cheng,1 Jagat Podduturi,1 Don A. Sibley,1 Yoshinobu Odaka,1 Larry Smart,1 Xiao L. Li,1 David T. Curiel,2 Alexander Pereboev,2 J. Michael Mathis.1

1Gene Therapy Program, Dept. of Cellular Biology and Anatomy,Feist-Weiller Cancer Center, LSU Health Sciences Center, Shreveport, LA
2Division of Human Gene Therapy, Departments of Medicine, Surgery, Pathology and the Gene Therapy Center, University of Alabama at Birmingham, Birmingham, AL.

Introduction: A major challenge for efficient vaccines against tumor antigens is the identification of mmunogenic antigens against which an effective immune response can be induced. Thus, the selection of highly immunogenic antigens will greatly increase the prospects of effective vaccines against tumor cells bearing those antigens. However, the current process of evaluating the target antigens for their potential use in vaccination is time-consuming, cumbersome and inefficient. We explored the possibility of expressing the target antigen directly into antigen presenting cells (APCs) such as dendritic cells (DCs) *in vivo* using a CD40-targeted adenoviral vector expressing the target antigen. This method has the advantage of using the APC machinery to address antigen processing and HLA binding rather than reconstituting antigen processing in vitro, and predicting and then testing the binding of peptides to MHC molecules. In addition, this in vivo model is less likely to be influenced by external factors. Importantly, CD40-targeted adenoviral vectors can serve a dual function, both in the assessment of immunogenicity of target antigens and as the vaccine itself.
Methods: We used two target antigens to test the potential of this model to evaluate immunogenicity of target antigens. One of the antigens was SV40 T-Ag, which is highly immunogenic and other was the firefly luciferase enzyme, which is poorly immunogenic in mice. Ten mice were immunized with 10^9 ifu CD40-targeted Ad5 SV40 T-Ag (combined with 1200 ng CFm40L bispecific adaptor protein) and another ten mice were immunized with 10^9 ifu CD40-targeted Ad5-luc (combined with 1200 ng CFm40L bispecific adaptor protein). Mice that received only saline were used as a control. Two weeks later, the mice received a boost immunization with the same viruses at the same dose. At one day after the second immunization, the mice were bled by retro-orbital bleeding and serum was harvested from the blood of the immunized mice. The serum was analyzed for the induction of secretion of inflammatory cytokines and chemokines by the bioplex cytokine bead array using 23-plex cytokine panel.
Results: The sera of mice immunized with CD40-targeted Ad5 SV40 T-Ag showed elevated levels in 18 of 23 cytokines and chemokines compared to control mice. The highest increase was seen in Th1 cytokines such as IL-12, IFN-γ and TNF-α. The sera of mice immunized with CD40-targeted Ad5-luc showed elevated levels in only 2 of 23 cytokines and chemokines compared to control mice. This increase was seen in the levels of the Th2 cytokines IL-5 and G-CSF.
Conclusion: CD40-targeted adenoviral vectors expressing target antigen can be used to transduce APCs *in vivo* and induce an antigen-specific immune response. The induced immune responses can then be measured and compared to compare the immunogenicity of different target antigens.

SUPPORTING DATA:

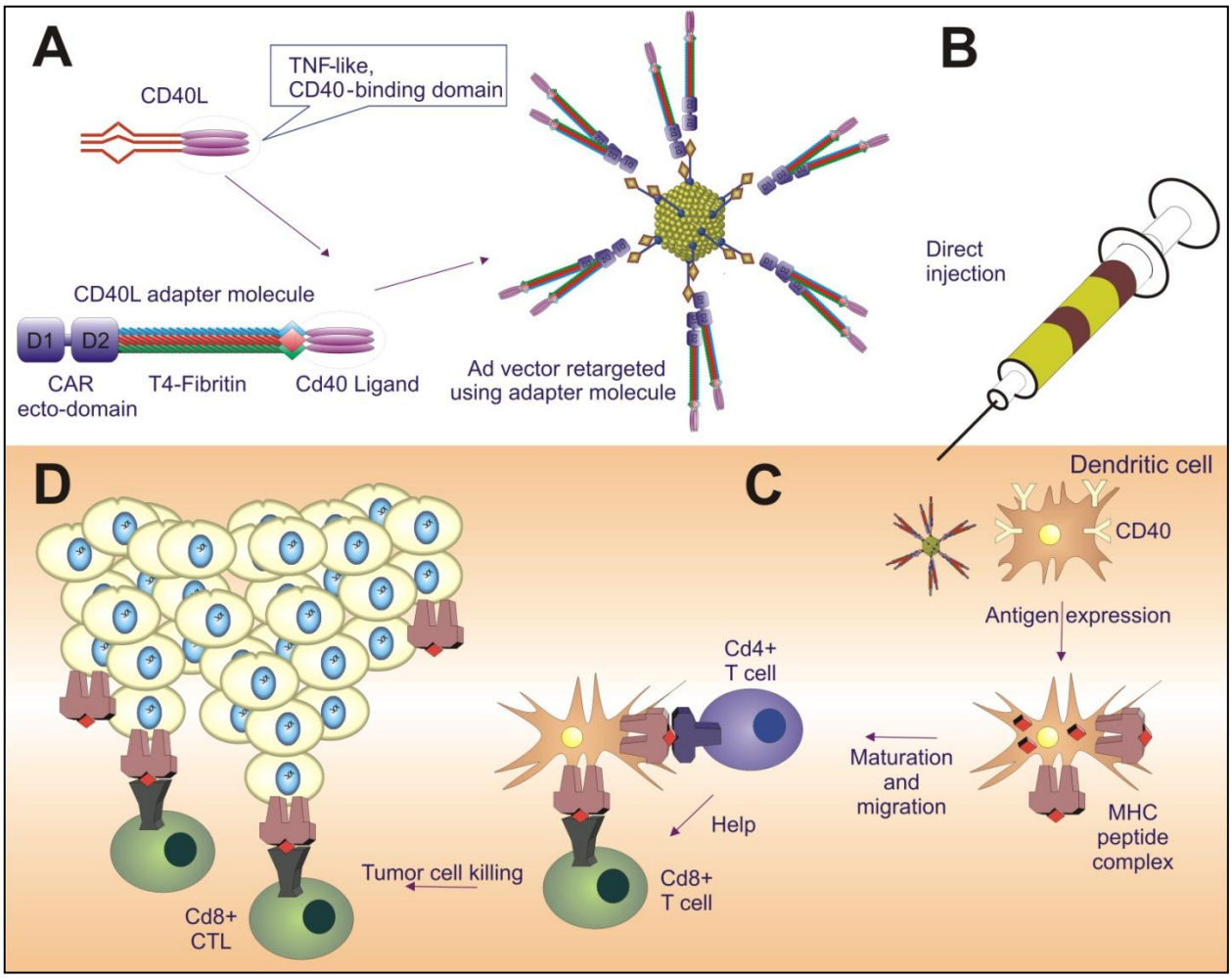

Figure 1.1 Targeting of Ad5 vector to CD40 with TNF-Like domain of CD40L provides flexible platform for DC infection. The development of an *in vivo* approach based on DC vaccination without isolation and culturing of DCs *ex vivo* would be clinically significant. However, a critical component of *in vivo* infection is efficient targeting of the vector to DCs without perturbation of DC function. To this end, we generated Ad vector systems that specifically target human and mouse DCs via the CD40 receptor using CAR-CD40L bi-specific adapter molecules (A) and showed that CD40-targeted Ads efficiently infect DCs *in vitro* without interfering with DC function. We evaluated a dendritic cell-targeted Ad vaccine expressing the simian virus 40 (SV40) large T antigen (T-Ag) in a mouse model of ovarian cancer. We hypothesize that immunization of DCs (B) with the SV40 T-Ag will be effective in inducing antigen-specific cytotoxic T-lymphocyte (CTL) responses (C), an

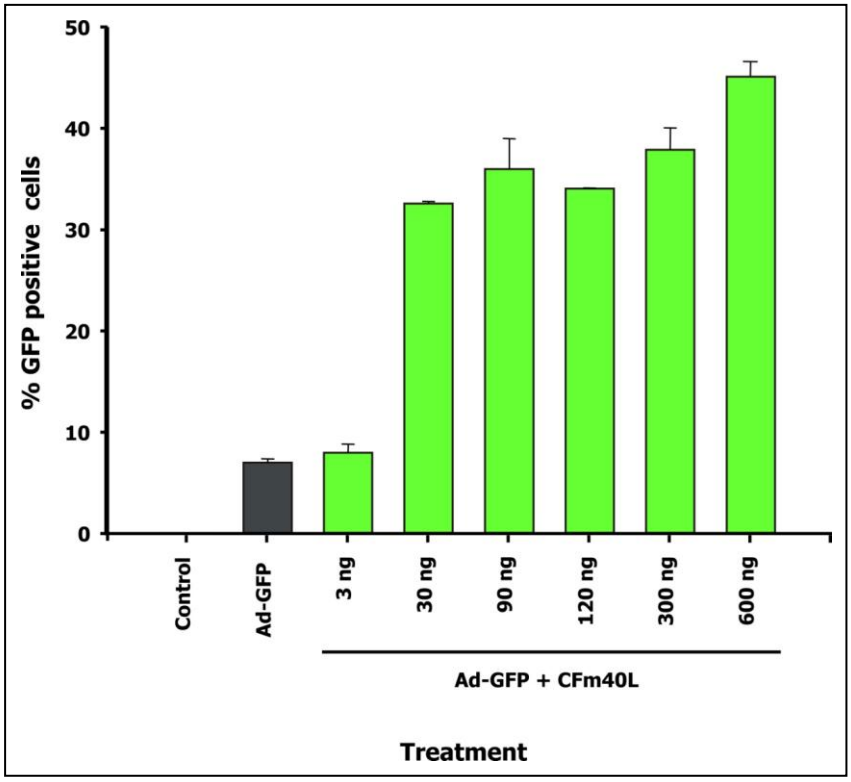

Figure 2.1 Ad-CMV-GFP targeted to CD40 by CFm40L enhances efficacy of gene transfer to DCs. DCs were cultured in triplicate 60 mm tissue culture dishes at a density of 1×10^6 cells/dish. Indicated amounts of CFm40L were incubated with 1×10^8 ifu Ad5-CMV-GFP virus for 30 min at 37°C. The CFm40L/Ad5-CMV-GFP mixtures were then transferred to the DCs and incubated for 4 h at 37°C followed by virus removal by medium change. Forty-eight h post-infection the cells were harvested and the % GFP positive cells were determined by flow cytometry. Each bar represents the mean values ± SD.

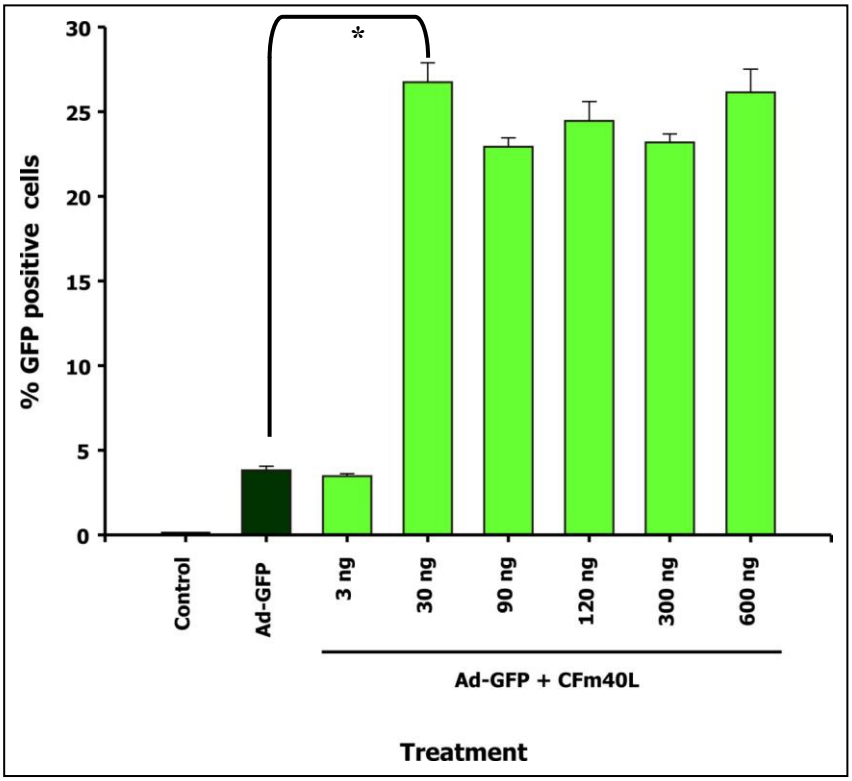

Figure 2.2 Ad-CMV-GFP targeted to CD40 by CFm40L enhances efficacy of gene transfer to RAW 264.7 cells. Raw 264.7 cells were cultured in triplicate 60 mm tissue culture dishes at a density of 1×10^6 cells/dish. Indicated amounts of CFm40L were incubated with 1×10^8 ifu Ad5-CMV-GFP virus for 30 min at 37°C. The CFm40L/Ad5-CMV-GFP mixtures were then transferred to the Raw 264.7 cells and incubated for 4 h at 37°C followed by virus removal by medium change. Forty-eight h post-infection the cells were harvested and the % GFP positive cells were determined by flow cytometry. Each bar represents the mean values ± SD. * $P < 0.05$ versus cells infected with Ad-GFP alone.

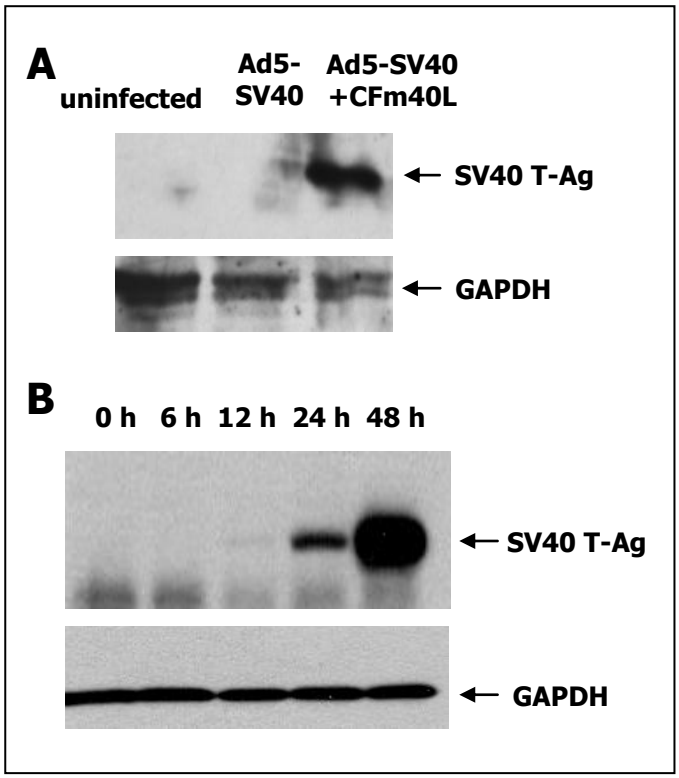

Figure 2.3 Western blot assay of dendritic cells. (A) Western blot assay of uninfected dendritic cells and dendritic cells infected with untargeted Ad5-CMV-SV40 T-Ag and CD40-targeted Ad5-CMV-SV40 T-Ag. The expression of SV40 T-Ag was detected only in dendritic cells that were infected with CD40-targeted Ad5-CMV-SV40 T-Ag. (B) Western blot assay of dendritic cells infected with CD40-targeted Ad5-CMV-SV40 T-Ag. The expression of SV40 T-Ag was maximal at 48 h post-infection.

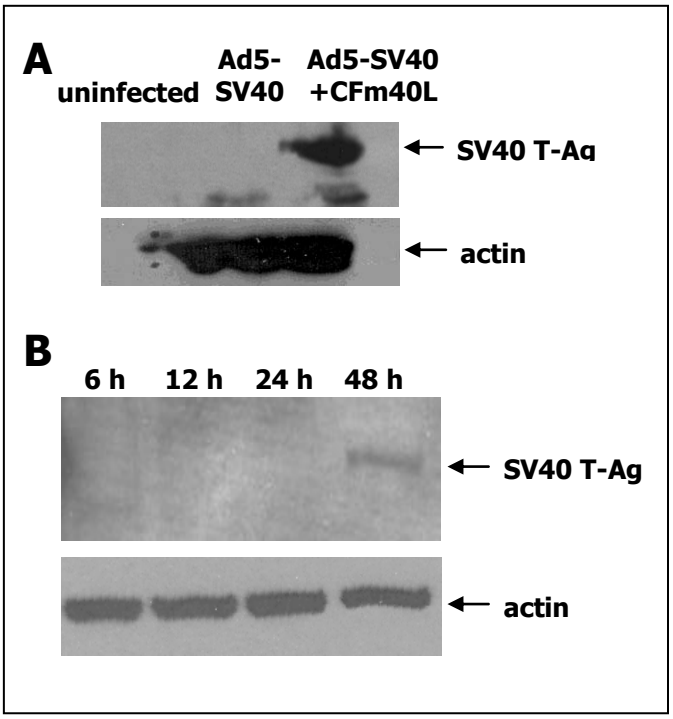

Figure 2.4 Western blot assay of RAW 264.7 cells. (A) Western blot assay of RAW 264.7 cells infected with CD40-targeted Ad5-CMV-SV40 T-Ag. The expression of SV40 T-Ag was detected in the RAW cells at 48 h post-infection. (B) Western blot assay of RAW 264.7 cells infected with CD40-targeted Ad5-CMV-SV40 T-Ag. The expression of SV40 T-Ag was maximal at 48 h post-infection.

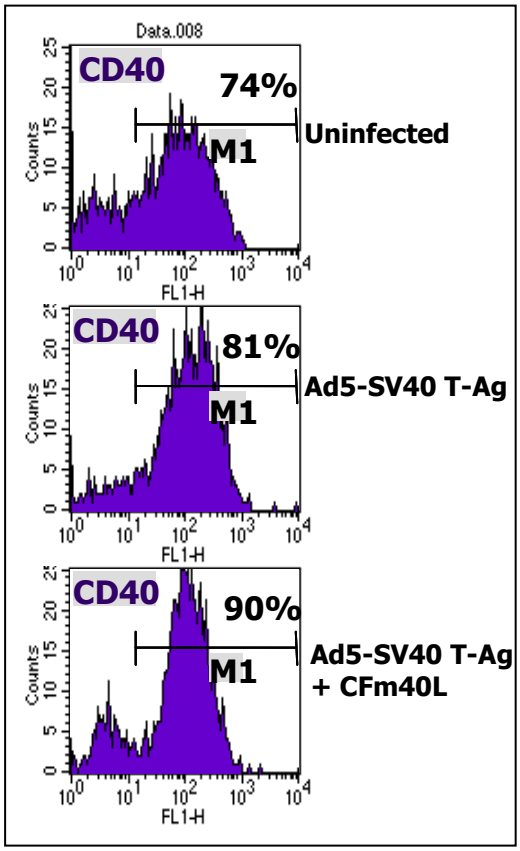

Markers	Treatment		
	Un infected	Ad5-SV40 T-Ag	Ad5-SV40 T-Ag + CFm40L
CD40	65.8% +/- 9.7	71.1% +/- 9.5	79.3% +/- 2.7
CD80	12.8% +/- 7.4	14.8% +/- 8.4	12.9% +/- 5.6
CD86	8.1% +/- 2.8	9.2% +/- 5.0	12.8% +/- 5.6

Figure 2.5 Flow cytometric analysis of uninfected dendritic cells and dendritic cells infected with untargeted Ad5-CMV-SV40 T-Ag and CD40-targeted Ad5-CMV-SV40 T-Ag. The cells were stained with FITC-labeled antibody against activation marker CD40, CD80, CD86, and CD11c.

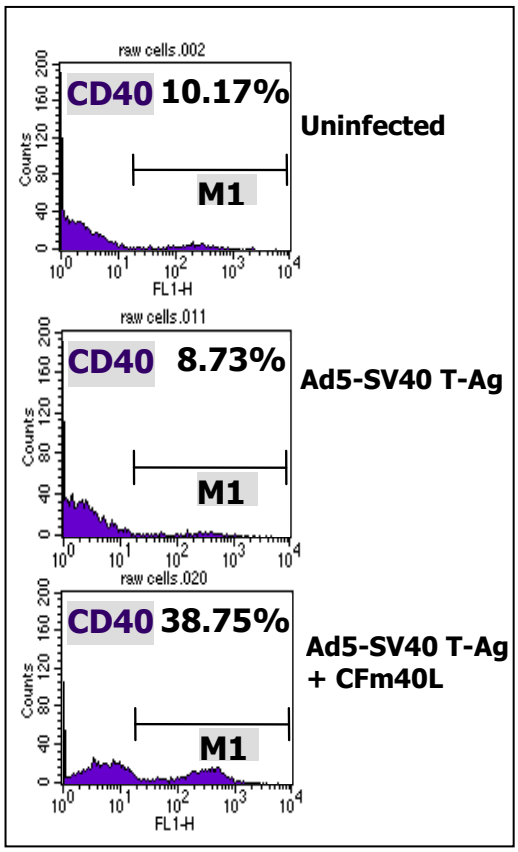

Markers	Treatment		
	Un infected	Ad5-SV40 T-Ag	Ad5-SV40 T-Ag + CFm40L
CD40	10%	9%	39%
CD80	1.5%	0.3%	0.9%
CD86	0.1%	0.1%	0.1%

Figure 2.6 Flow cytometric analysis of uninfected RAW 264.7 cells and RAW 264.7 cells infected with untargeted Ad5-CMV-SV40 T-Ag and CD40-targeted Ad5-CMV-SV40 T-Ag. The cells were stained with FITC-labeled antibody against activation marker CD40, CD80, CD86, and CD11c.

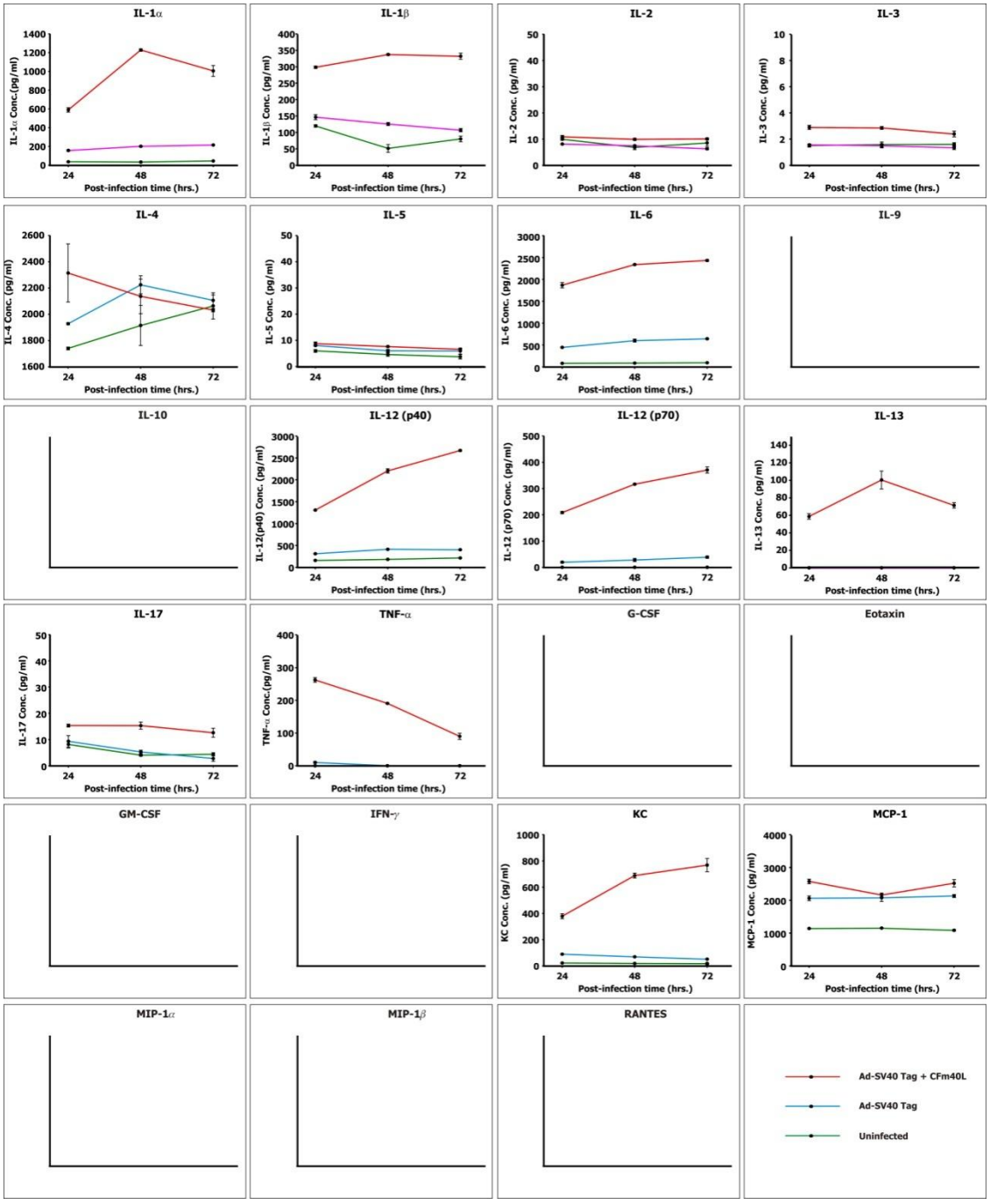

Figure 2.7 Bio-Plex cytokine assay of DCs infected with untargeted Ad5-CMV-SV40 T-Ag and CD40-targeted Ad5-CMV-SV40 T-Ag. DCs infected with CD40-targeted Ad5-CMV-SV40 T-Ag showed increased secretion of cytokines compared with uninfected DCs or DCs infected with untargeted Ad5-CMV-SV40 T-Ag. The relative increase in secretion of cytokines was maximal at 48 h post-infection. * $P < 0.05$ versus uninfected DCs, ** $P < 0.05$ versus uninfected DCs and DCs infected with untargeted Ad5-CMV-SV40 T-Ag, *** $P < 0.05$ versus DCs infected with untargeted Ad5-CMV-SV40 T-Ag.

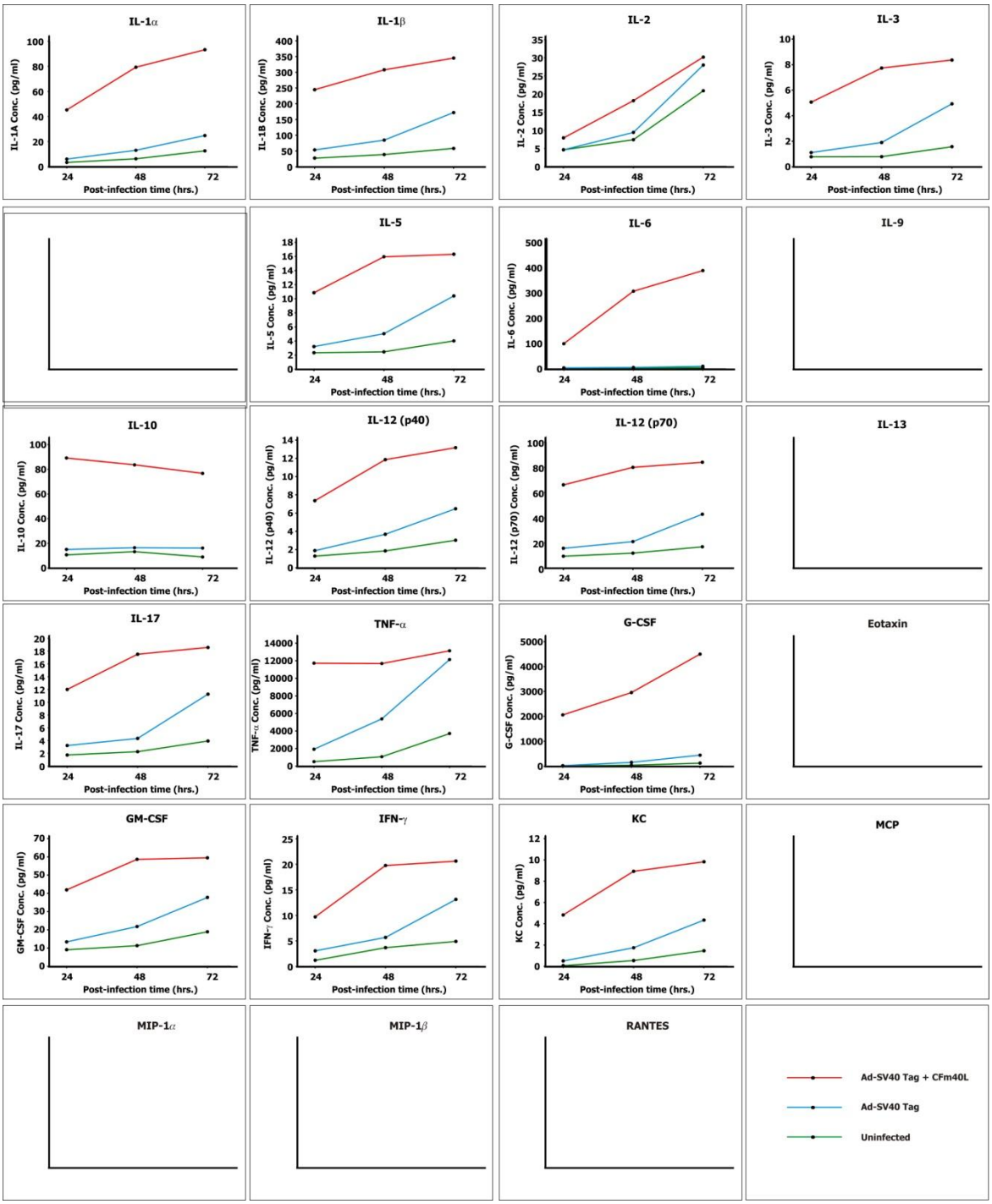

Figure 2.8 Bio-Plex cytokine assay of RAW 264.7 cells infected with untargeted Ad5-CMV-SV40 T-Ag and CD40-targeted Ad5-CMV-SV40 T-Ag. RAW 264.7 cells infected with CD40-targeted Ad5-CMV-SV40 T-Ag showed increased secretion of cytokines compared with uninfected RAW 264.7 cells or cells infected with untargeted Ad5-CMV-SV40 T-Ag. The relative increase in secretion of cytokines was maximal at 48 h post-infection.

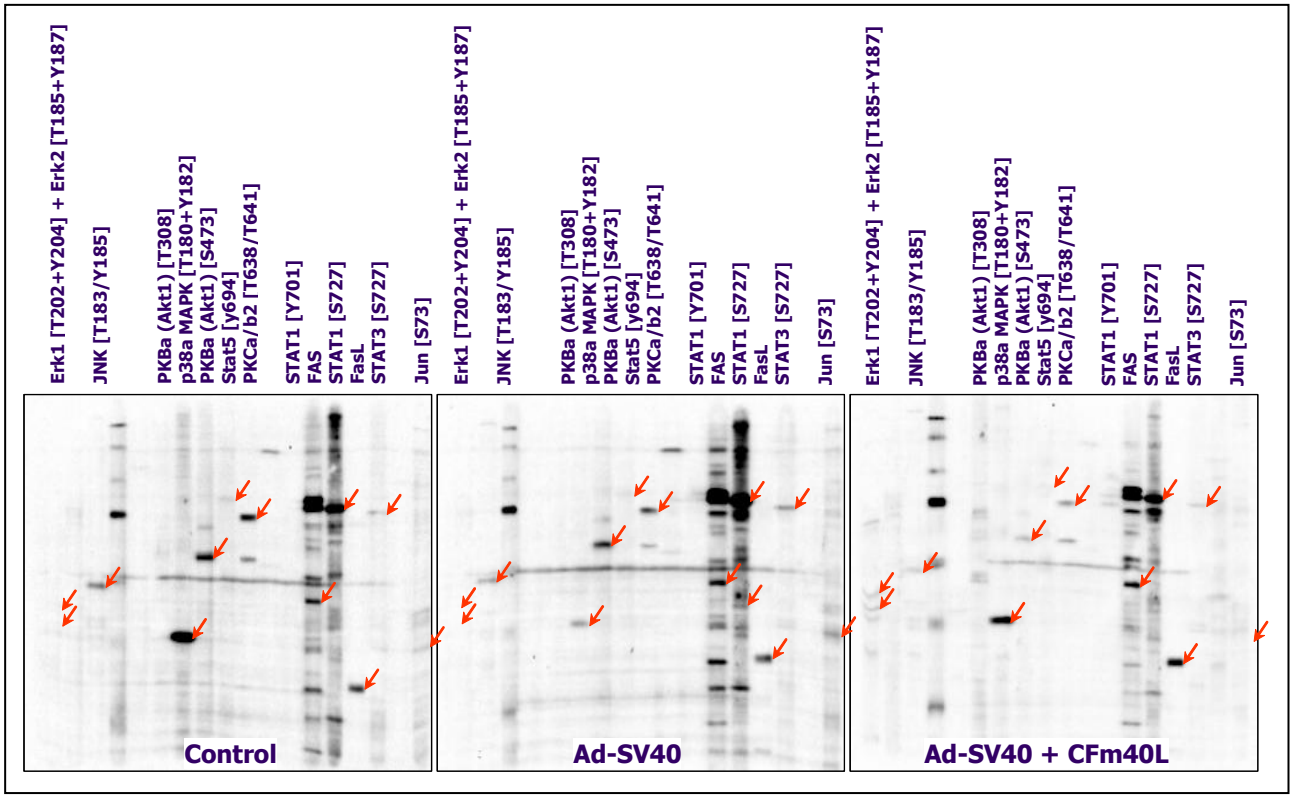

Figure 3.1 Immunoblot analysis of phosphorylation and expression of cell signaling proteins in DCs. The phosphorylation status and expression of several cell signaling proteins was altered in DCs infected by CD40-targeted Ad5-CMV-SV40 T-Ag at 24 h post-infection compared with DCs infected by untargeted Ad5-CMV-SV40 T-Ag and the control uninfected DCs.

	FULL NAME OF PROTEIN	ABBREV
1	Extracellular regulated protein-serine kinase 1 (p44 MAP kinase) [T202+Y204]	Erk1
2	Extracellular regulated protein-serine kinase 2 (p42 MAP kinase) [T185+Y187]	Erk2
3	Inhibitor of NF-kappa-B protein-serine kinase alpha (CHUK) [S180]	IKKa
4	Inhibitor of NF-kappa-B protein-serine kinase beta [S181]	IKKb
5	Janus protein-tyrosine kinase 2 [Y1007/Y1008]	JAK2
6	Jun N-terminus protein-serine kinase (stress-activated protein kinase (SAPK)) [T183/Y185] (37)	JNK
7	Jun N-terminus protein-serine kinase (stress-activated protein kinase (SAPK)) [T183/Y185] (38)	JNK
8	Jun N-terminus protein-serine kinase (stress-activated protein kinase (SAPK)) [T183/Y185] (44)	JNK
9	Jun N-terminus protein-serine kinase (stress-activated protein kinase (SAPK)) [T183/Y185] (46)	JNK
10	Jun proto-oncogene-encoded AP1 transcription factor [S63]	Jun
11	Jun-c trascription factor [S73]	Jun
12	Mitogen-activated protein-serine kinase p38 alpha [T180+Y182] (36)	p38a MAPK
13	Mitogen-activated protein-serine kinase p38 alpha [T180+Y182] (40)	p38a MAPK
14	Protein-serine kinase B alpha (Akt1) [S473]	PKBa (Akt1)
15	Protein-serine kinase B alpha (Akt1) [T308]	PKBa (Akt1)
16	Protein-serine kinase C alpha/beta 2 [T638/T641]	PKCa/b2
17	Signal transducer and activator of transcription 1 [S727] (78)	STAT1
18	Signal transducer and activator of transcription 1 [S727] (87)	STAT1
19	Signal transducer and activator of transcription 1 [Y701] (78)	STAT1
20	Signal transducer and activator of transcription 1 [Y701] (87)	STAT1
21	Signal transducer and activator of transcription 2 [S690]	STAT2
22	Signal transducer and activator of transcription 3 [S727]	STAT3
23	Signal transducer and activator of transcription 5 [Y694]	STAT5
24	Tumor necrosis factor ligand, member 6	FasL
25	Tumor necrosis factor superfamily member 6 (Apo1, CD95)	FAS
26	Yes-related protein-tyrosine kinase	Lyn

	FULL NAME OF PROTEIN	ABBREV
27	B23 (Nucleophosmin) [S4]	B23 (NPM)
28	Extracellular regulated protein-serine kinase 5 (Big MAP kinase 1) [T218/Y220]	Erk5 (BMK1)
29	Fos-c FBJ murine osteosarcoma oncoprotein-related transcription factor [T232]	Fos
30	Glycogen synthase-serine kinase 3 alpha [S21]	GSK3a
31	Glycogen synthase-serine kinase 3 alpha [Y279] (44)	GSK3a
32	Glycogen synthase-serine kinase 3 alpha [Y279] (49)	GSK3a
33	Glycogen synthase-serine kinase 3 beta [S9]	GSK3b
34	Glycogen synthase-serine kinase 3 beta [Y216] (34)	GSK3b
35	Glycogen synthase-serine kinase 3 beta [Y216] (39)	GSK3b
36	MAP kinase protein-serine kinase 3/6 (MKK3/6) [S189/S207]	MEK3/6
37	MAP kinase protein-serine kinase 4 (MKK4) [S257+T261]	MEK4
38	MAP kinase protein-serine kinase 6 (MKK6) [S207]	MEK6
39	MAPK/ERK protein-serine kinase 1 (MKK1) [S297]	MEK1
40	MAPK/ERK protein-serine kinase 1 (MKK1) [T291]	MEK1
41	MAPK/ERK protein-serine kinase 1 (MKK1) [T385]	MEK1
42	MAPK/ERK protein-serine kinase 1/2 (MKK1/2) [S217/S221]	MEK1/2
43	MAPK/ERK protein-serine kinase 2 (MKK2) [T394] (mouse)	MEK2 mouse
44	Mitogen-activated protein kinase-activated protein kinase 2 [T222]	MAPKAPK2
45	Mitogen-activated protein kinase-activated protein kinase 2 alpha [T334]	MAPKAPK2a
46	Mitogen-activated protein kinase-activated protein kinase 2 beta [T334]	MAPKAPK2b
47	p21-activated protein-serine kinase 1/2/3 [S144/S141/S154] (54)	PAK1/2/3
48	p21-activated protein-serine kinase 1/2/3 [S144/S141/S154] (56)	PAK1/2/3
49	SMA- and mothers against decapentaplegic homolog 2 [S465+S467]	Smad2
50	SMA- and mothers against decapentaplegic homologs 1/5/9 [S463+S465/S463+S465/S465+S467]	Smad1/5/9
51	Src protein-tyrosine kinase [Y418] (44)	Src
52	Src protein-tyrosine kinase [Y418] (46)	Src
53	Src protein-tyrosine kinase [Y529] (44)	Src
54	Src protein-tyrosine kinase [Y529] (46)	Src

Table 3.1 List Of The Different Signal Transduction Proteins Analyzed

	FULL NAME OF PROTEIN	ABBREV	% CHAN
			Untreated
1	Extracellular regulated protein-serine kinase 1 (p44 MAP kinase) [T202+Y204]	Erk1	**0**
2	Extracellular regulated protein-serine kinase 2 (p42 MAP kinase) [T185+Y187]	Erk2	**0**
3	Inhibitor of NF-kappa-B protein-serine kinase alpha (CHUK) [S180]	IKKa	n.d.
4	Inhibitor of NF-kappa-B protein-serine kinase beta [S181]	IKKb	n.d.
5	Janus protein-tyrosine kinase 2 [Y1007/Y1008]	JAK2	n.d.
6	Jun N-terminus protein-serine kinase (stress-activated protein kinase (SAPK)) [T183/Y185] (37)	JNK	n.d.
7	Jun N-terminus protein-serine kinase (stress-activated protein kinase (SAPK)) [T183/Y185] (38)	JNK	n.d.
8	Jun N-terminus protein-serine kinase (stress-activated protein kinase (SAPK)) [T183/Y185] (44)	JNK	n.d.
9	Jun N-terminus protein-serine kinase (stress-activated protein kinase (SAPK)) [T183/Y185] (46)	JNK	**100**
10	Jun proto-oncogene-encoded AP1 transcription factor [S63]	Jun	n.d.
11	Jun-c trascription factor [S73]	Jun	**100**
12	Mitogen-activated protein-serine kinase p38 alpha [T180+Y182] (36)	p38a MAPK	**100**
13	Mitogen-activated protein-serine kinase p38 alpha [T180+Y182] (40)	p38a MAPK	n.d.
14	Protein-serine kinase B alpha (Akt1) [S473]	PKBa (Akt1)	**100**
15	Protein-serine kinase B alpha (Akt1) [T308]	PKBa (Akt1)	**0**
16	Protein-serine kinase C alpha/beta 2 [T638/T641]	PKCa/b2	**100**
17	Signal transducer and activator of transcription 1 [S727] (78)	STAT1	**100**
18	Signal transducer and activator of transcription 1 [S727] (87)	STAT1	n.d.
19	Signal transducer and activator of transcription 1 [Y701] (78)	STAT1	**0**
20	Signal transducer and activator of transcription 1 [Y701] (87)	STAT1	n.d
21	Signal transducer and activator of transcription 2 [S690]	STAT2	n.d

Table 3.2 Semi-quantitative analysis of phosphorylation and expression of several cell signaling proteins in DCs. The phosphorylation status and expression of several cell signaling proteins was altered in DCs infected by CD40-targeted Ad5-CMV-SV40 T-Ag at 24 h post-infection compared with DCs infected by untargeted Ad5-CMV-SV40 T-Ag and the control uninfected DCs.

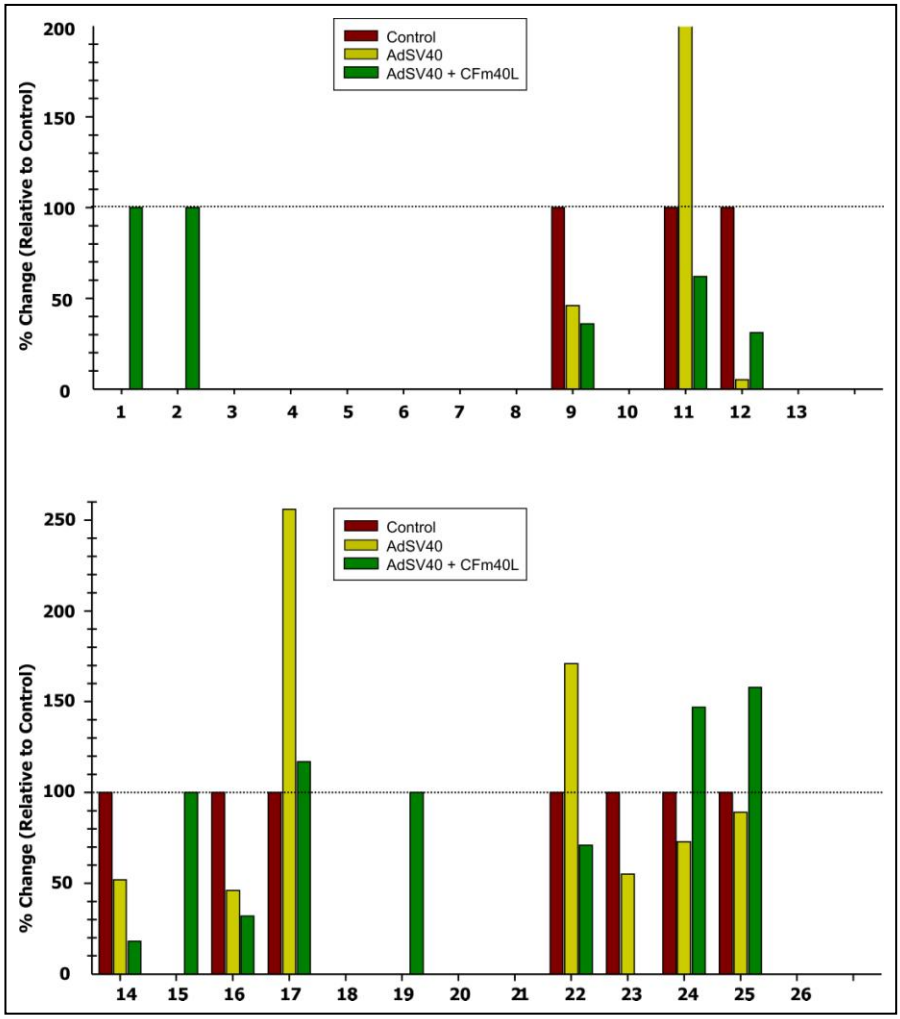

Figure 3.2 Graphical representation of semi-quantitative analysis of phosphorylation and expression of several cell signaling proteins in DCs. The phosphorylation status and expression of several cell signaling proteins was altered in DCs infected by CD40-targeted Ad5-CMV-SV40 T-Ag at 24 h post-infection compared with DCs infected by untargeted Ad5-CMV-SV40 T-Ag and the control uninfected DCs.

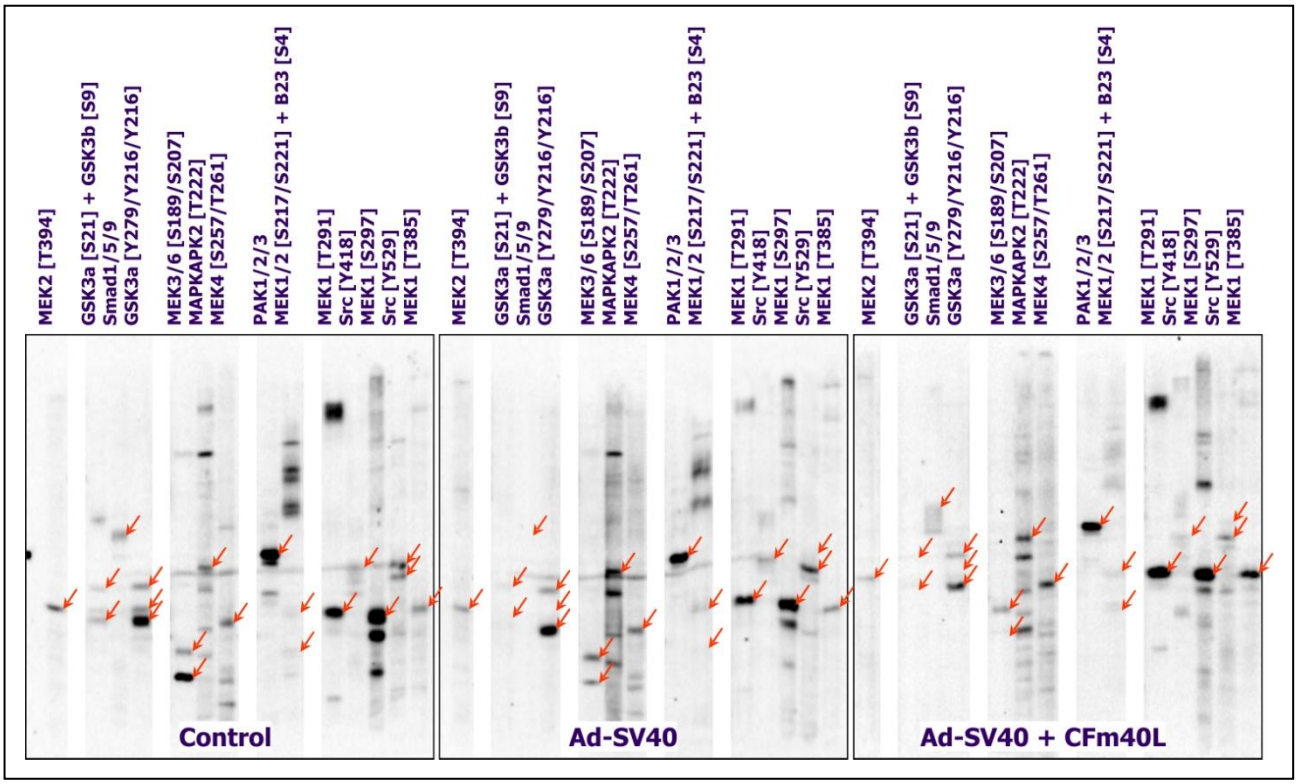

Figure 3.3 Immunoblot analysis of phosphorylation and expression of cell signaling proteins in DCs. The phosphorylation status and expression of several cell signaling proteins was altered in DCs infected by CD40-targeted Ad5-CMV-SV40 T-Ag at 24 h post-infection compared with DCs infected by untargeted Ad5-CMV-SV40 T-Ag and the control uninfected DCs.

	FULL NAME OF PROTEIN	ABBREV	% CHANGE RELATIVE TO CONTROL		
			Untreated	AdSV40	AdSV40 + CFm40L
27	B23 (Nucleophosmin) [S4]	B23 (NPM)	**100**	**0**	**143**
28	Extracellular regulated protein-serine kinase 5 (Big MAP kinase 1) [T218/Y220]	Erk5 (BMK1)	n.d.	n.d.	n.d.
29	Fos-c FBJ murine osteosarcoma oncoprotein-related transcription factor [T232]	Fos	n.d.	n.d.	n.d.
30	Glycogen synthase-serine kinase 3 alpha [S21]	GSK3a	**100**	**88**	**0**
31	Glycogen synthase-serine kinase 3 alpha [Y279] (44)	GSK3a	**100**	**178**	**97**
32	Glycogen synthase-serine kinase 3 alpha [Y279] (49)	GSK3a	n.d.	n.d.	n.d.
33	Glycogen synthase-serine kinase 3 beta [S9]	GSK3b	**100**	**0**	**0**
34	Glycogen synthase-serine kinase 3 beta [Y216] (34)	GSK3b	**100**	**182**	**69**
35	Glycogen synthase-serine kinase 3 beta [Y216] (39)	GSK3b	**100**	**0**	**31**
36	MAP kinase protein-serine kinase 3/6 (MKK3/6) [S189/S207]	MEK3/6	**100**	**243**	**123**
37	MAP kinase protein-serine kinase 4 (MKK4) [S257+T261]	MEK4	**100**	**159**	**193**
38	MAP kinase protein-serine kinase 6 (MKK6) [S207]	MEK6	**100**	**17**	**0**
39	MAPK/ERK protein-serine kinase 1 (MKK1) [S297]	MEK1	**100**	**128**	**143**
40	MAPK/ERK protein-serine kinase 1 (MKK1) [T291]	MEK1	**100**	**117**	**279**
41	MAPK/ERK protein-serine kinase 1 (MKK1) [T385]	MEK1	**100**	**141**	**469**
42	MAPK/ERK protein-serine kinase 1/2 (MKK1/2) [S217/S221]	MEK1/2	**100**	**268**	**123**
43	MAPK/ERK protein-serine kinase 2 (MKK2) [T394] (mouse)	MEK2 mouse	**100**	**81**	**54**
44	Mitogen-activated protein kinase-activated protein kinase 2 [T222]	MAPKAPK2	**100**	**253**	**199**
45	Mitogen-activated protein kinase-activated protein kinase 2 alpha [T334]	MAPKAPK2a	n.d.	n.d.	n.d.
46	Mitogen-activated protein kinase-activated protein kinase 2 beta [T334]	MAPKAPK2b	n.d.	n.d.	n.d.
47	p21-activated protein-serine kinase 1/2/3 [S144/S141/S154] (54)	PAK1/2/3	**100**	**106**	**95**
48	p21-activated protein-serine kinase 1/2/3 [S144/S141/S154] (56)	PAK1/2/3	n.d	n.d	n.d
49	SMA- and mothers against decapentaplegic homolog 2 [S465+S467]	Smad2	n.d	n.d	n.d
50	SMA- and mothers against decapentaplegic homologs 1/5/9 [S463+S465/S463+S465/S465+S467]	Smad1/5/9	**100**	**0**	**139**
51	Src protein-tyrosine kinase [Y418] (44)	Src	n.d	n.d	n.d
52	Src protein-tyrosine kinase [Y418] (46)	Src	**100**	**160**	**56**
53	Src protein-tyrosine kinase [Y529] (44)	Src	**100**	**64**	**36**
54	Src protein-tyrosine kinase [Y529] (46)	Src	**100**	**205**	**74**

Table 3.3 Semi-quantitative analysis of phosphorylation and expression of several cell signaling proteins in DCs. The phosphorylation status and expression of several cell signaling proteins was altered in DCs infected by CD40-targeted Ad5-CMV-SV40 T-Ag at 24 h post-infection compared with DCs infected by untargeted Ad5-CMV-SV40 T-Ag and the control uninfected DCs.

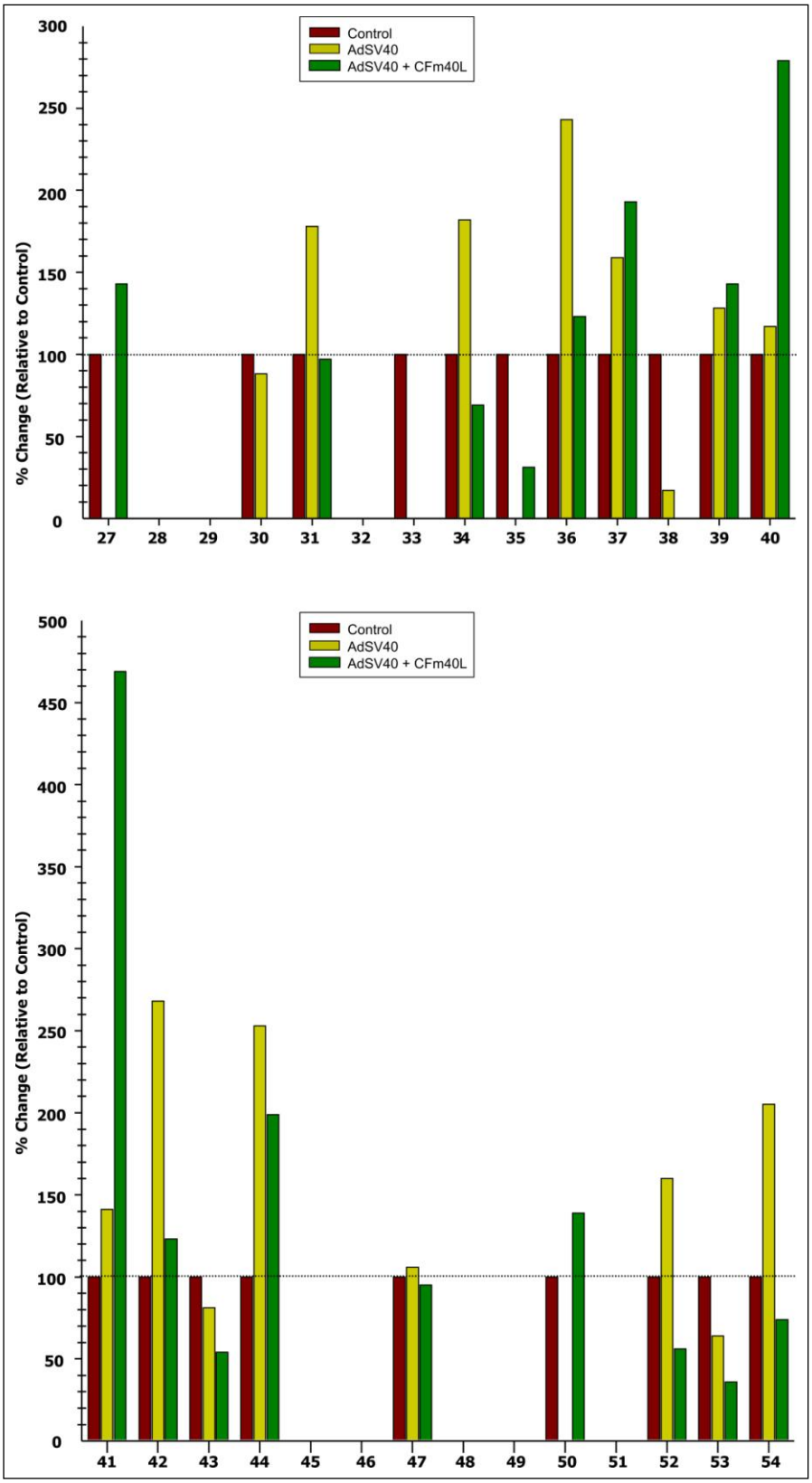

Figure 3.4 Graphical representation of semi-quantitative analysis of phosphorylation and expression of several cell signaling proteins in DCs. The phosphorylation status and expression of several cell signaling proteins was altered in DCs infected by CD40-targeted Ad5-CMV-SV40 T-Ag at 24 h post-infection compared with DCs infected by untargeted Ad5-CMV-SV40 T-Ag and the control uninfected DCs.

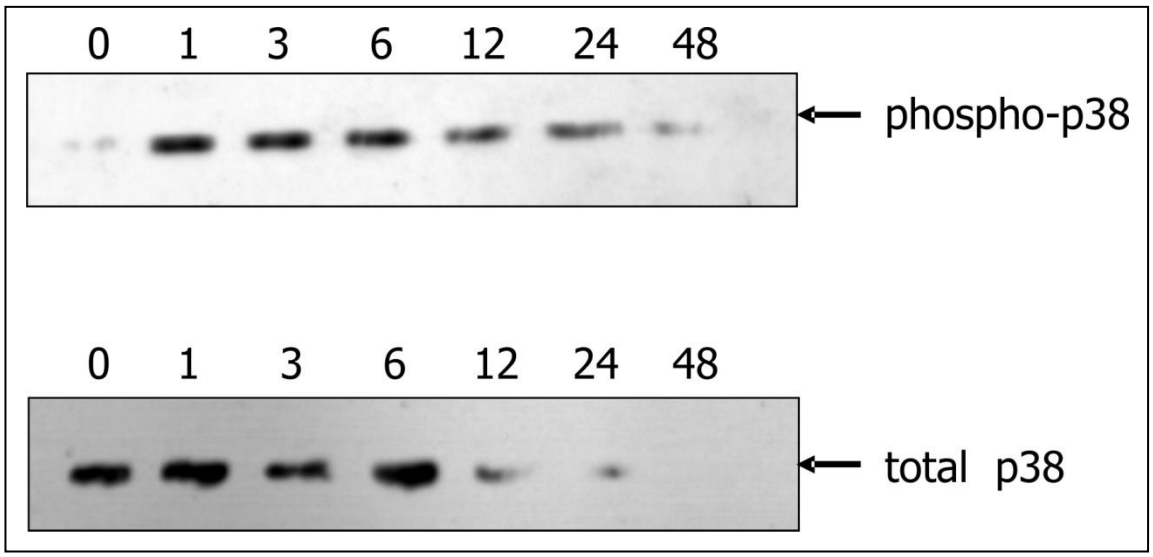

Figure 3.5 Western blot analysis of phosphorylation of p38 MAPK in DCs infected by CD40-targeted Ad5-CMV-SV40 T-Ag. The phosphorylation of p38 MAPK was induced within 1 h after infection with CD40-targeted Ad5-CMV-SV40 T-Ag.

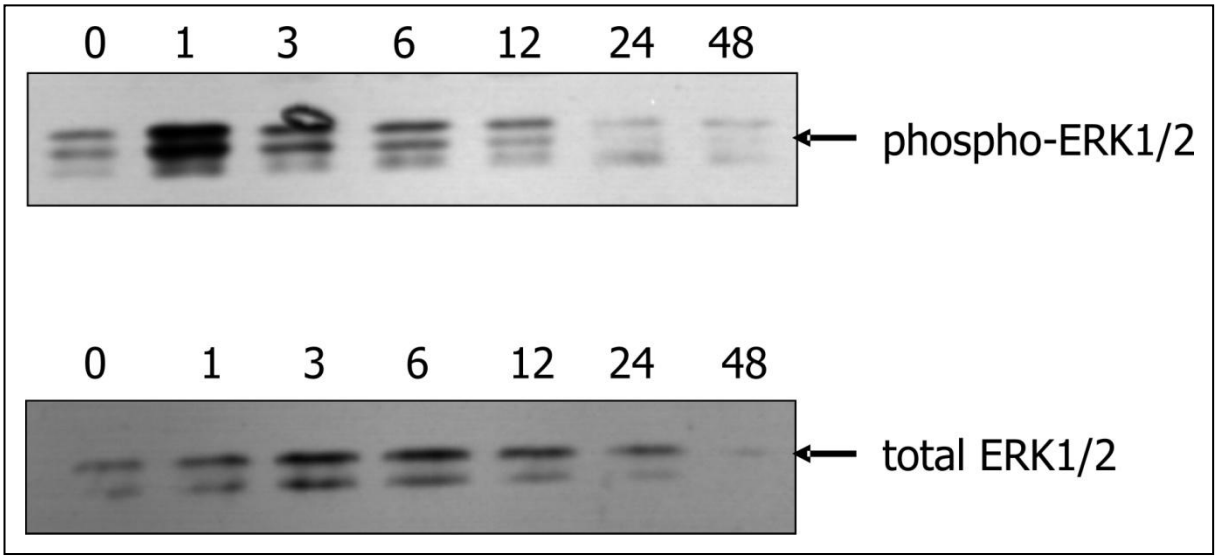

Figure 3.6 Western blot analysis of phosphorylation of ERK1/2 MAPK in DCs infected by CD40-targeted Ad5-CMV-SV40 T-Ag. The phosphorylation of ERK1/2 MAPK was induced within 1 h after infection with CD40-targeted Ad5-CMV-SV40 T-Ag.

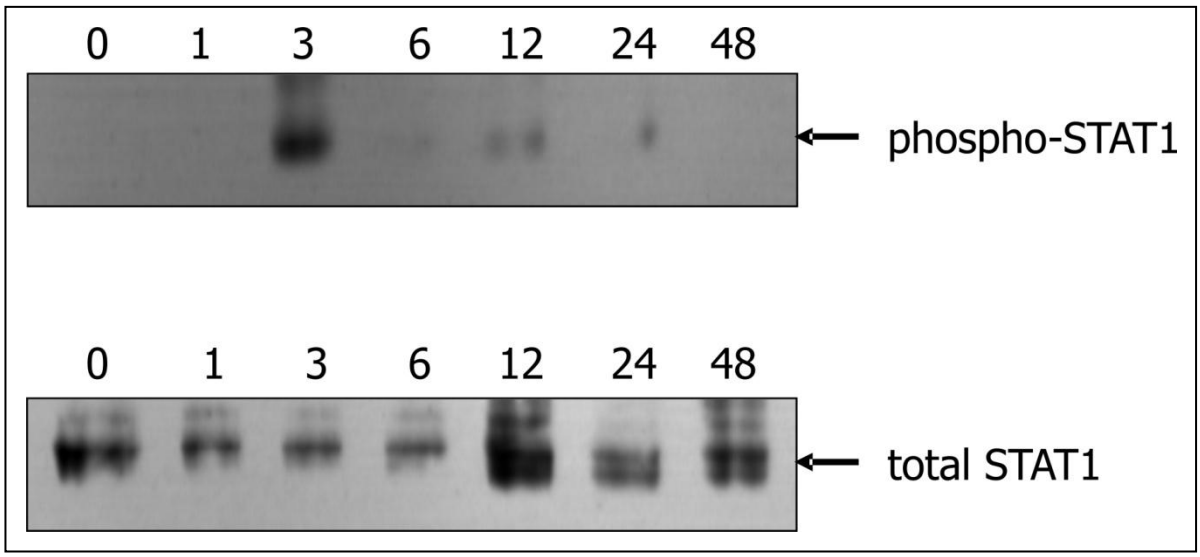

Figure 3.7 Western blot analysis of phosphorylation of STAT1 in DCs infected by CD40-targeted Ad5-CMV-SV40 T-Ag. The phosphorylation of STAT1 occurs in between 1 and 3 h after infection with CD40-targeted Ad5-CMV-SV40 T-Ag.

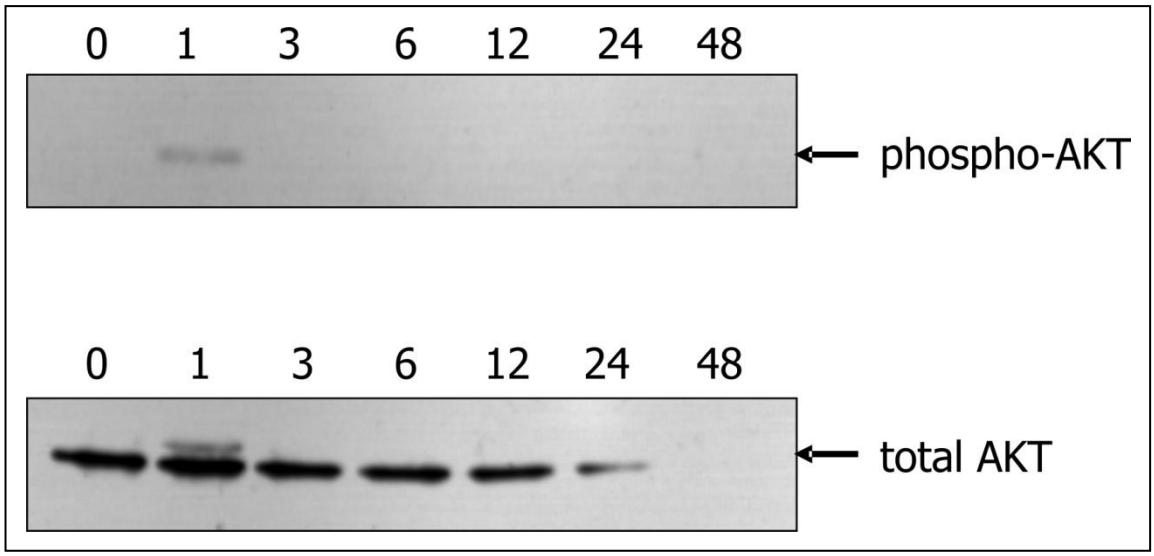

Figure 3.8 Western blot analysis of phosphorylation of AKT in DCs infected by CD40-targeted Ad5-CMV-SV40 T-Ag. The phosphorylation of AKT was induced within 1 h after infection with CD40-targeted Ad5-CMV-SV40 T-Ag.

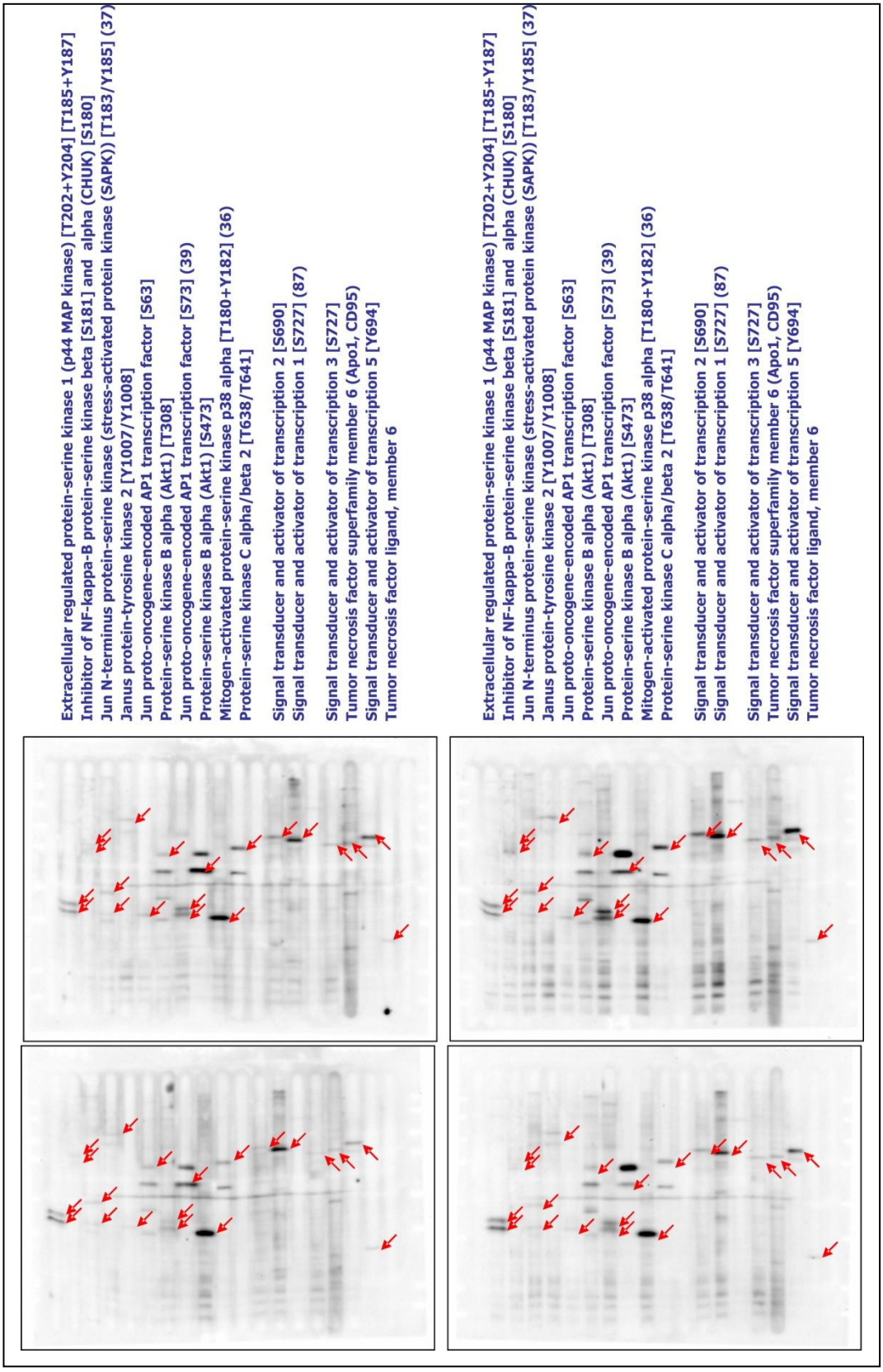

Figure 3.9 Immunoblot analysis of phosphorylation and expression of several cell signaling proteins in DCs. The phosphorylation status and expression of several cell signaling proteins was altered in DCs infected by CD40-targeted Ad5-CMV-SV40 T-Ag at 1 h post-infection compared with DCs infected by untargeted Ad5-CMV-SV40 T-Ag, DCs treated with CFm40L alone and the control uninfected DCs.

	FULL NAME OF PROTEIN	ABBREV	% CHANGE RELATIVE TO CONTROL			
			Untreated	CFm40L	AdSV40	AdSV40 + CFm40L
1	Extracellular regulated protein-serine kinase 1 (p44 MAP kinase) [T202+Y204]	Erk1	**100**	**80**	**107**	**134**
2	Extracellular regulated protein-serine kinase 2 (p42 MAP kinase) [T185+Y187]	Erk2	**100**	**79**	**184**	**175**
3	Inhibitor of NF-kappa-B protein-serine kinase alpha (CHUK) [S180]	IKKa	**100**	**153**	**46**	**74**
4	Inhibitor of NF-kappa-B protein-serine kinase beta [S181]	IKKb	**100**	**88**	**90**	**80**
5	Janus protein-tyrosine kinase 2 [Y1007/Y1008]	JAK2	**100**	**120**	**110**	**118**
6	Jun N-terminus protein-serine kinase (stress-activated protein kinase (SAPK)) [T183/Y185] (37)	JNK	**100**	**76**	**155**	**118**
7	Jun N-terminus protein-serine kinase (stress-activated protein kinase (SAPK)) [T183/Y185] (38)	JNK	**100**	**82**	**87**	**62**
8	Jun N-terminus protein-serine kinase (stress-activated protein kinase (SAPK)) [T183/Y185] (44)	Jun	**100**	**56**	**50**	**55**
9	Jun N-terminus protein-serine kinase (stress-activated protein kinase (SAPK)) [T183/Y185] (46)	Jun	**100**	**100**	**80**	**108**
10	Jun proto-oncogene-encoded AP1 transcription factor [S63]	Jun	**100**	**112**	**53**	**98**
11	Jun-c trascription factor [S73]	Jun	n.d.	n.d.	n.d.	n.d.
12	Mitogen-activated protein-serine kinase p38 alpha [T180+Y182] (36)	p38a MAPK	**100**	**68**	**182**	**128**
13	Mitogen-activated protein-serine kinase p38 alpha [T180+Y182] (40)	p38a MAPK	n.d.	n.d.	n.d.	n.d.
14	Protein-serine kinase B alpha (Akt1) [S473]	PKBa (Akt1)	**100**	**34**	**41**	**25**
15	Protein-serine kinase B alpha (Akt1) [T308]	PKBa (Akt1)	**100**	**67**	**83**	**87**
16	Protein-serine kinase C alpha/beta 2 [T638/T641]	PKCa/b2 [T638/T641]	**100**	**92**	**57**	**53**
17	Signal transducer and activator of transcription 1 [S727] (78)	STAT1	n.d.	n.d.	n.d.	n.d.
18	Signal transducer and activator of transcription 1 [S727] (87)	STAT1	**100**	**98**	**60**	**91**
19	Signal transducer and activator of transcription 1 [Y701] (78)	STAT1	n.d.	n.d.	n.d.	n.d.
20	Signal transducer and activator of transcription 1 [Y701] (87)	STAT1	n.d.	n.d.	n.d.	n.d.
21	Signal transducer and activator of transcription 2 [S690]	STAT2	**100**	**114**	**82**	**74**
22	Signal transducer and activator of transcription 3 [S727]	STAT3	**100**	**111**	**52**	**92**
23	Signal transducer and activator of transcription 5 [Y694]	STAT5	**100**	**36**	**57**	**98**
24	Tumor necrosis factor ligand, member 6	FasL	**100**	**91**	**150**	**125**
25	Tumor necrosis factor superfamily member 6 (Apo1, CD95)	FAS	**100**	**41**	**102**	**42**
26	Yes-related protein-tyrosine kinase	Lyn	n.d.	n.d.	n.d.	n.d.

Table 3.4 Semi-quantitative analysis of phosphorylation and expression of several cell signaling proteins in DCs. The phosphorylation status and expression of several cell signaling proteins was altered in DCs infected by CD40-targeted Ad5-CMV-SV40 T-Ag at 1 h post-infection compared with DCs infected by untargeted Ad5-CMV-SV40 T-Ag, DCs treated with CFm40L alone and the control uninfected DCs.

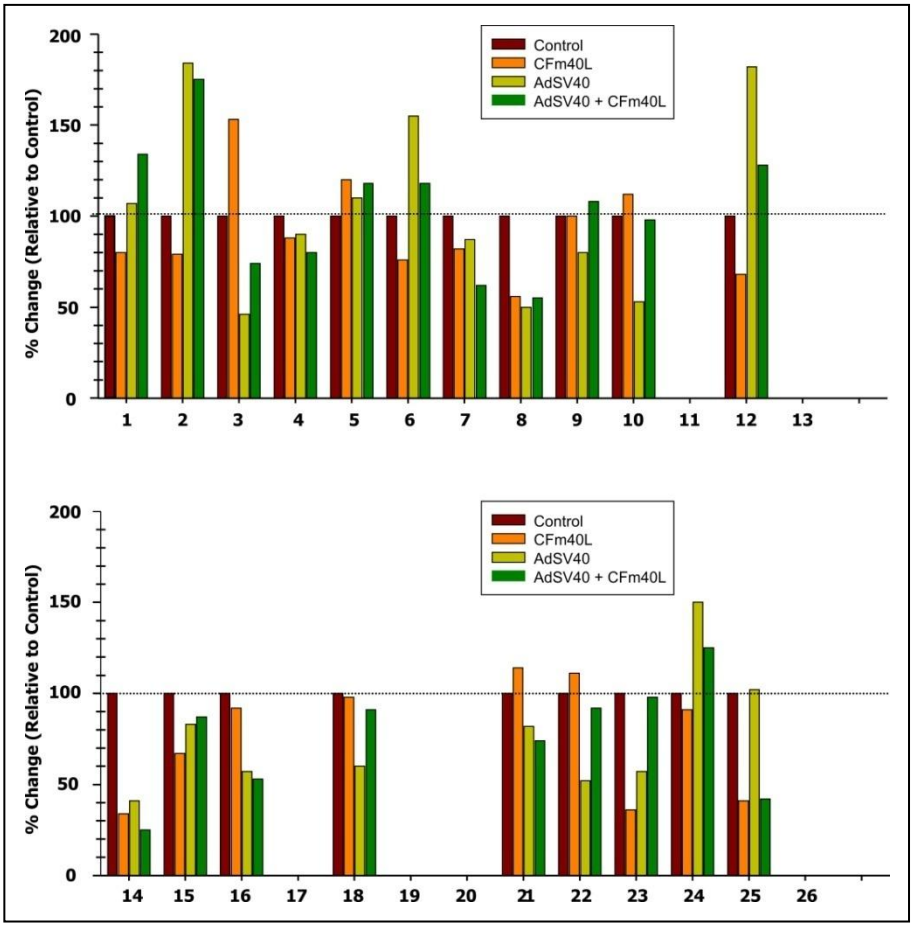

Figure 3.10 Graphical representation of semi-quantitative analysis of phosphorylation and expression of several cell signaling proteins in DCs. The phosphorylation status and expression of several cell signaling proteins was altered in DCs infected by CD40-targeted Ad5-CMV-SV40 T-Ag at 1 h post-infection compared with DCs infected by untargeted Ad5-CMV-SV40 T-Ag, DCs treated with CFm40L alone and the control uninfected DCs.

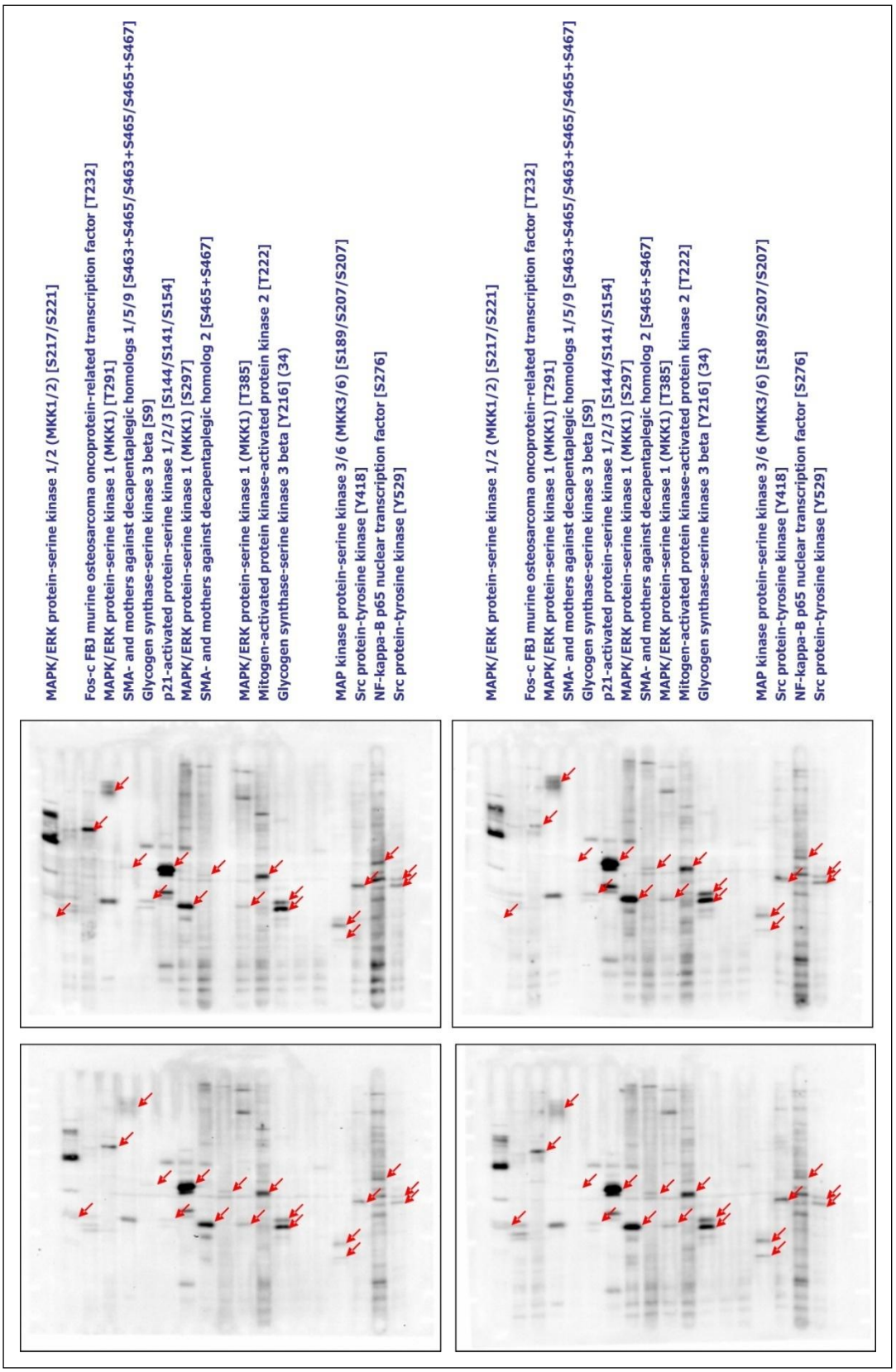

Figure 3.11 Immunoblot analysis of phosphorylation and expression of several cell signaling proteins in DCs. The phosphorylation status and expression of several cell signaling proteins was altered in DCs infected by CD40-targeted Ad5-CMV-SV40 T-Ag at 1 h post-infection compared with DCs infected by untargeted Ad5-CMV-SV40 T-Ag, DCs treated with CFm40L alone and the control uninfected DCs.

	FULL NAME OF PROTEIN	ABBREV	% CHANGE RELATIVE TO CONTROL			
			Untreated	CFm40L	AdSV40	AdSV40 + CFm40L
27	B23 (Nucleophosmin) [S4]	B23 (NPM)	n.d.	n.d.	n.d.	n.d.
28	Extracellular regulated protein-serine kinase 5 (Big MAP kinase 1) [T218/Y220]	Erk5 (BMK1)	n.d.	n.d.	n.d.	n.d.
29	Fos-c FBJ murine osteosarcoma oncoprotein-related transcription factor [T232]	Fos	**100**	**27**	**70**	**68**
30	Glycogen synthase-serine kinase 3 alpha [S21]	GSK3a	n.d.	n.d.	n.d.	n.d.
31	Glycogen synthase-serine kinase 3 alpha [Y279] (44)	GSK3a	n.d.	n.d.	n.d.	n.d.
32	Glycogen synthase-serine kinase 3 alpha [Y279] (49)	GSK3a	n.d.	n.d.	n.d.	n.d.
33	Glycogen synthase-serine kinase 3 beta [S9]	GSK3b	**100**	**107**	**62**	**67**
34	Glycogen synthase-serine kinase 3 beta [Y216] (34)	GSK3b	**100**	**134**	**108**	**125**
35	Glycogen synthase-serine kinase 3 beta [Y216] (39)	GSK3b	**100**	**128**	**99**	**132**
36	MAP kinase protein-serine kinase 3/6 (MKK3/6) [S189/S207]	MEK3/6	**100**	**94**	**85**	**105**
37	MAP kinase protein-serine kinase 4 (MKK4) [S257+T261]	MEK6	**100**	**188**	**196**	**372**
38	MAP kinase protein-serine kinase 6 (MKK6) [S207]	MEK1	**100**	**156**	**123**	**167**
39	MAPK/ERK protein-serine kinase 1 (MKK1) [S297]	MEK1	**100**	**94**	**82**	**103**
40	MAPK/ERK protein-serine kinase 1 (MKK1) [T291]	MEK1	**100**	**173**	**188**	**169**
41	MAPK/ERK protein-serine kinase 1 (MKK1) [T385]	MEK1/2	**100**	**43**	**135**	**154**
42	MAPK/ERK protein-serine kinase 1/2 (MKK1/2) [S217/S221]	MEK2 mouse	n.d.	n.d.	n.d.	n.d.
43	MAPK/ERK protein-serine kinase 2 (MKK2) [T394] (mouse)	MAPKAPK2	**100**	**114**	**121**	**130**
44	Mitogen-activated protein kinase-activated protein kinase 2 [T222]	MAPKAPK2a	n.d.	n.d.	n.d.	n.d.
45	Mitogen-activated protein kinase-activated protein kinase 2 alpha [T334]	MAPKAPK2b	n.d.	n.d.	n.d.	n.d.
46	Mitogen-activated protein kinase-activated protein kinase 2 beta [T334]	NFkappaB p65	**100**	**75**	**103**	**74**
47	p21-activated protein-serine kinase 1/2/3 [S144/S141/S154] (54)	PAK1/2/3	n.d.	n.d.	n.d.	n.d.
48	p21-activated protein-serine kinase 1/2/3 [S144/S141/S154] (56)	PAK1/2/3	**100**	**108**	**131**	**110**
49	SMA- and mothers against decapentaplegic homolog 2 [S465+S467]	Smad2	**100**	**168**	**171**	**113**
50	SMA- and mothers against decapentaplegic homologs 1/5/9 [S463+S465/S463+S465/S465+S467]	Smad1/5/9	**100**	**46**	**72**	**38**
51	Src protein-tyrosine kinase [Y418] (44)	Src	n.d.	n.d.	n.d.	n.d.
52	Src protein-tyrosine kinase [Y418] (46)	Src	**100**	**120**	**79**	**125**
53	Src protein-tyrosine kinase [Y529] (44)	Src	**100**	**122**	**76**	**98**
54	Src protein-tyrosine kinase [Y529] (46)	Src	**100**	**114**	**74**	**95**

Table 3.5 Semi-quantitative analysis of phosphorylation and expression of several cell signaling proteins in DCs. The phosphorylation status and expression of several cell signaling proteins was altered in DCs infected by CD40-targeted Ad5-CMV-SV40 T-Ag at 1 h post-infection compared with DCs infected by untargeted Ad5-CMV-SV40 T-Ag, DCs treated with CFm40L alone and the control uninfected DCs.

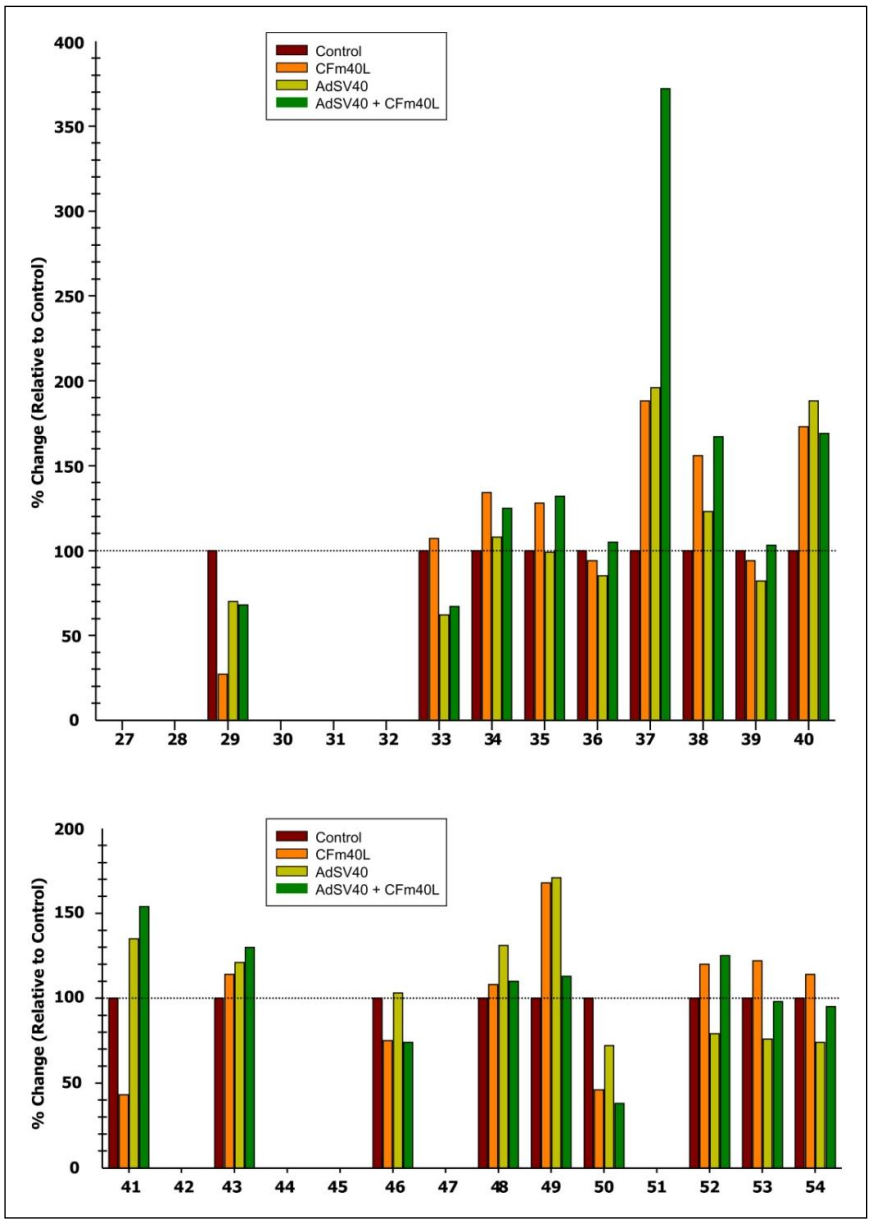

Figure 3.12 Graphical representation of semi-quantitative analysis of phosphorylation and expression of several cell signaling proteins in DCs. The phosphorylation status and expression of several cell signaling proteins was altered in DCs infected by CD40-targeted Ad5-CMV-SV40 T-Ag at 1 h post-infection compared with DCs infected by untargeted Ad5-CMV-SV40 T-Ag, DCs treated with CFm40L alone and the control uninfected DCs.

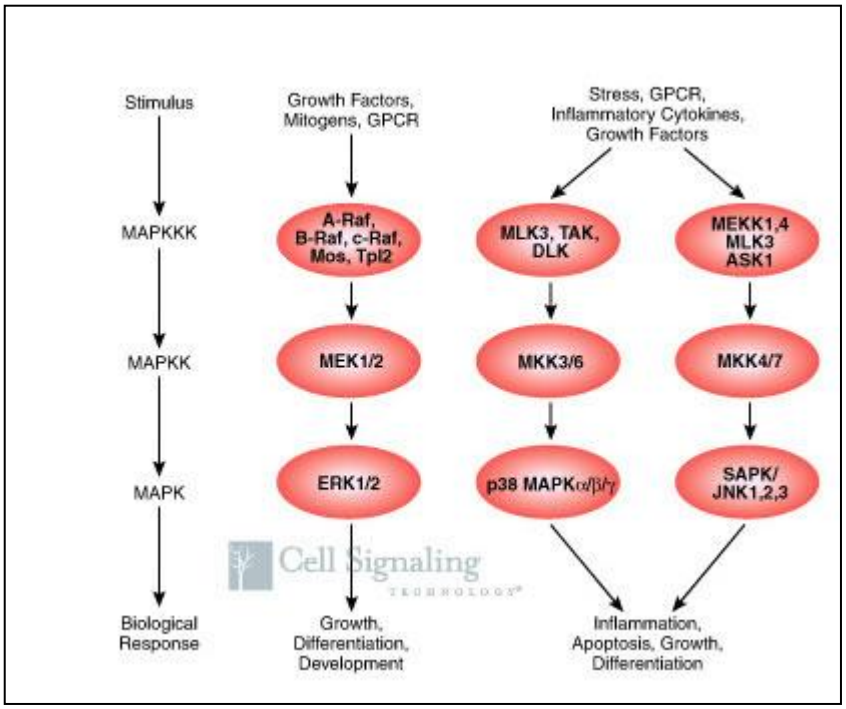

Figure 3.13 MAP kinase signaling Pathways

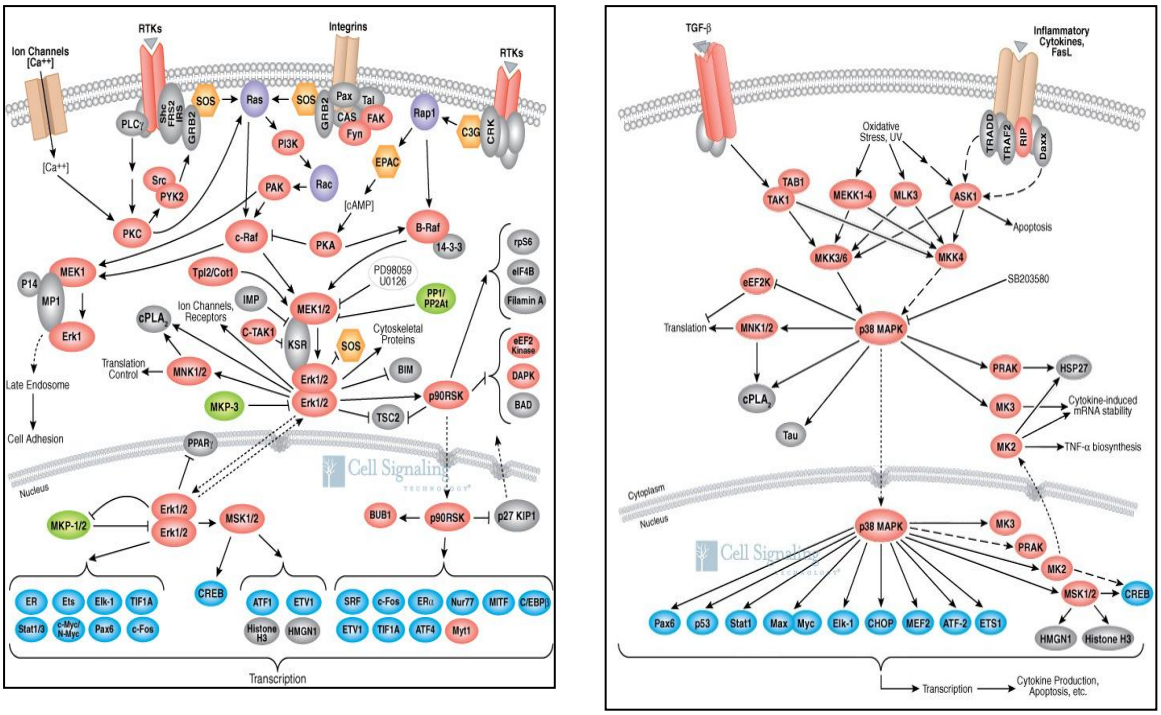

Figure 3.14 ERK1/2 and p38 MAP kinase signaling Pathways

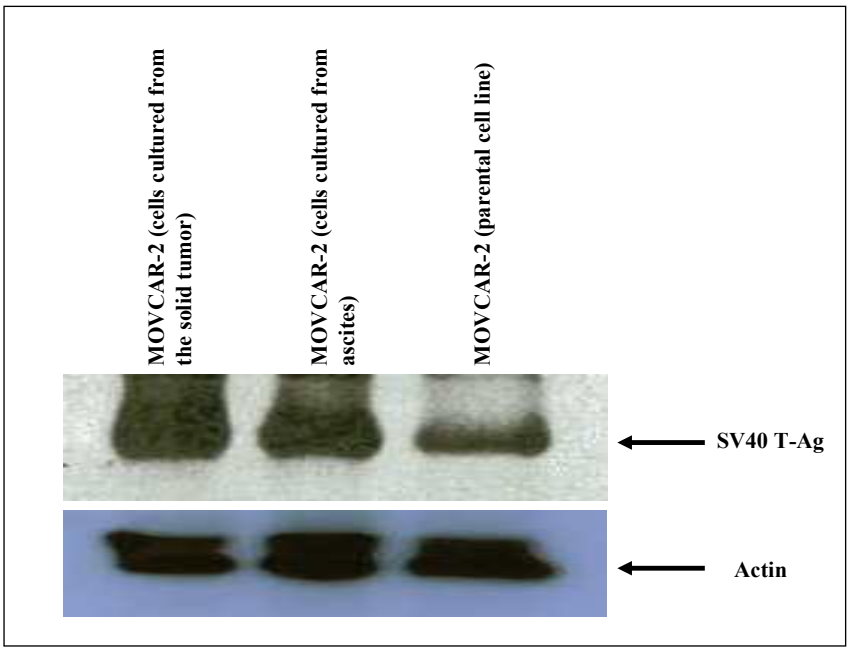

Figur vas detected in
MOV(tes (lane 2) and
the pa

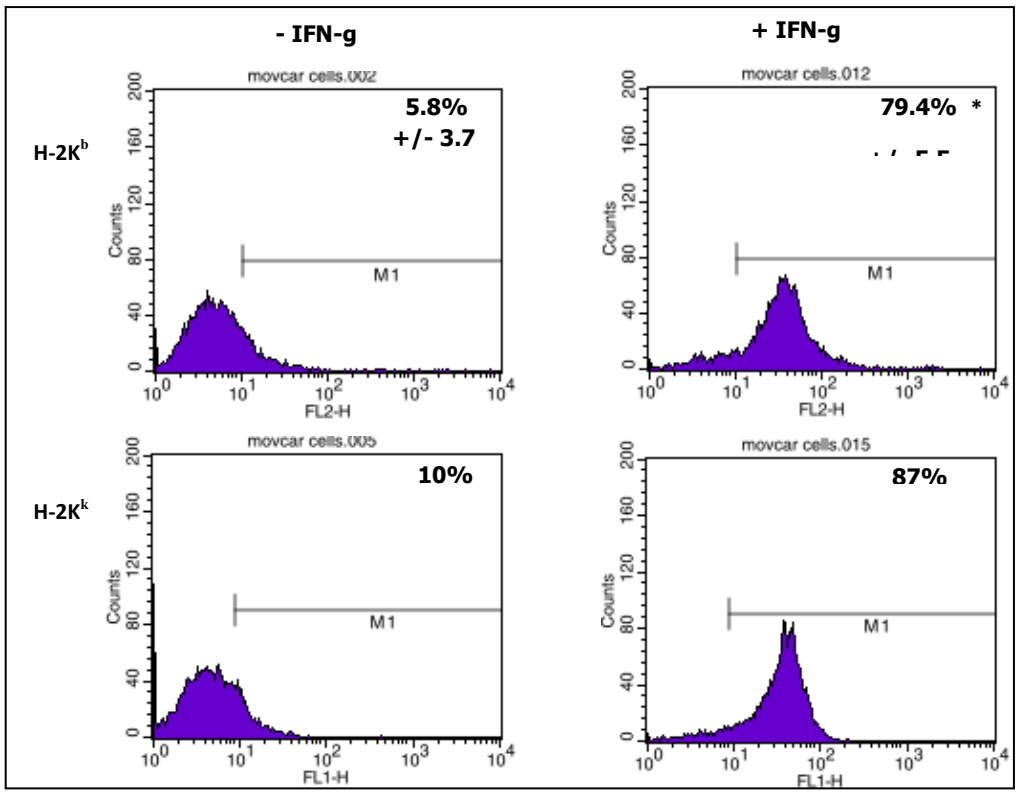

Figure 4.2 Flow cytometric analysis of the parental MOVCAR-2. The cells were stained with FITC-labeled antibody against MHC class I haplotypes Kb and Kk. * P < 0.05 versus control MOVCAR-2 cells, not treated with IFN-g.

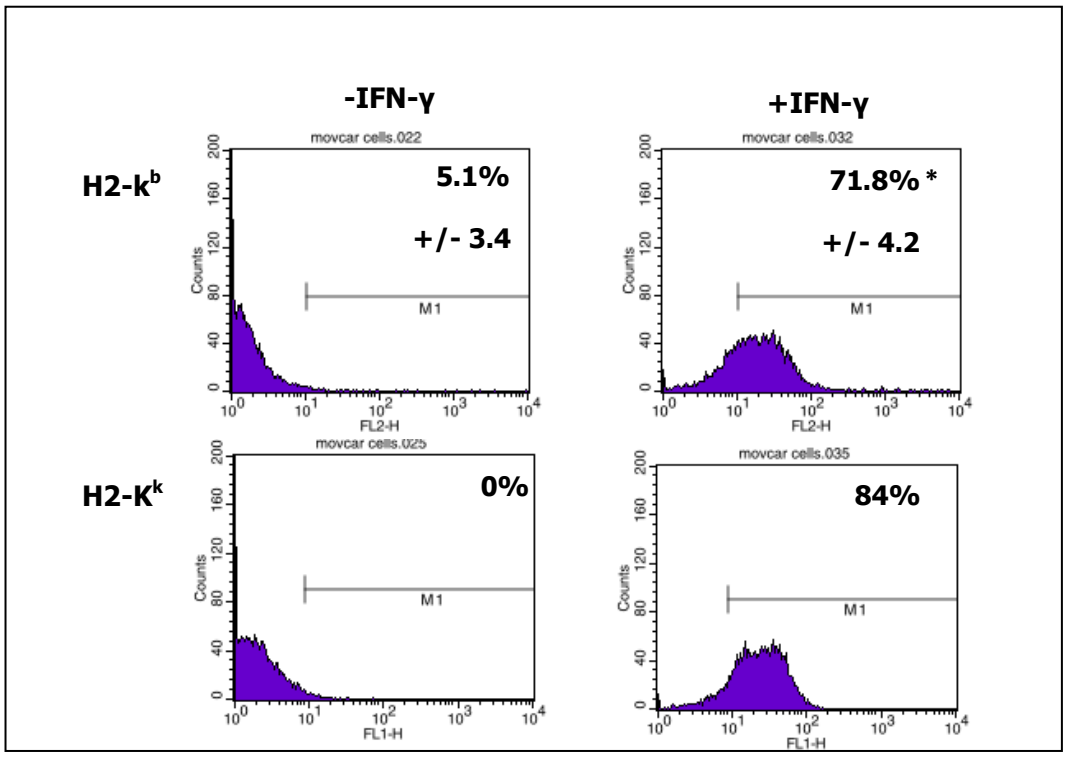

Figure 4.3 Flow cytometric analysis of MOVCAR-2 cells cultured from the ascites. The cells were stained with FITC-labeled antibody against MHC class I haplotypes Kb and Kk. * P < 0.05 versus control MOVCAR-2 cells, not treated with IFN-g.

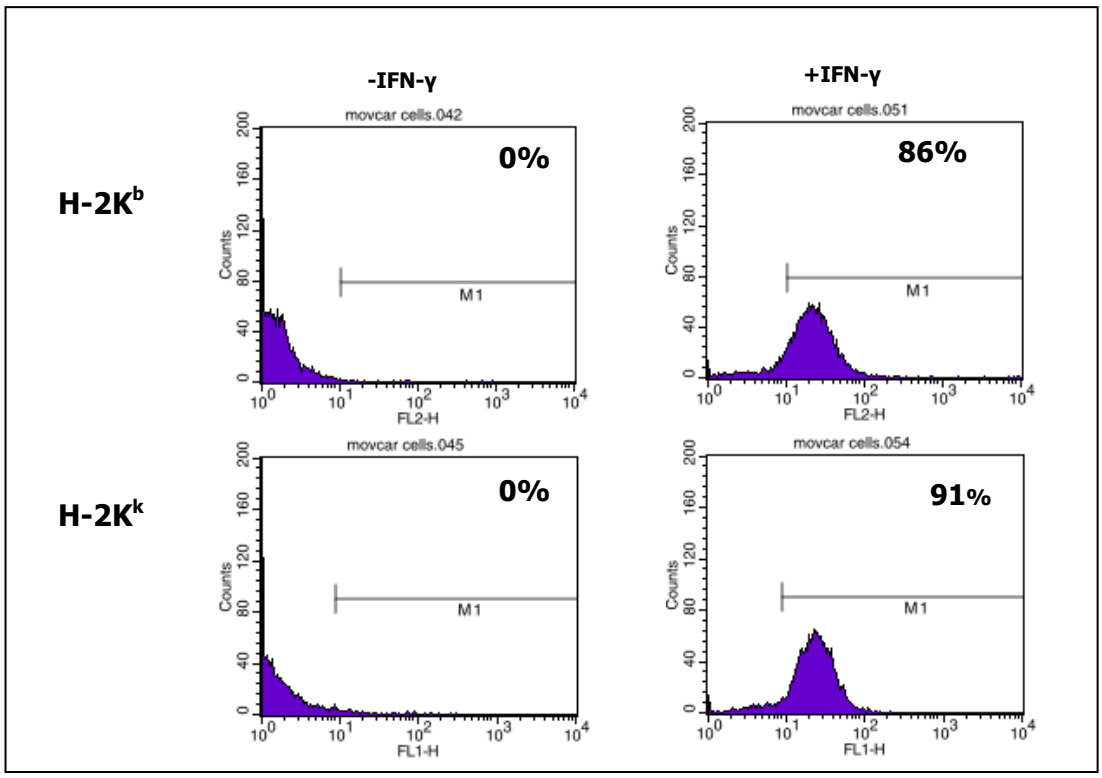

Figure 4.4 Flow cytometric analysis of MOVCAR-2 cultured from the solid tumor. The cells were stained with FITC-labeled antibody against MHC class I haplotypes Kb and Kk. * P < 0.05 versus control MOVCAR-2 cells, not treated with IFN-g.

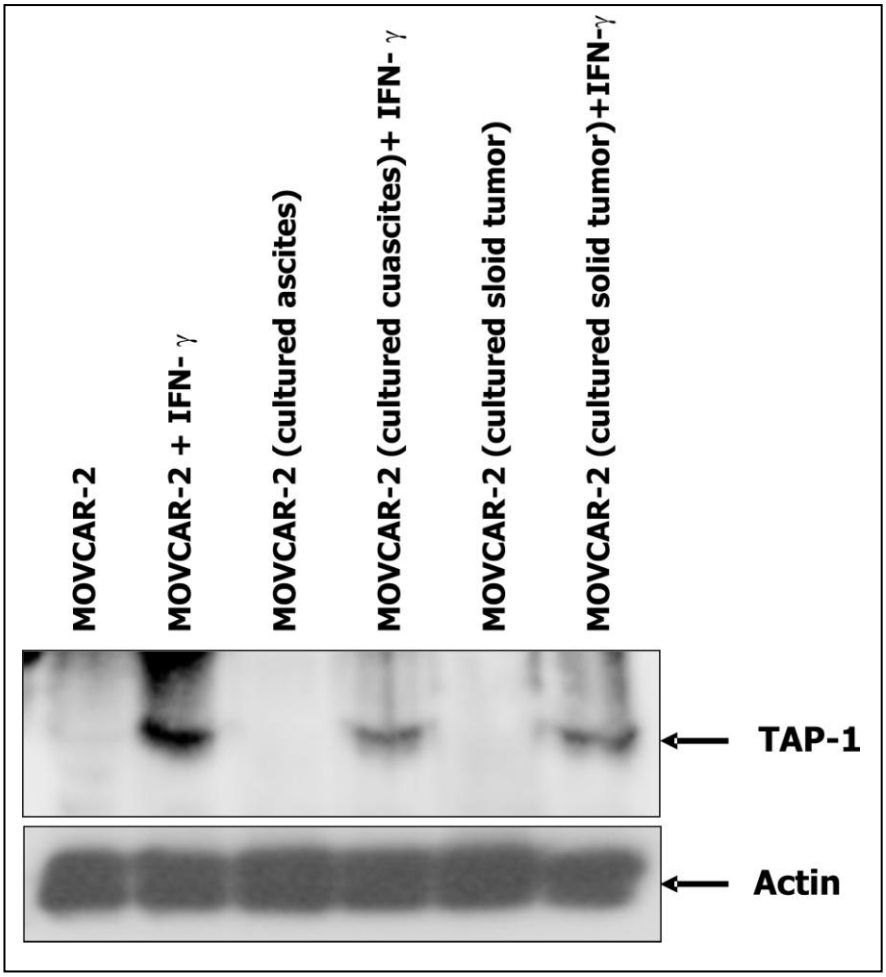

Figure 4.5 Western blot assay of MOVCAR-2 cells before and after treatment with IFN-gamma. The expression of TAP-1 was detected in MOVCAR-2 cells only after treatment with IFN-gamma. The IFN-gamma treated parental MOVCAR-2 cell line (lane 2), MOVCAR-2 cells cultured from the ascites (lane 4), MOVCAR-2 cells cultured from the solid tumor (lane 6) show expression of TAP-1, but not the untreated MOVCAR-2 cells (lanes 1, 3 and 5).

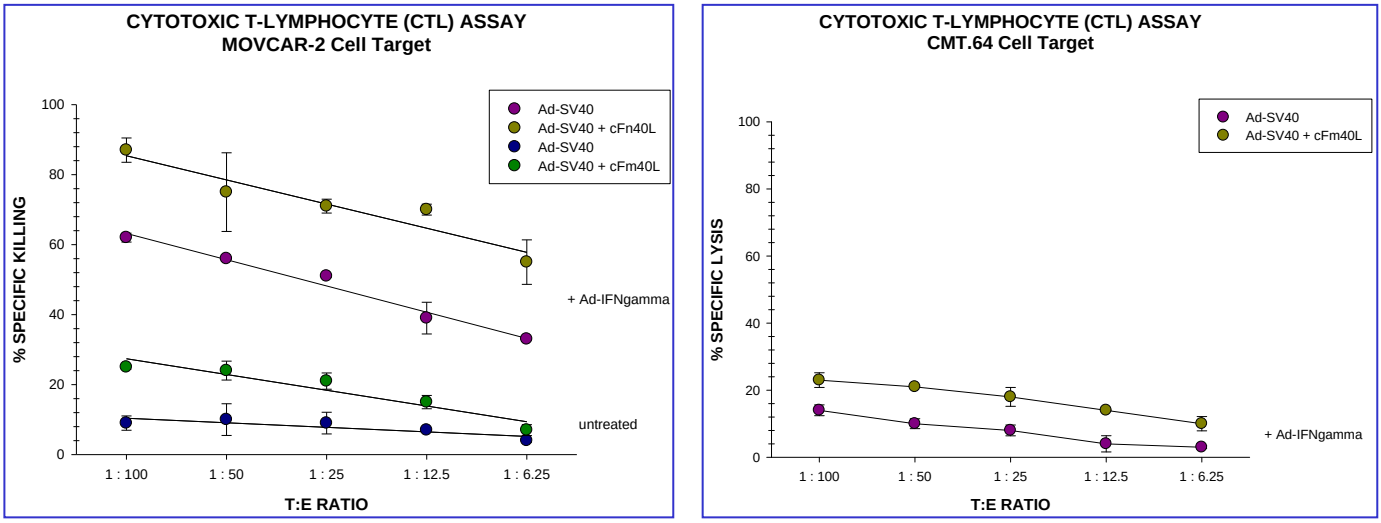

Figure 4.6 A standard 4 h ^{51}Cr release assay against target cells, MOVCAR-2 (IFN-γ treated as well as untreated) and negative control cells, CMT.64 (IFN-γ treated). The T-cells that were obtained from mice that were treated with Ad5-CMV-SV40 T-Ag + CFm40L showed higher cytolytic activity against the target MOVCAR-2 cells compared with the T-cells obtained from mice that were treated with Ad5-CMV-SV40 T-Ag alone. Each bar represents the mean ± standard error.

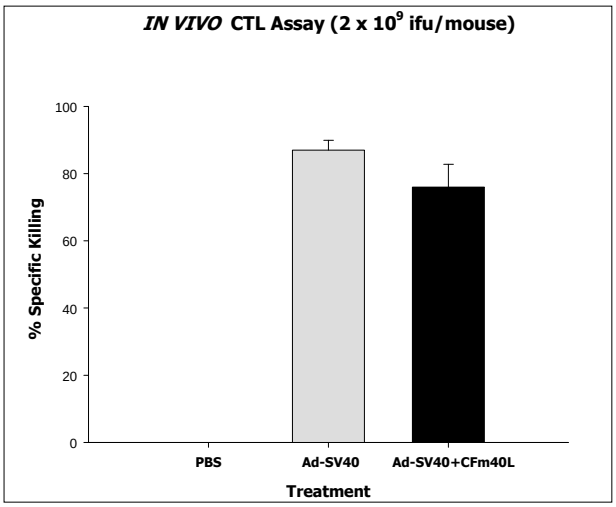

Figure 4.7 CFSE-l ; and untargeted Ad5-CMV-SV40 T-A vity. To prepare target cells for dete B6C3F1 spleen suspensions by osmotic lysis. The cells were then washed and split into two populations. One population was pulsed with 5 μM CKG and 5 μM VVY peptide, incubated at 37°C for 90 min, and labeled with a high concentration of CFSE (5 μM) (CFSEhigh cells). The second control target population was left unpulsed and labeled with a low concentration of CFSE (0.5 μM) (CFSElow cells). For i.v. injection, an equal number of cells from each population was mixed together such that each mouse received a total of 2×10^7 cells in 500 μl of PBS. The target cells were then injected into mice that had previously been immunized using CD40-targeted Ad5-CMV-SV40 T-Ag (2×10^9 ifu of virus complexed with 2400 ng of CFm40L) and untargeted Ad5-CMV-SV40 T-Ag (2×10^9 ifu of virus). Five h after i.v. injection of target cells, mice were sacrificed and harvested of their spleens. Cell suspensions were analyzed by flow cytometry, and each population was detected by their differential CFSE fluorescence intensities. Up to 5×10^3 CFSE-positive cells were collected for analysis. To calculate specific lysis, the following formula was used: ratio = (percentage $CFSE^{low}$/percentage $CFSE^{high}$). Percentage of specific lysis = [1 - (ratio unprimed/ratio primed)] × 100. The bars represent the mean values ± standard error of results obtained from 5 mice per treatment. * $P < 0.05$ versus control mice that received only PBS.

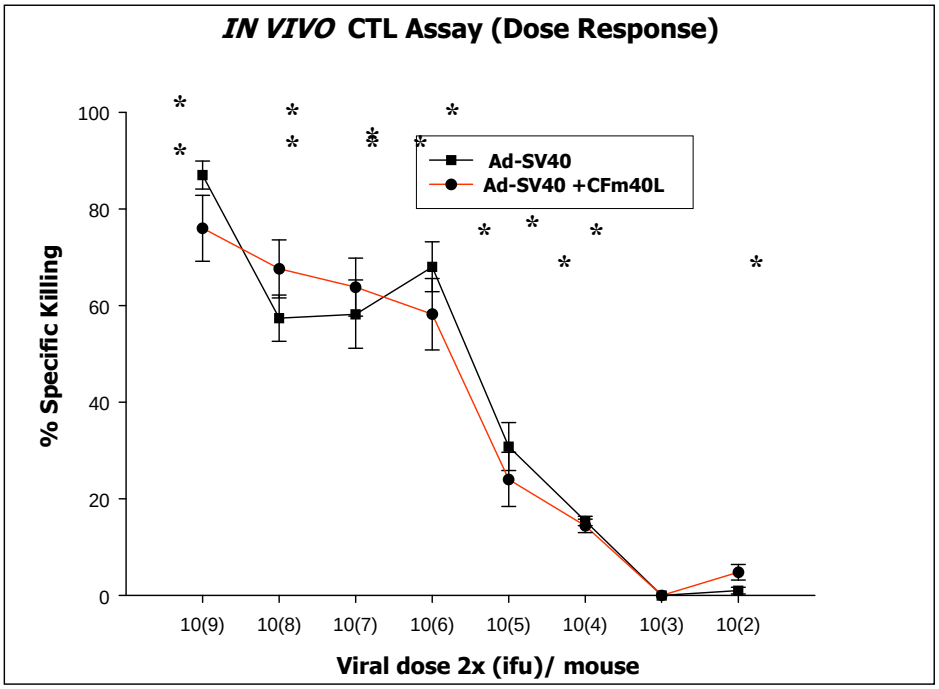

Figure 4.8 CFSE-based *in vivo* cytotoxicity assay. CD40-targeted Ad5-CMV-SV40 T-Ag and untargeted Ad5-CMV-SV40 T-Ag vaccines induce similar SV40 T-Ag specific cytotoxic T lymphocyte activity at all the doses of virus that were used for immunization. The B6C3F1 mice were immunized using various doses of CD40-targeted and untargeted Ad5-CMV-SV40 T-Ag, as described in materials and methods. The labeled target and control splenocyte cells, mixed 1:1, were injected intravenously in the immunized mice. After 5 h, the mice were sacrificed, spleens were harvested, and the two populations of splenocytes were analyzed by flow cytometry based on their differential labeling. The percentage of specific killing was also calculated as described in materials and methods. The symbols ● and ■ represent the mean value of percentage specific killing obtained in B6C3F1 mice immunized using CD40-targeted and untargeted Ad5-CMV-SV40 T-Ag respectively. Five mice were used per treatment for each dose of virus used for immunization. Each bar represents the mean ± standard error. * $P < 0.05$ versus control mice that received only PBS.

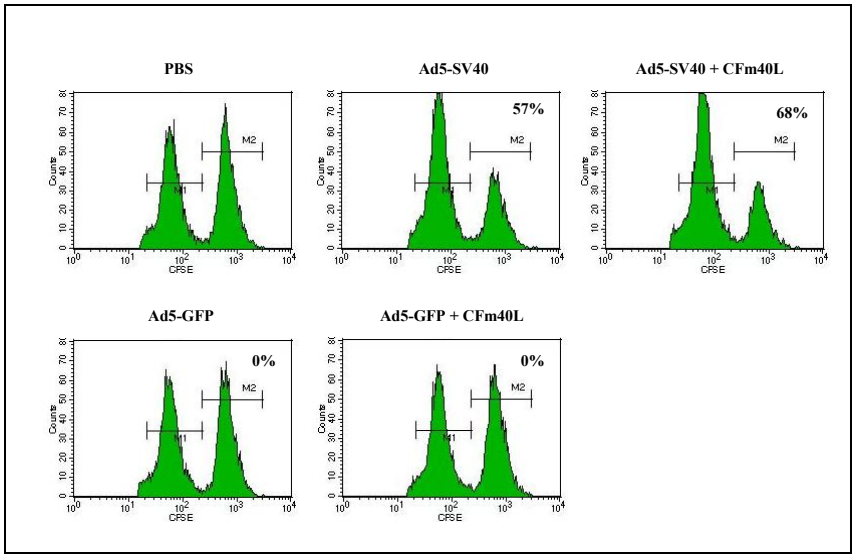

Figure 4.9 Representative histograms from the spleens of mice immunized using PBS, Ad5-CMV-SV40 T-Ag and Ad5-CMV-SV40 T-Ag complexed with CFm40L, Ad5-CMV-GFP and Ad5-CMV-GFP complexed with CFm40L to determine the *in vivo* killing of CFSE-labeled target cells. The B6C3F1 mice were immunized using 1×10^8 ifu of the above viruses and 240 ng of CFm40L, as described in materials and methods. The target cells were splenocytes harvested from naïve B6C3F1 mice that were pulsed with antigens corresponding to the antigenic epitopes of SV40 T-Ag and labeled with 5 μM of the dye CFSE. Non-pulsed splenocytes from the syngeneic B6C3F1 mice were labeled with 0.5 μM of the same dye CFSE and used as negative control. Both cell types were mixed 1:1 and injected intravenously in the immunized B6C3F1 mice. After 5 h the spleens were harvested from these mice and the splenocytes were analyzed by flow cytometry. The percentage of target and control cells was determined based on their differential labeling intensities. Up to 5×10^3 CFSE-positive cells were collected for analysis. Each peak M1 represents the control non-pulsed splenocytes and peak M2 represents the splenocytes pulsed with peptides CKG and VVY that correspond to the antigenic epitopes of SV40 T-Ag.

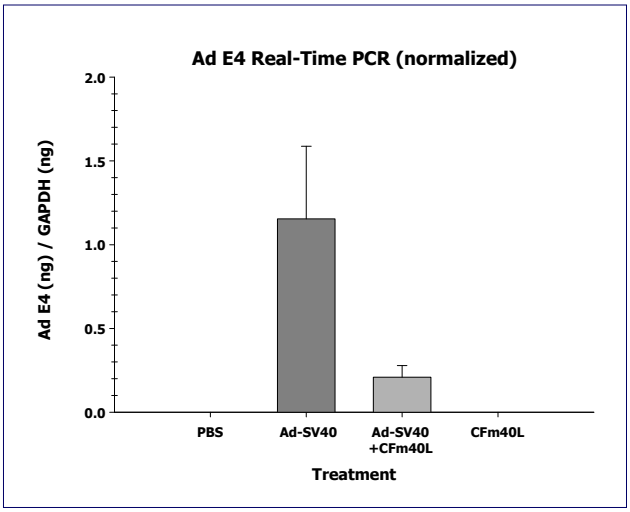

Figure 5.1 Quantitative comparison of adenoviral E4 DNA in livers of B6C3F1 mice immunized using CD40-targeted Ad5-CMV-SV40 T-Ag and untargeted Ad5-CMV-SV40 T-Ag by TaqMan Real-time PCR. The amount of adenoviral E4 DNA was expressed in nanograms (ng) and was normalized to the amount of mouse GAPDH DNA (ng), present in the liver tissue. There was increased amount of E4 DNA present in the livers of mice immunized using untargeted Ad5-CMV-SV40 T-Ag than the mice immunized using CD40-targeted Ad5-CMV-SV40 T-Ag. n = 5 mice was used per group. Each bar represents the mean ± standard error.

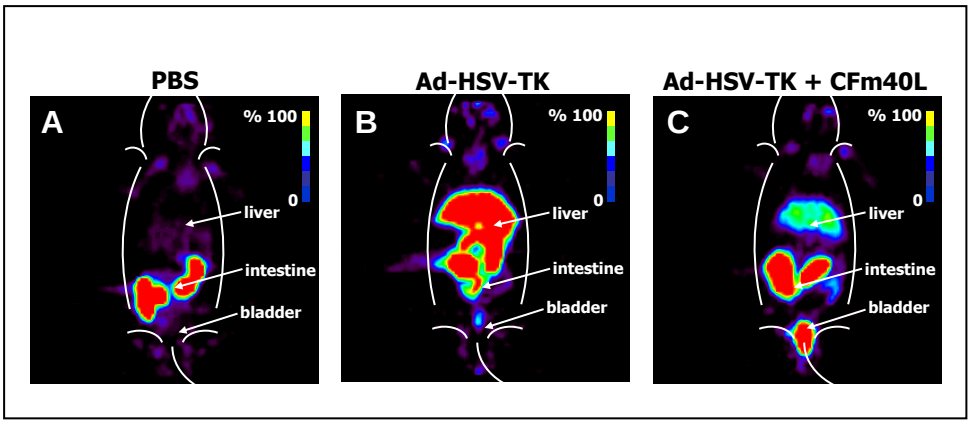

Figure 5.2 MicroPET imaging illustrating expression of TK in mice injected intraperitoneally with CD40-targeted Ad-HSV-TK and untargeted Ad-HSV-TK. (A) Image data from control mouse that received 500 μl of PBS. (B) Image data from mouse that received 1×10^9 ifu of untargeted Ad-HSV-TK. (C) Image data from mouse that received 1×10^9 ifu of CD40-targeted Ad-HSV-TK. There was higher expression of TK in the livers of mice that received untargeted Ad-HSV-TK than the mice that received CD40-targeted Ad-HSV-TK. The signal bars indicate 0 to 100% activity. The signal bars indicate 0 to 100% relative signal.

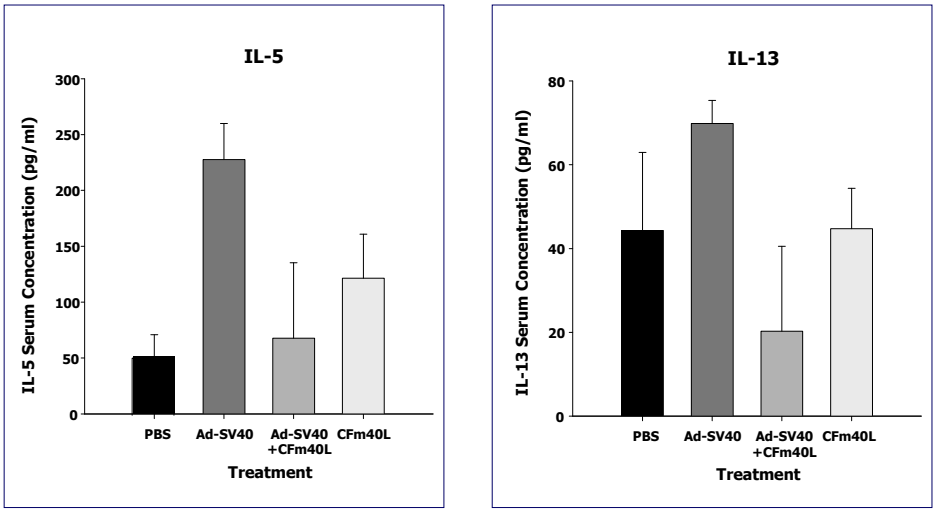

Figure 5.3 Quantitative analysis of inflammatory cytokines released in the blood of B6C3F1 mice immunized using CD40-targeted Ad5-CMV-SV40 T-Ag, untargeted Ad5-CMV-SV40 T-Ag and CFm40L by the cytokine bead array. Serum samples were collected from the immunized mice and analyzed for presence of cytokines using the *Bio-Plex* cytokine bead array. There was increased amounts of Th-2-type cytokines such as IL-5 and IL-13 in the serum of the mice immunized using untargeted Ad5-CMV-SV40 T-Ag (Ad-SV40) than the mice immunized using CD40-targeted Ad5-CMV-SV40 T-Ag (Ad-SV40 + CFm40L) and the control mice (PBS and CFm40L). n = 3 mice was used per group. Each bar represents the mean ± standard error. * P < 0.05 versus control mice that received only PBS. ** P < 0.05 versus mice that were immunized with CD40-targete

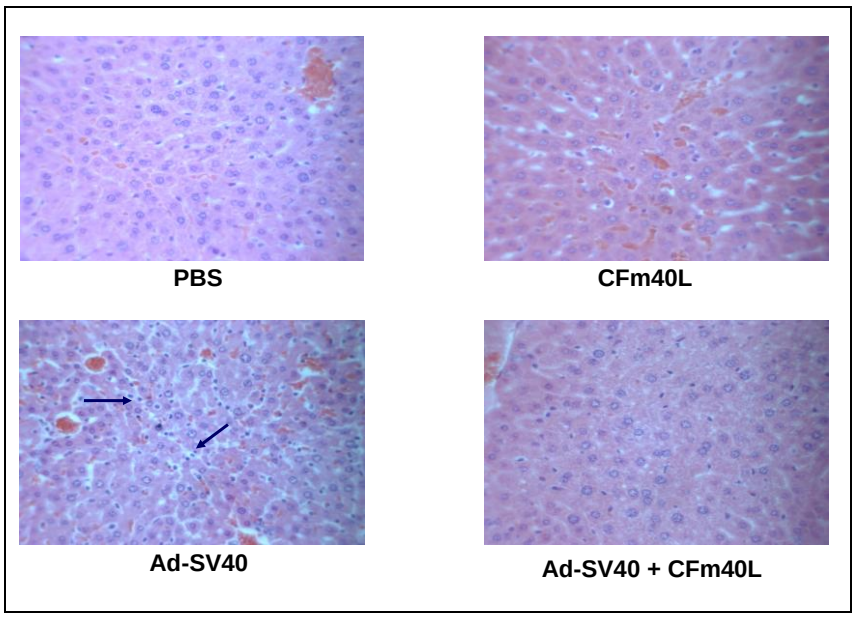

Figure 5.4 Hematoxylin and Eosin Staining of liver tissue from B6C3F1 mice immunized using CD40-targeted Ad5-CMV-SV40 T-Ag, untargeted Ad5-CMV-SV40 T-Ag and CFm40L. The mice injected with untargeted Ad5-CMV-SV40 T-Ag (Ad-SV40) showed increased infiltration of the liver by mononuclear inflammatory cells compared with livers of mice injected with CD40-targeted Ad5 SV40 Tag (Ad-SV40 + CFm40L) and control treatments (PBS, CFm40L).

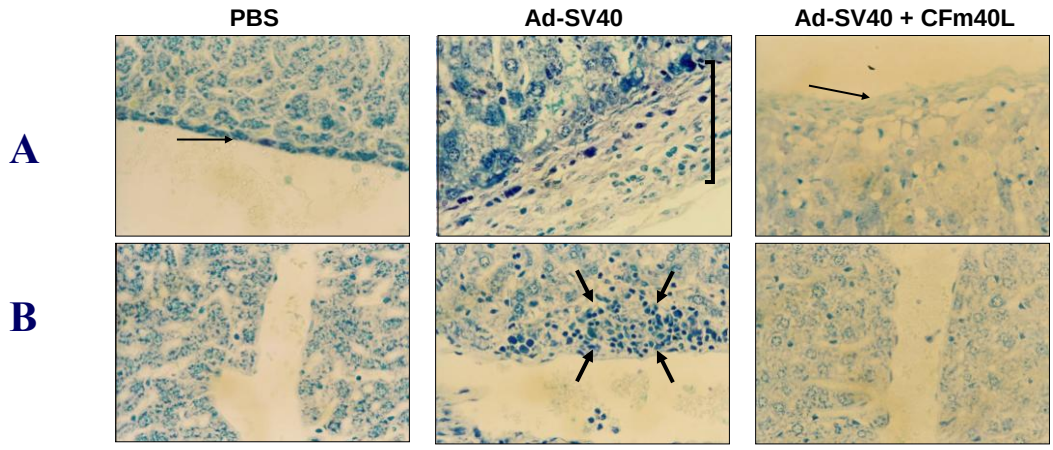

Figure 5.5 Romanowski staining of liver tissue from B6C3F1 mice immunized using CD40-targeted Ad5-CMV-SV40 T-Ag and untargeted Ad5-CMV-SV40 T-Ag. The mice injected with untargeted Ad5-CMV-SV40 T-Ag (Ad-SV40) showed increased (A) inflammation of the capsule of the liver and (B) infiltration of the mononuclear inflam e mice immunized using CD40-target).

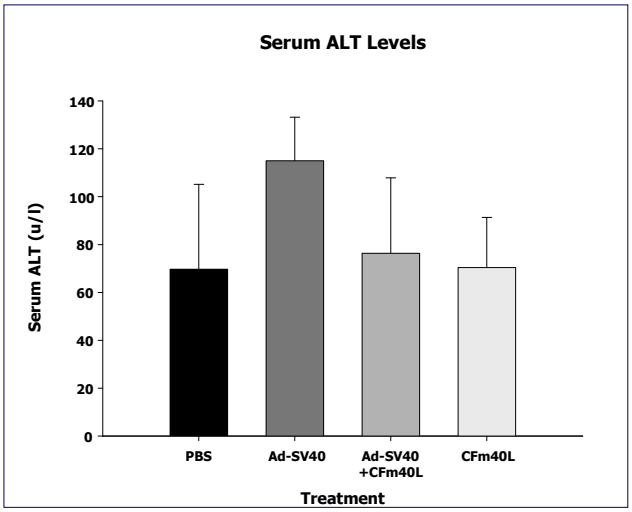

Figure 5.6 Analysis of serum marker for Liver damage, alanine aminotransferase (ALT), by ELISA. There was increased levels of ALT in the serum of mice immunized using untargeted Ad5-CMV-SV40 T-Ag (Ad-SV40) compared with the mice immunized using CD40-targeted Ad5-CMV-SV40 T-Ag (Ad-SV40 + CFm40L) and control treatments (PBS, CFm40L). n = 5 mice per group was used. Each bar represents the mean ± standard error.

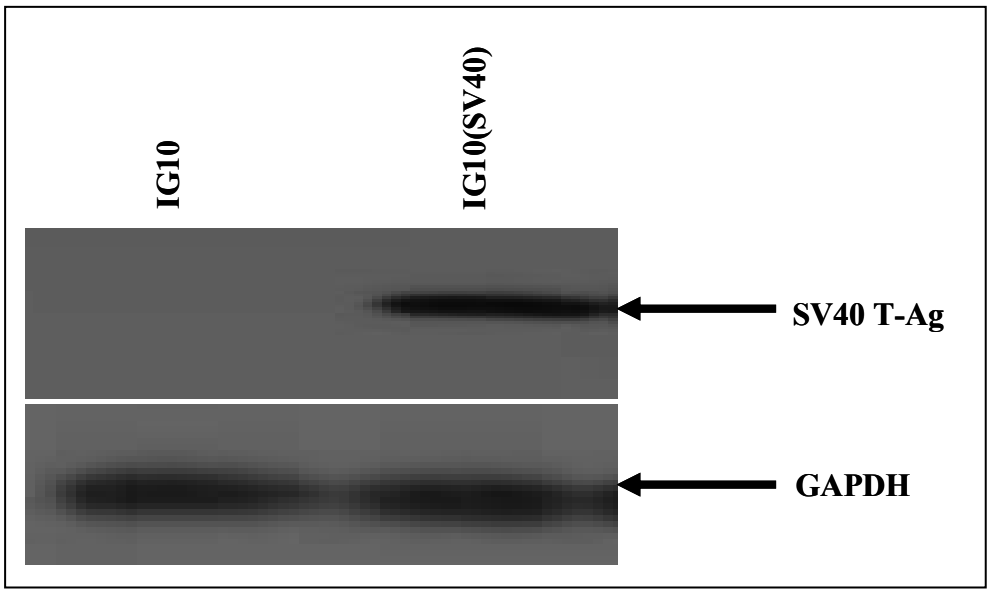

Figure 6.1 Western blot assay of IG10-Luc and IG10-SV40 cells. The expression of SV40 T-Ag was detected in IG10-SV40-Luc cells (lane 2) but not in IG10-Luc cells (lane 1).

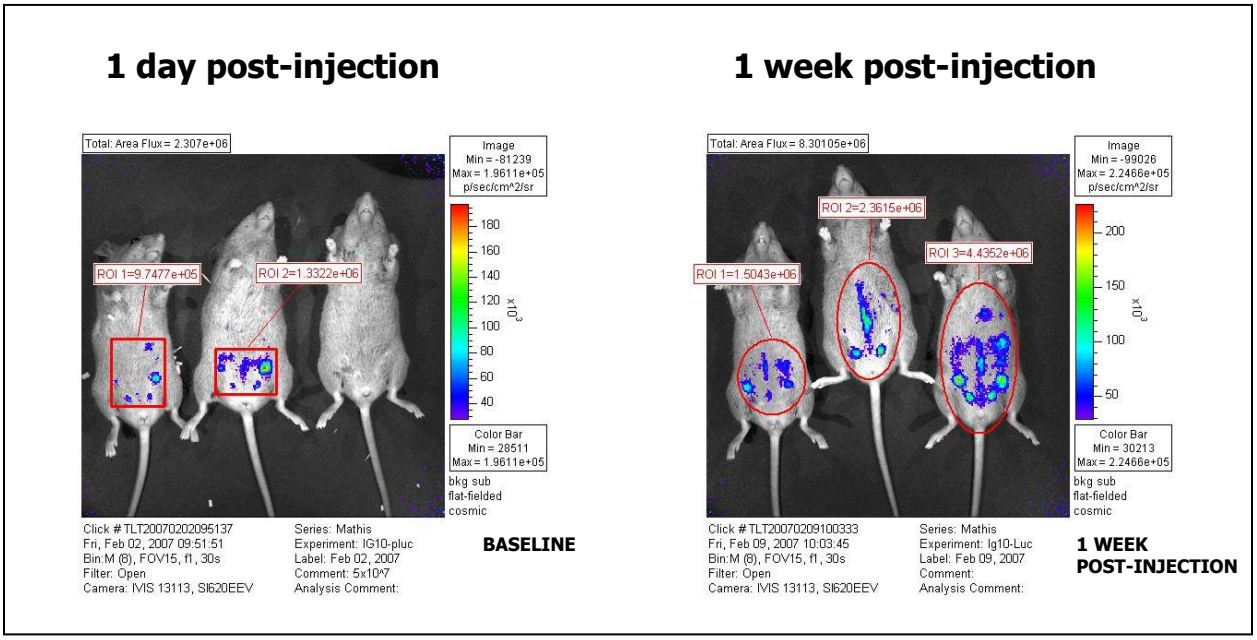

Figure 6.2 Bioluminescent Imaging. B6C3F1 mice were injected with IG10-Luc cells. Three mice were injected with 1×10^7 cells per mouse. The mice were subjected to bioluminescent imaging at 1 day and then 1 week after injection. The signal bars indicate relative photons light intensity.

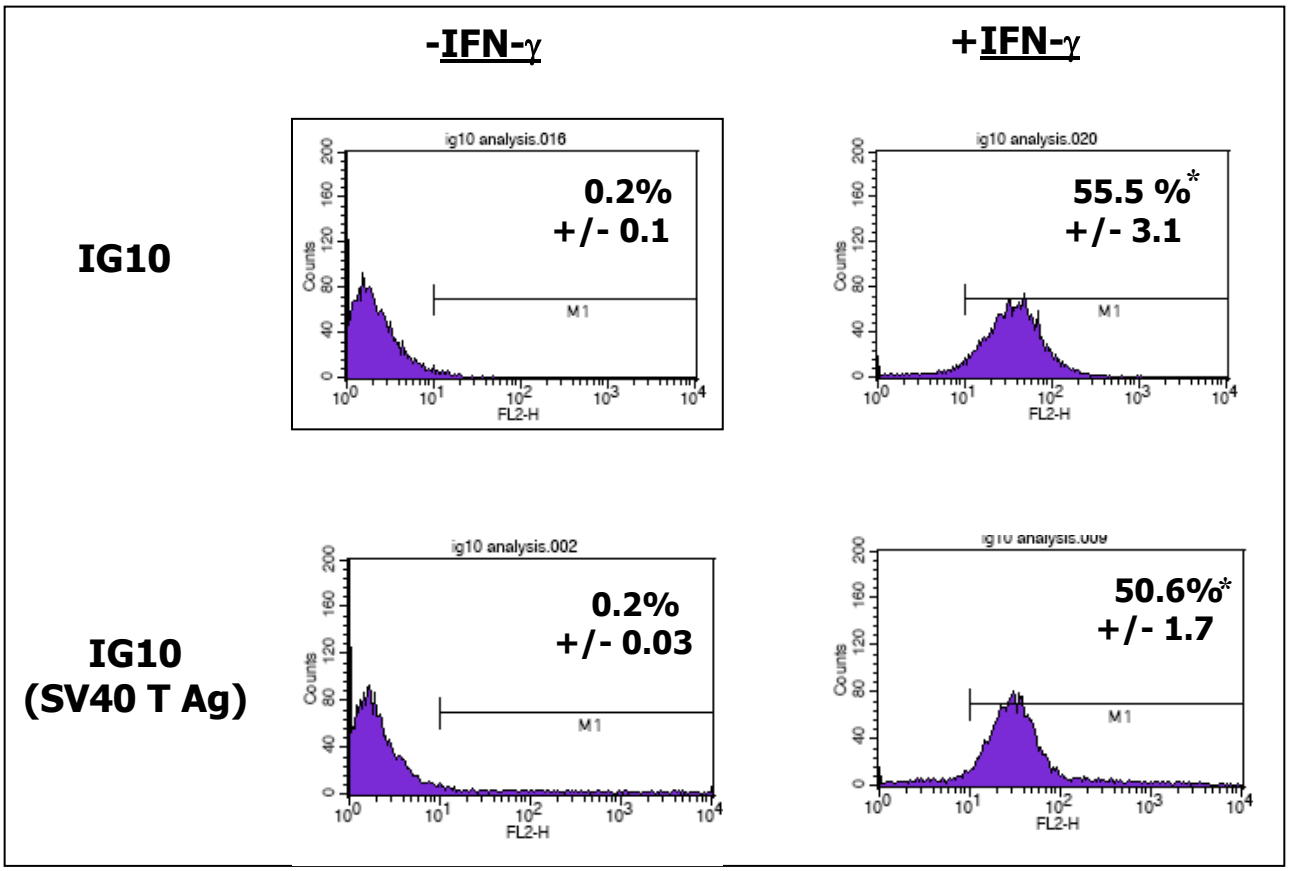

Figure 6.3 Flow cytometric analysis of the IG10-Luc and IG10-SV40-Luc cells without and with IFN-gamma treatment. The cells were stained with FITC-labeled antibody against MHC class I.
* P < 0.05 versus control IG10 and IG10(SV40) cells, not treated with IFN-g.

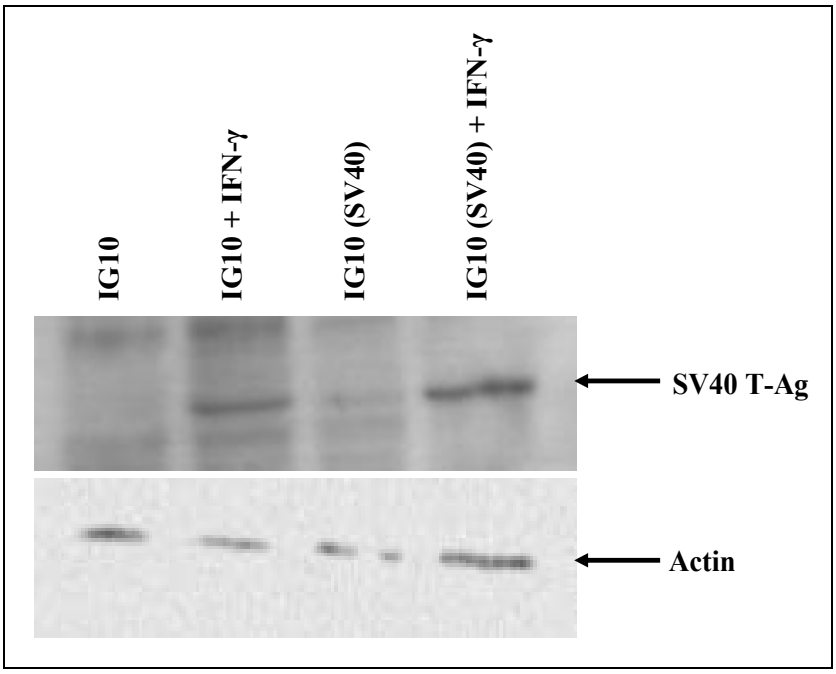

Figure 6.4 Western blot assay of IG10 and IG10-SV40 cells before and after treatment with IFN-gamma. a. ot

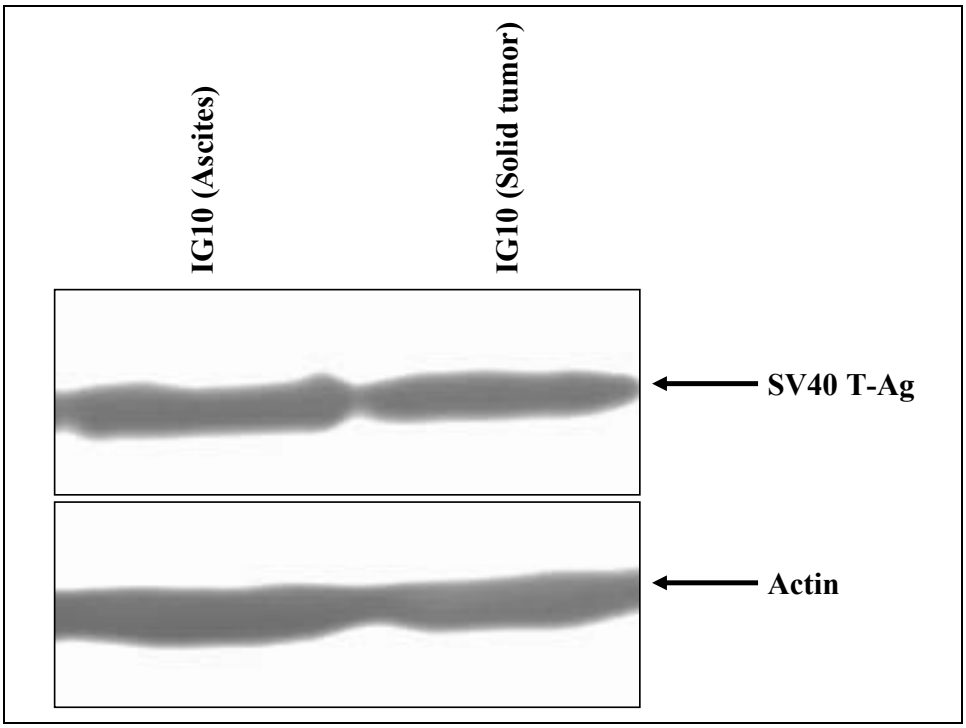

Figure 6.5 Western blot assay of IG10-SV40 cells. The expression of SV40 T-Ag was detected in tumor cells cultured from the ascites (lane 1) and cells cultured from the solid tumor (lane 2).

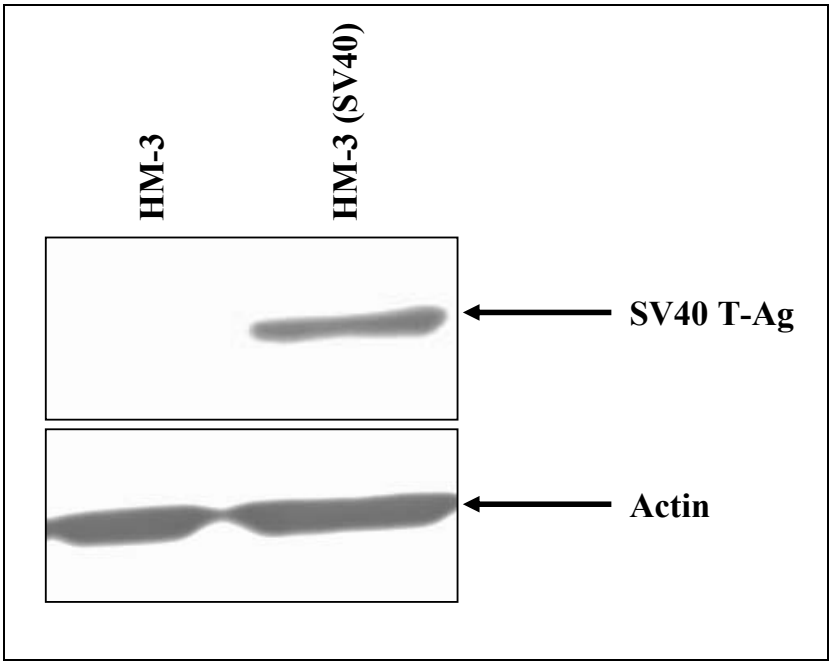

Figure 6.6 Western blot assay of HM-3-Luc and HM-3-SV40-Luc cells. The expression of SV40 T-Ag was detected in HM-3-SV40-Luc cells (lane 2) but not in HM-3-Luc cells (lane 1).

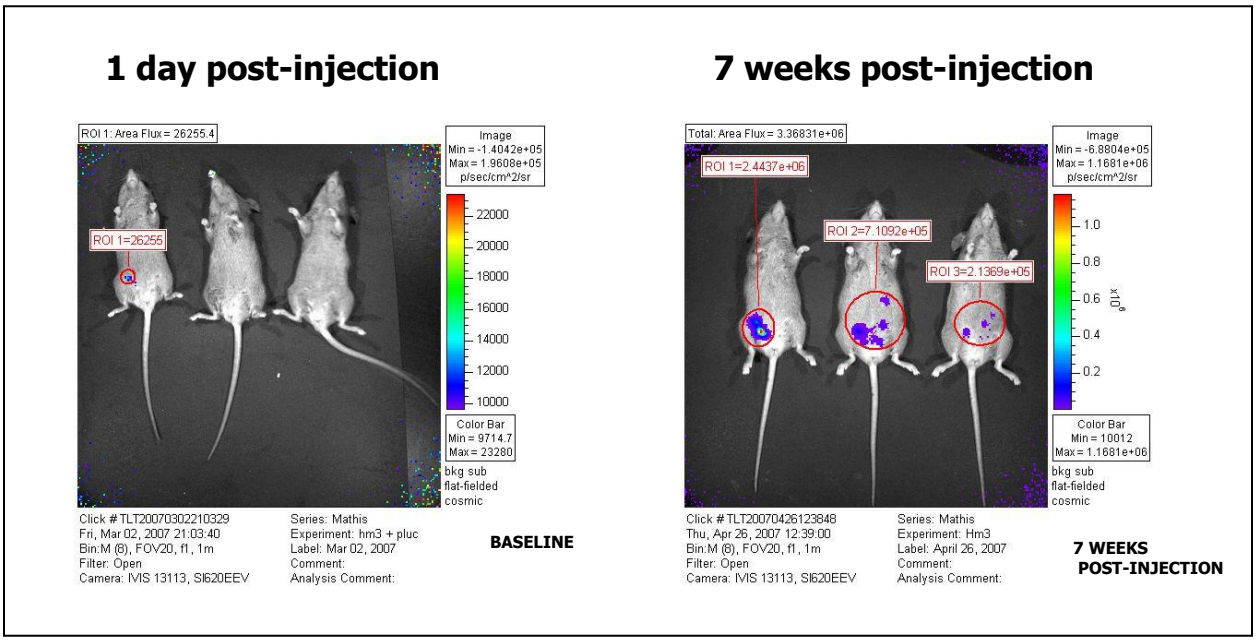

Figure 6.7 Bioluminescent Imaging. B6C3F1 mice were injected with HM-3-Luc cells. Three mice were injected with 1×10^7 cells per mouse. The mice were subjected to bioluminescent imaging at 1 day and then every week after injection until 7 weeks. The signal bars indicate relative photons light intensity.

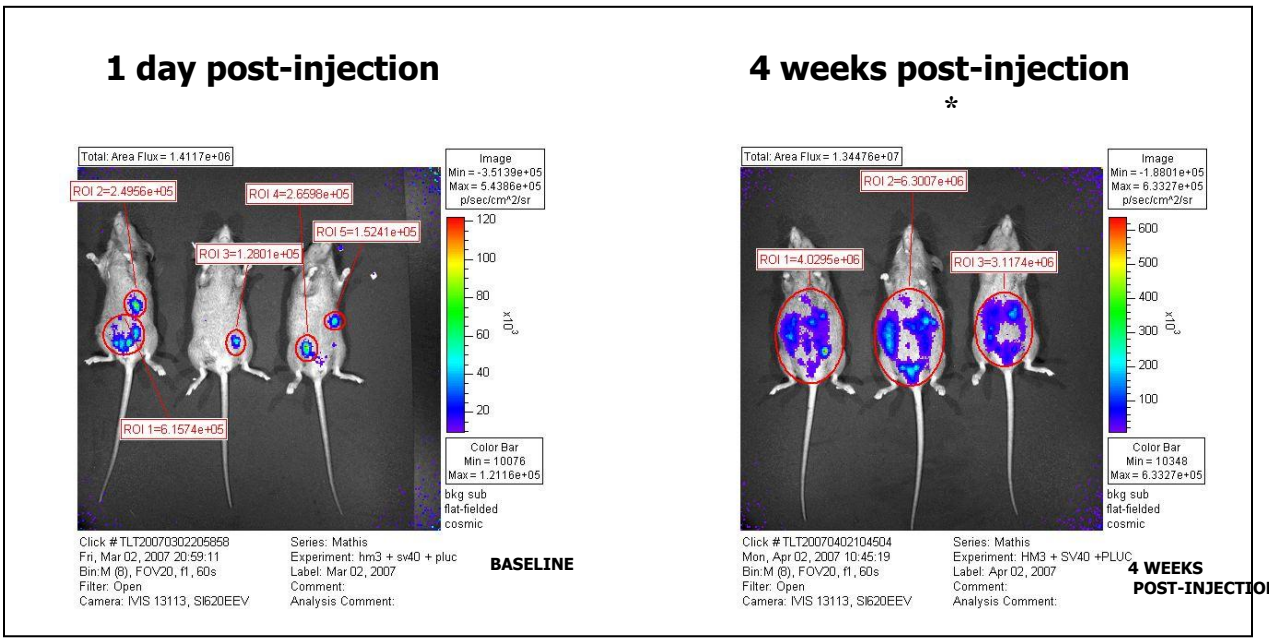

Figure 6.8 Bioluminescent Imaging. B6C3F1 mice were injected with HM-3-SV40-Luc cells. Three mice were injected with 1×10^7 cells per mouse. The mice were subjected to bioluminescent imaging at 1 day and then every week after injection until 4 weeks. The signal bars indicate relative photons light intensity. * $P < 0.05$ versus mice injected with HM-3(SV40) cells at 1 day post-injection.

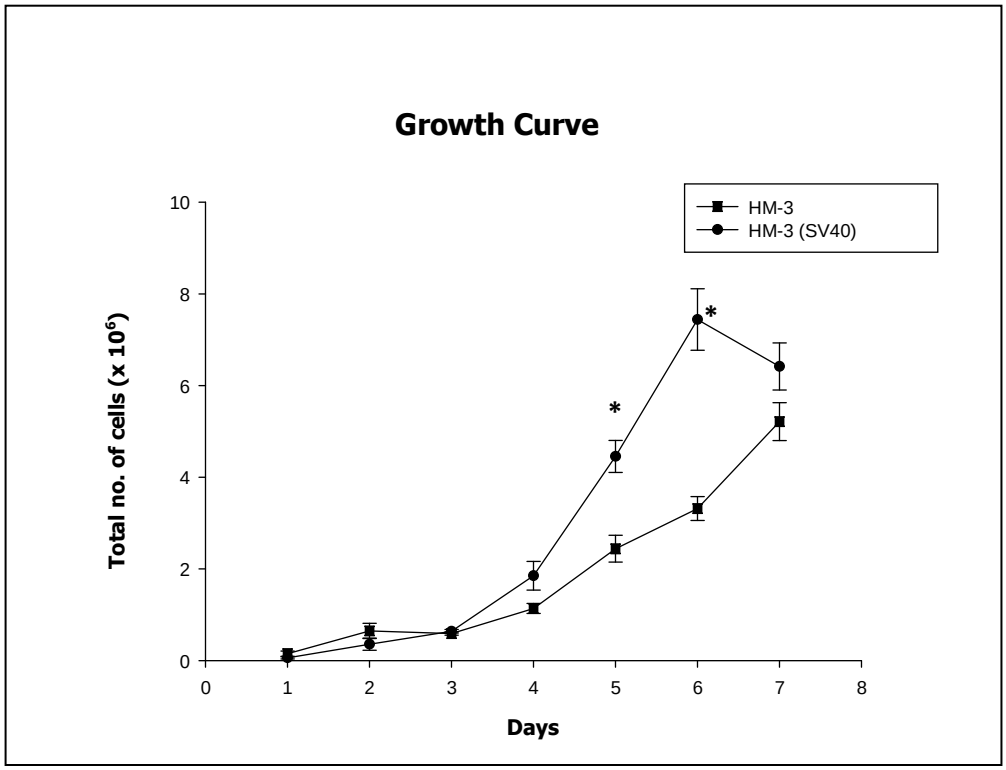

Figure 6.9 Growth curves of HM-3 and HM-3(SV40) cells. Each cell group was maintained in DMEM media supplemented with 10% FBS and cells numbers were counted on the indicated days. Mean no. of cells +/- SE obtained from three observations, is plotted against the number days at which the cells were counted. HM-3(SV40) has a higher growth curve than HM-3 cells. * $P < 0.05$ versus HM-3 cells.

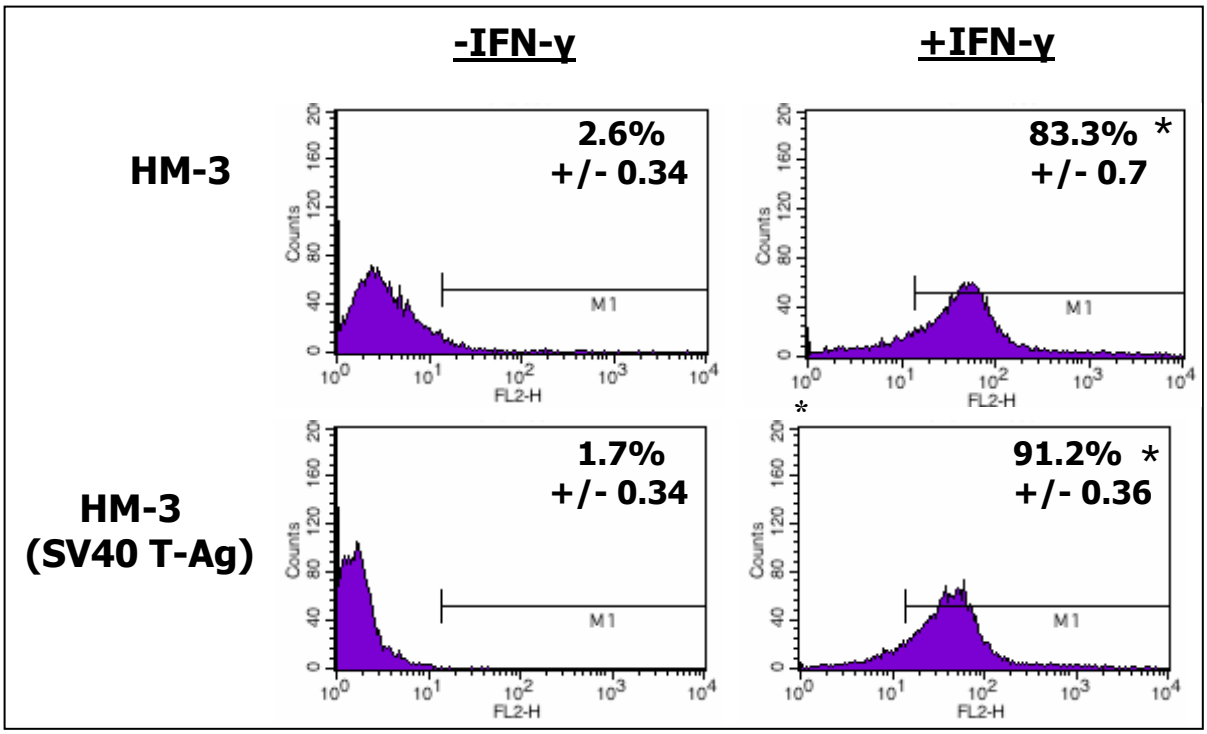

Figure 6.10 Flow cytometric analysis of the HM-3-Luc and HM-3(SV40)-Luc cells without and with IFN-gamma treatment. The cells were stained with FITC-labeled antibody against MHC class I. * P < 0.05 versus control HM-3 and HM-3(SV40) cells, not treated with IFN-g.

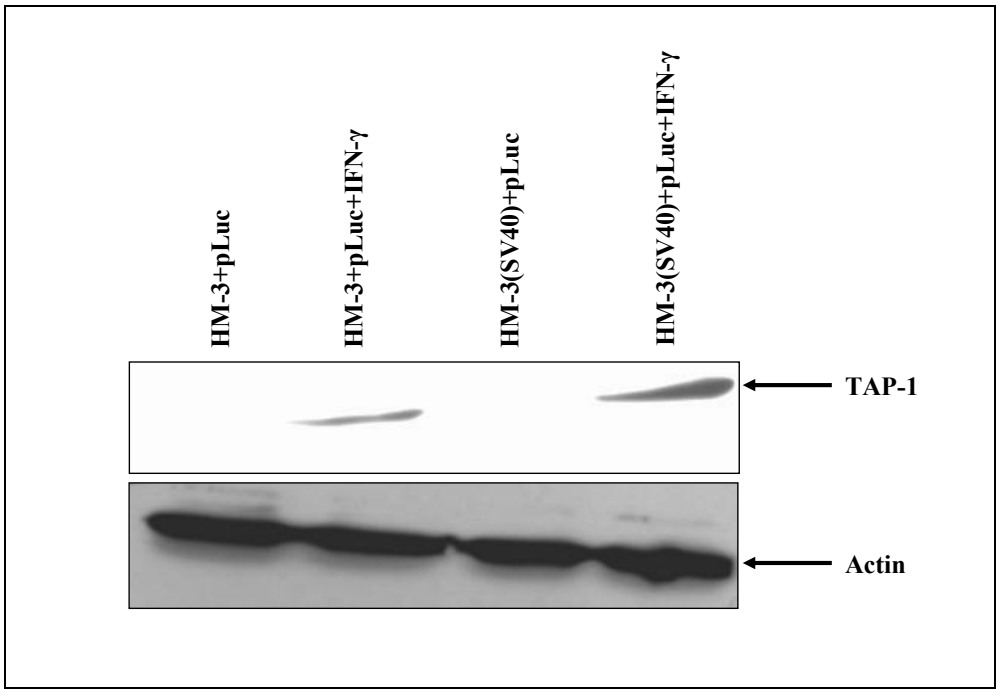

Figure 6.11 Western blot assay of HM-3 and HM-3-SV40 cells before and after treatment with IFN-gamma. The expression of TAP-1 was detected in HM-3 and HM-3-SV40 cells only after treatment with IFN-gamma. The IFN-gamma treated HM-3 cells (lane 2) and HM-3-SV40 (lane 4) cells show expression of TAP-1, but not the untreated HM-3 and HM-3-SV40 cells (lanes 1 and 3).

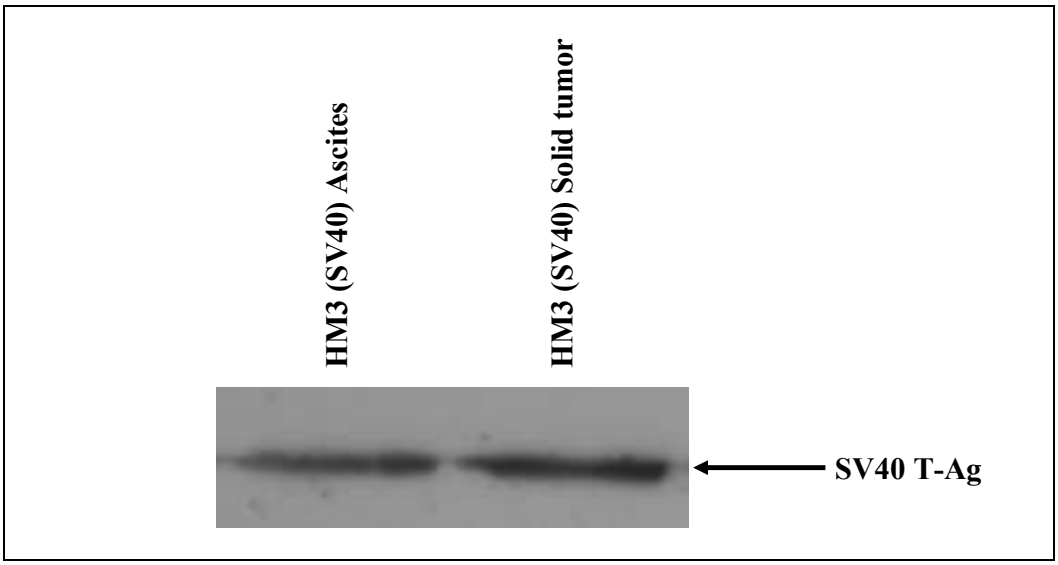

Figure 6.12 Western blot assay of HM-3-SV40 cells. The expression of SV40 T-Ag was detected in tumor cells cultured from the ascites (lane 1) and cells cultured from the solid tumor (lane 2).

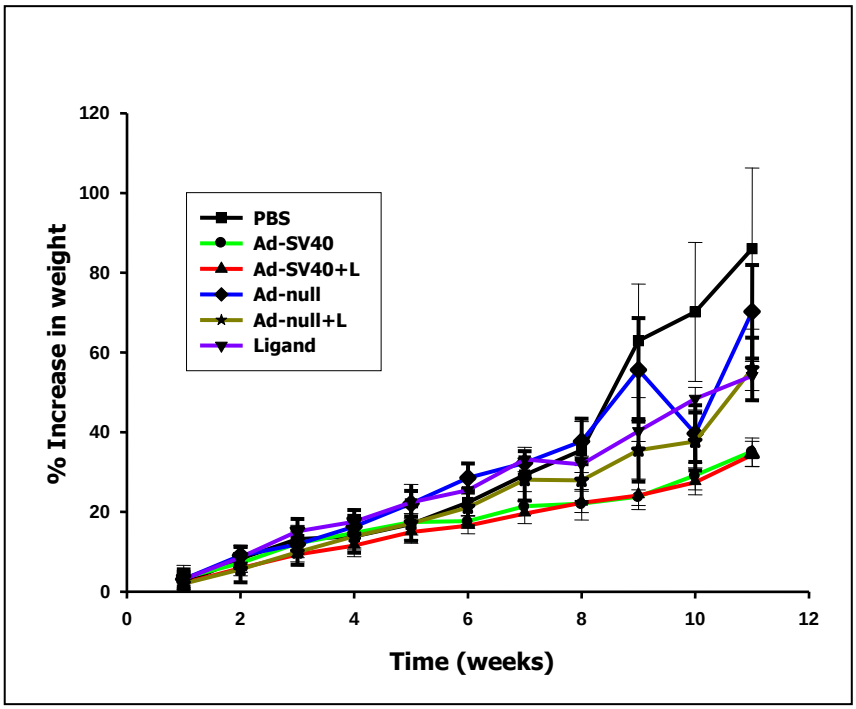

Figure 6.13 Analysis of percentage change in bodyweight . The B6C3F1 mice immunized with CD40-targeted Ad5-CMV-SV40 T-Ag (Ad-SV40+L) and untargeted Ad5-CMV-SV40 T-Ag (Ad-SV40) were challenged with IG10-SV40 tumor cells. The mice immunized with CD40-targeted Ad5-null (Ad-null+L), untargeted Ad5-null (Ad5-null), CFm40L (Ligand) and saline (PBS), also challenged with IG10-SV40 tumor cells, were used as controls. The mice immunized with CD40-targeted and untargeted Ad5-CMV-SV40 T-Ag showed similar percentage of increase in bodyweight, which was significantly less ($P < 0.05$) than that shown by the control mice. * $P < 0.05$ versus mice immunized with CD40-targeted Ad5-null (Ad-null+L), untargeted Ad5-null (Ad-null), CFm40L (Ligand) and saline (PBS).

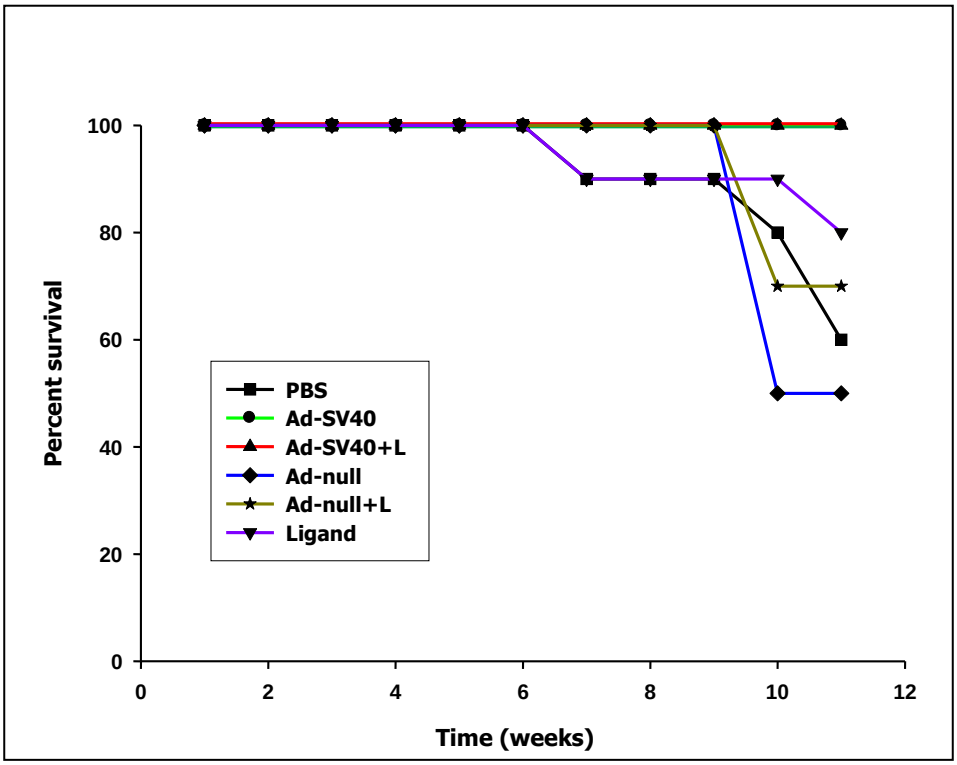

Figure 6.14 Analysis of survival. The B6C3F1 mice immunized with CD40-targeted Ad5-CMV-SV40 T-Ag (Ad-SV40+L) and untargeted Ad5-CMV-SV40 T-Ag (Ad-SV40) were challenged with IG10-SV40 tumor cells. The mice immunized with CD40-targeted Ad5-null (Ad-null+L), untargeted Ad5-null (Ad5-null), CFm40L (Ligand) and saline (PBS), also challenged with IG10-SV40 tumor cells, were used as controls. The mice immunized with CD40-targeted and untargeted Ad5-CMV-SV40 T-Ag showed 100% survival till 11 weeks after challenge with the tumor cells, while the control mice showed significant decrease in their survival.